



National Library  
of Canada

Acquisitions and  
Bibliographic Services Branch

395 Wellington Street  
Ottawa, Ontario  
K1A 0N4

Bibliothèque nationale  
du Canada

Direction des acquisitions et  
des services bibliographiques

395, rue Wellington  
Ottawa (Ontario)  
K1A 0N4

*Your file - Votre référence*

*Our file - Notre référence*

## NOTICE

The quality of this microform is heavily dependent upon the quality of the original thesis submitted for microfilming. Every effort has been made to ensure the highest quality of reproduction possible.

If pages are missing, contact the university which granted the degree.

Some pages may have indistinct print especially if the original pages were typed with a poor typewriter ribbon or if the university sent us an inferior photocopy.

Reproduction in full or in part of this microform is governed by the Canadian Copyright Act, R.S.C. 1970, c. C-30, and subsequent amendments.

## AVIS

La qualité de cette microforme dépend grandement de la qualité de la thèse soumise au microfilmage. Nous avons tout fait pour assurer une qualité supérieure de reproduction.

S'il manque des pages, veuillez communiquer avec l'université qui a conféré le grade.

La qualité d'impression de certaines pages peut laisser à désirer, surtout si les pages originales ont été dactylographiées à l'aide d'un ruban usé ou si l'université nous a fait parvenir une photocopie de qualité inférieure.

La reproduction, même partielle, de cette microforme est soumise à la Loi canadienne sur le droit d'auteur, SRC 1970, c. C-30, et ses amendements subséquents.

Canada

**UNIVERSITY OF ALBERTA**

**THE DIRECT ANALYSIS OF MATERIALS WITH INDUCTIVELY COUPLED  
PLASMA SPECTROMETRY**

by

**XIANG RONG LIU**



**A Thesis Submitted to the Faculty of Graduate Studies and Research in Partial  
Fulfillment of the Requirements for the Degree of Doctor of Philosophy**

**DEPARTMENT OF CHEMISTRY**

**EDMONTON, ALBERTA**

**FALL, 1994**



National Library  
of Canada

Acquisitions and  
Bibliographic Services Branch

395 Wellington Street  
Ottawa, Ontario  
K1A 0N4

Bibliothèque nationale  
du Canada

Direction des acquisitions et  
des services bibliographiques

395, rue Wellington  
Ottawa (Ontario)  
K1A 0N4

*Your file - Votre référence*

*Our file - Notre référence*

**The author has granted an irrevocable non-exclusive licence allowing the National Library of Canada to reproduce, loan, distribute or sell copies of his/her thesis by any means and in any form or format, making this thesis available to interested persons.**

**L'auteur a accordé une licence irrévocable et non exclusive permettant à la Bibliothèque nationale du Canada de reproduire, prêter, distribuer ou vendre des copies de sa thèse de quelque manière et sous quelque forme que ce soit pour mettre des exemplaires de cette thèse à la disposition des personnes intéressées.**

**The author retains ownership of the copyright in his/her thesis. Neither the thesis nor substantial extracts from it may be printed or otherwise reproduced without his/her permission.**

**L'auteur conserve la propriété du droit d'auteur qui protège sa thèse. Ni la thèse ni des extraits substantiels de celle-ci ne doivent être imprimés ou autrement reproduits sans son autorisation.**

ISBN 0-315-95219-9

**Canada**

Name XIANG RONG LIU

Dissertation Abstracts International is arranged by broad, general subject categories. Please select the one subject which most nearly describes the content of your dissertation. Enter the corresponding four-digit code in the spaces provided.

0486

U·M·I

SUBJECT TERM

SUBJECT CODE

## Subject Categories

### THE HUMANITIES AND SOCIAL SCIENCES

#### COMMUNICATIONS AND THE ARTS

Architecture ..... 0729  
Art History ..... 0377  
Cinema ..... 0900  
Dance ..... 0378  
Fine Arts ..... 0357  
Information Science ..... 0723  
Journalism ..... 0391  
Library Science ..... 0399  
Mass Communications ..... 0708  
Music ..... 0413  
Speech Communication ..... 0459  
Theater ..... 0465

#### EDUCATION

General ..... 0515  
Administration ..... 0514  
Adult and Continuing ..... 0516  
Agricultural ..... 0517  
Art ..... 0273  
Bilingual and Multicultural ..... 0282  
Business ..... 0688  
Community College ..... 0275  
Curriculum and Instruction ..... 0727  
Early Childhood ..... 0518  
Elementary ..... 0524  
Finance ..... 0277  
Guidance and Counseling ..... 0519  
Health ..... 0680  
Higher ..... 0745  
History of ..... 0520  
Home Economics ..... 0278  
Industrial ..... 0521  
Language and Literature ..... 0279  
Mathematics ..... 0280  
Music ..... 0522  
Philosophy of ..... 0998  
Physical ..... 0573

Psychology ..... 0525  
Reading ..... 0535  
Religious ..... 0527  
Sciences ..... 0714  
Secondary ..... 0533  
Social Sciences ..... 0534  
Sociology of ..... 0340  
Special ..... 0529  
Teacher Training ..... 0530  
Technology ..... 0710  
Tests and Measurements ..... 0288  
Vocational ..... 0747

#### LANGUAGE, LITERATURE AND LINGUISTICS

Language ..... 0679  
General ..... 0289  
Ancient ..... 0290  
Linguistics ..... 0291  
Modern ..... 0401  
Literature ..... 0294  
Classical ..... 0295  
Comparative ..... 0297  
Medieval ..... 0298  
Modern ..... 0316  
African ..... 0591  
American ..... 0305  
Asian ..... 0352  
Canadian (English) ..... 0355  
Canadian (French) ..... 0593  
English ..... 0311  
Germanic ..... 0312  
Latin American ..... 0315  
Middle Eastern ..... 0313  
Romance ..... 0314  
Slavic and East European ..... 0314

#### PHILOSOPHY, RELIGION AND THEOLOGY

Philosophy ..... 0422  
Religion ..... 0318  
General ..... 0321  
Biblical Studies ..... 0319  
Clergy ..... 0320  
History of ..... 0322  
Philosophy of ..... 0469  
Theology ..... 0323

#### SOCIAL SCIENCES

American Studies ..... 0323  
Anthropology ..... 0324  
Archaeology ..... 0326  
Cultural ..... 0327  
Physical ..... 0310  
Business Administration ..... 0272  
General ..... 0770  
Accounting ..... 0454  
Banking ..... 0338  
Management ..... 0385  
Marketing ..... 0501  
Canadian Studies ..... 0503  
Economics ..... 0505  
General ..... 0508  
Agricultural ..... 0509  
Commerce-Business ..... 0510  
Finance ..... 0511  
History ..... 0358  
Labor ..... 0366  
Theory ..... 0351  
Folklore ..... 0578  
Geography ..... 0366  
Gerontology ..... 0351  
History ..... 0578

Ancient ..... 0579  
Medieval ..... 0581  
Modern ..... 0582  
Black ..... 0328  
African ..... 0331  
Asia, Australia and Oceania ..... 0332  
Canadian ..... 0334  
European ..... 0335  
Latin American ..... 0336  
Middle Eastern ..... 0337  
United States ..... 0585  
History of Science ..... 0398  
Law ..... 0615  
Political Science ..... 0616  
General ..... 0617  
International Law and Relations ..... 0814  
Public Administration ..... 0452  
Recreation ..... 0626  
Social Work ..... 0627  
Sociology ..... 0938  
General ..... 0631  
Criminology and Penology ..... 0628  
Demography ..... 0629  
Ethnic and Racial Studies ..... 0630  
Individual and Family Studies ..... 0629  
Industrial and Labor Relations ..... 0630  
Public and Social Welfare ..... 700  
Social Structure and Development ..... 344  
Theory and Methods ..... 0707  
Transportation ..... 0997  
Urban and Regional Planning ..... 0453  
Women's Studies ..... 0453

### THE SCIENCES AND ENGINEERING

#### BIOLOGICAL SCIENCES

Agriculture ..... 0473  
General ..... 0285  
Agronomy ..... 0475  
Animal Culture and Nutrition ..... 0476  
Animal Pathology ..... 0359  
Food Science and Technology ..... 0478  
Forestry and Wildlife ..... 0479  
Plant Culture ..... 0480  
Plant Pathology ..... 0817  
Plant Physiology ..... 0777  
Range Management ..... 0746  
Wood Technology ..... 0306  
Biology ..... 0287  
General ..... 0308  
Anatomy ..... 0309  
Biostatistics ..... 0379  
Botany ..... 0329  
Cell ..... 0353  
Ecology ..... 0369  
Entomology ..... 0793  
Genetics ..... 0410  
Limnology ..... 0307  
Microbiology ..... 0317  
Molecular ..... 0416  
Neuroscience ..... 0433  
Oceanography ..... 0821  
Physiology ..... 0778  
Radiation ..... 0472  
Veterinary Science ..... 0786  
Zoology ..... 0760  
Biophysics ..... 0425  
General ..... 0996  
Medical ..... 0575

#### EARTH SCIENCES

Biogeochemistry ..... 0425  
Geochemistry ..... 0996

Geodesy ..... 0370  
Geology ..... 0372  
Geophysics ..... 0373  
Hydrology ..... 0388  
Mineralogy ..... 0411  
Paleobotany ..... 0345  
Paleoecology ..... 0426  
Paleontology ..... 0418  
Paleozoology ..... 0985  
Palynology ..... 0427  
Physical Geography ..... 0368  
Physical Oceanography ..... 0415

#### HEALTH AND ENVIRONMENTAL SCIENCES

Environmental Sciences ..... 0768  
Health Sciences ..... 0566  
General ..... 0300  
Audiology ..... 0992  
Chemotherapy ..... 0567  
Dentistry ..... 0350  
Education ..... 0769  
Hospital Management ..... 0758  
Human Development ..... 0982  
Immunology ..... 0564  
Medicine and Surgery ..... 0347  
Mental Health ..... 0569  
Nursing ..... 0570  
Nutrition ..... 0380  
Obstetrics and Gynecology ..... 0354  
Occupational Health and Therapy ..... 0381  
Ophthalmology ..... 0571  
Pathology ..... 0419  
Pharmacology ..... 0572  
Pharmacy ..... 0382  
Physical Therapy ..... 0573  
Public Health ..... 0574  
Radiology ..... 0575  
Recreation ..... 0575

Speech Pathology ..... 0460  
Toxicology ..... 0383  
Home Economics ..... 0386

#### PHYSICAL SCIENCES

Pure Sciences ..... 0485  
Chemistry ..... 0749  
General ..... 0486  
Agricultural ..... 0487  
Analytical ..... 0488  
Biochemistry ..... 0738  
Inorganic ..... 0490  
Nuclear ..... 0491  
Organic ..... 0494  
Pharmaceutical ..... 0495  
Physical ..... 0754  
Polymer ..... 0755  
Radiation ..... 0605  
Mathematics ..... 0986  
Physics ..... 0606  
General ..... 0608  
Acoustics ..... 0748  
Astronomy and Astrophysics ..... 0607  
Elementary Particles and High Energy ..... 0798  
Fluid and Plasma ..... 0759  
Molecular ..... 0609  
Nuclear ..... 0610  
Optics ..... 0752  
Radiation ..... 0611  
Solid State ..... 0463  
Statistics ..... 0346  
Applied Sciences ..... 0984  
Applied Mechanics ..... 0346  
Computer Science ..... 0984

Engineering ..... 0537  
General ..... 0538  
Aerospace ..... 0539  
Agricultural ..... 0540  
Automotive ..... 0541  
Biomedical ..... 0542  
Chemical ..... 0543  
Civil ..... 0544  
Electronics and Electrical ..... 0348  
Heat and Thermodynamics ..... 0545  
Hydraulic ..... 0546  
Industrial ..... 0547  
Marine ..... 0794  
Materials Science ..... 0548  
Mechanical ..... 0743  
Metallurgy ..... 0551  
Mining ..... 0552  
Nuclear ..... 0549  
Packaging ..... 0765  
Petroleum ..... 0554  
Sanitary and Municipal ..... 0790  
System Science ..... 0428  
Geotechnology ..... 0796  
Operations Research ..... 0795  
Physics Technology ..... 0994  
Textile Technology ..... 0994

#### PSYCHOLOGY

General ..... 0621  
Behavioral ..... 0384  
Clinical ..... 0622  
Developmental ..... 0620  
Experimental ..... 0623  
Industrial ..... 0624  
Personality ..... 0625  
Physiological ..... 0989  
Psychobiology ..... 0349  
Psychometrics ..... 0632  
Social ..... 0451



UNIVERSITY OF ALBERTA

RELEASE FORM

NAME OF AUTHOR: Xiang Rong Liu

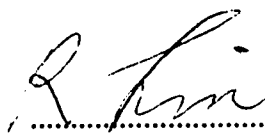
TITLE OF THESIS: The Direct Analysis of Materials with Inductively Coupled Plasma Spectrometry.

DEGREE: Ph.D.

YEAR THIS DEGREE GRANTED: 1994

Permission is hereby granted to the University of Alberta Library to reproduce single copies of this thesis and to lend or sell such copies for private, scholarly or scientific research purposes only.

The author reserves all other publication and other right in association with the copyright in the thesis, and except as hereinbefore provided neither the thesis nor any substantial portion thereof may be printed or otherwise reproduced in any material form whatever without the author's prior written permission.

  
.....  
(Student's Signature)

Permanent Address:

#101, 10726-85 Avenue

Edmonton Alberta

Canada T6E 2K8

Sept. 9, 1994  
Date: .....

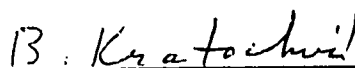
UNIVERSITY OF ALBERTA

FACULTY OF GRADUATE STUDIES AND RESEARCH

The undersigned certify that they have read, and recommend to the Faculty of Graduate Studies and Research for acceptance, a thesis entitled THE DIRECT ANALYSIS OF MATERIALS WITH INDUCTIVELY COUPLED PLASMA SPECTROMETRY submitted by XIANG RONG LIU in partial fulfillment of the requirements for the degree of Doctor of Philosophy.



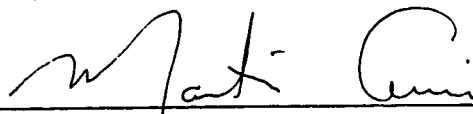
Dr. G. Horlick, Supervisor



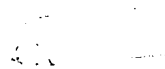
Dr. B. Kratochvil



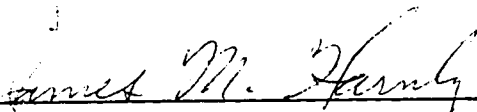
Dr. J. A. Plambeck



Dr. M. Cowie



Dr. J. Tulip



Dr. J. M. Harnly External Examiner

Date: \_\_\_\_\_

Sept. 9, 1994

**To Caroline and Juying**

## Abstract

Two solid sample introduction techniques, direct sample insertion and laser ablation, have been studied in this thesis.

It is shown that a direct sample insertion (DSI) device can be used in conjunction with inductively coupled plasma atomic emission spectrometry for the direct determination of trace elements in a variety of materials. The majority of analyses involving DSI devices have concerned samples in the form of small aqueous solution volumes or dried solution residues. Different mixed gas DSI-ICP have been studied in order to extend the DSI-ICP capability for the difficult to vaporize elements and refractory samples. Successful analyses have now been carried out for the direct insertion of  $\text{Al}_2\text{O}_3$ , Al metal, oil, and botanical samples. The key operational feature that has allowed the successful direct determination of trace elements in these materials, with essentially no *a priori* sample treatment, is the utilization of an argon-oxygen mixed gas plasma. The calibration curves are linear over a dynamic range of 3 to 4 orders of magnitude and detection limits are in the range of 10's of picograms.

In the second part of the thesis an *in situ* laser ablation system for inductively coupled plasma- atomic emission spectrometry (ICP-AES) is described that eliminates the aerosol transport step associated with conventional laser ablation sample introduction systems. The concept of this system is to place the sample inside the ICP torch immediately below the plasma discharge. This can be accomplished using a direct sample insertion system. The laser is then focused on the sample by a lens placed above the plasma and ablated material is directly injected into the plasma. For ablation with a Q-switched Nd-YAG laser (single pulse) this results in an emission signal that has a duration of about 0.7 ms, in contrast to a conventional ablation system where signal duration is measured in seconds. This translates to a dramatic improvement in sensitivity for the *in*



*situ* system over a conventional system. Detection limits for most elements in the Al alloy and steel samples are in the range of ppm to subppm level with absolute detection limits as low as fg/pulse. Measurement considerations are discussed, results are presented for the analysis of Al and steel samples, and the *in situ* system is compared to a conventional laser ablation system.

### **Acknowledgements**

I would like to thank my supervisor, Professor Gary Horlick for his invaluable advice and guidance throughout this work. I would also like to thank all members of the research group for their assistance and thoughtful discussions.

I also thanks to the staff of the Chemistry Department Electronics, Machine and Glass shops for their help.

Finally, I would like to acknowledge the Department of Chemistry for financial support.

## TABLE OF CONTENTS

CHAPTER	PAGE
1 General Introduction.....	2
1.1 Solution nebulization sample introduction for ICP .....	2
1.2 Alternative sample introduction systems for ICP spectrometry.....	5
1.2.1 Spark and arc ablation.....	7
1.2.2 Electrothermal vaporization (ETV) .....	8
1.2.3 Powder injection .....	10
1.2.4 Slurry nebulization .....	11
1.2.5 Vapor introduction.....	12
1.2.6 Laser ablation.....	13
1.2.7 DSI.....	14
1.2.7.1 Applications.....	16
1.2.7.2 Detection limits.....	17
1.2.7.3 Quantitation.....	19
1.2.8 Limitations of DSI and the scope of this research .....	19
References .....	23
2 Mixed Gas Direct Sample Insertion System.....	26
2.1 Introduction .....	26
2.2 System descriptions.....	29
2.2.1 Hardware.....	29
2.2.1.1 The DSI-ICP-AES setups.....	29
2.2.1.2 The sample insertion mechanism.....	33
2.2.1.3 The torch and matching network .....	35
2.2.1.4 The probe.....	38

2.2.1.5	The shutter.....	40
2.2.1.6	The filament and carrier gas.....	40
2.2.1.7	The heating chamber and drying process.....	41
2.2.1.8	The operation procedures.....	43
2.2.2	Software.....	43
2.2.3	Considerations for future signal readout and acquisition subsystem.....	50
2.3	Effect of incident power and gas content on the DSI signal.....	53
2.4	Effect of observation height.....	56
2.5	Effect of the probe's position and history on the signal's temporal profile .....	59
2.6	Studies of the mixed gas DSI-ICP-AES system with aqueous solution samples .....	62
2.7	Studies of the mixed gas DSI-ICP-AES system with solid samples .....	65
2.8	Summary.....	71
	References .....	73
3	Ar-O <sub>2</sub> mixed gas direct sample insertion system .....	76
3.1	Introduction .....	76
3.2	System descriptions and operations .....	77
3.3	Signal characteristics with an Ar-O <sub>2</sub> mixed gas plasma .....	80
3.4	Effect of probe geometry.....	88
3.5	Quantitative analytical performance of Ar-O <sub>2</sub> mixed gas DSI-ICP- AES.....	88
3.5.1	Aqueous solution samples.....	88
3.5.2	Engine oil samples .....	89
3.5.2.1	Introduction .....	89
3.5.2.2	Results and discussion .....	92

3.5.3	Particulate metals.....	95
3.5.3.1	Introduction .....	95
3.5.3.2	Results and discussion .....	97
3.5.4	Al <sub>2</sub> O <sub>3</sub> and SiO <sub>2</sub> based samples .....	99
3.5.4.1	Introduction .....	99
3.5.4.2	Analysis .....	101
3.5.4.3	Results and discussion .....	101
3.5.5	Botanical samples (with Lishi Ying and B. Kratochvil) .....	103
3.5.5.1	Introduction .....	103
3.5.5.2	Results and discussion .....	105
3.5.6	Clinical samples .....	105
3.6	Summary of analytical figures of merit.....	106
3.6.1	Detection limits.....	106
3.6.2	Quantitation.....	108
	References .....	111
4	Introduction to laser ablation in analytical atomic spectroscopy .....	114
4.1	Laser ablation in analytical atomic spectroscopy .....	114
4.2	Laser-material interactions .....	120
4.2.1	Basic equations.....	120
4.2.2	Free running vs. q-switched lasers.....	122
4.2.3	Sample properties that affect ablation.....	125
4.2.4	Conclusions .....	125
4.3	Laser ablation in ICP spectrometry.....	125
4.3.1	General features of LA-ICP system.....	126
4.3.2	Recent application .....	127
4.3.2.1	Detection limits .....	130
4.3.2.2	Precision and accuracy .....	131

4.3.2.3	Calibration curve and quantitative analysis.....	131
4.3.3	Limitations of conventional laser ablation ICP spectrometry.....	134
4.3.3.1	Memory effects .....	134
4.3.3.2	Matrix effects at the ablation stage .....	134
4.3.3.3	Matrix effects in the transportation stage .....	135
4.3.3.4	Limited detection power.....	135
4.3.3.5	Standardization problem.....	136
	References .....	137
5	<i>In situ</i> Laser ICP Spectrometry.....	140
5.1	Why <i>in situ</i> laser ablation ICP .....	140
5.2	Instrumentation .....	143
5.2.1	General description.....	143
5.2.2	Laser .....	144
5.2.3	Samples and the sample holder.....	144
5.2.4	Signal measurement considerations .....	146
5.3	Optimization of the operating parameters .....	150
5.4	Signal characteristics of <i>in situ</i> laser ablation ICP-AES.....	152
5.5	Analyte traveling speed in the plasma with <i>in situ</i> laser ablation ICP-AES.....	157
5.6	Time constant effect on the signals .....	159
5.7	Summary.....	162
	References .....	163
6	Applications of the <i>in situ</i> LA-ICP-AES for the analysis of solid Samples .....	164
6.1	Procedures for sample preparation and analysis .....	164
6.2	Evaluation of detection limits .....	166
6.3	Calibration curves for solid standards .....	171
6.4	Analyses of solution residues with <i>in situ</i> LA-ICP-AES.....	176

6.5 Problems and future work .....	180
References .....	181
7 Studies of conventional LA-ICP-AES .....	182
7.1 Introduction .....	182
7.2 Instrumentation .....	183
7.3 Signal characterization of conventional LA-ICP-AES .....	183
7.4 Summary .....	195
References .....	197
8 Summary and future work .....	198
8.1 DSI-ICP .....	198
8.2 LA-ICP .....	201
References .....	203

## LIST OF TABLES

TABLE	PAGE
2.1 Hardware specification and typical operating conditions for the Ar-O <sub>2</sub> and Ar-N <sub>2</sub> mix gas ICP-DSI system.....	32
2.2 Boiling point data for Zr, Ti, V, Al and their oxides and carbides .....	55
2.3 Detection limits for the solution residue sample.....	61
2.4 Signal relative intensities (relative to b1) of 12 sheet glass samples analyzed by Ar-N <sub>2</sub> (2%) mixed gas DSI-ICP-AES with SiO <sub>2</sub> coated probe .....	70
3.1 Metals analyzed in lubricating oils and areas associated with possible trouble .....	91
3.2 Sample information of ALCAN Al alloys .....	100
3.3 Sample information of ALCOA Al alloys .....	100
3.4 Detection limits for CONOSTAN S21 oil residue sample with Ar-O <sub>2</sub> mix gas DSI-ICP-AES .....	107
3.5 Detection limits for a botanical sample and Al <sub>2</sub> O <sub>3</sub> with Ar-O <sub>2</sub> mix gas DSI-ICP-AES .....	107
4.1 Some typical lasers and the parameters used in laser ablation application.....	118
6.1 Sample information for steels .....	165
6.2 Detection limits by <i>in situ</i> laser ablation ICP-AES evaluated from single pulse peak height and the base line noise.....	165
6.3 The improved detection limits of <i>in situ</i> LA-ICP-AES by multiple pulse averaging.....	168
6.4 Estimated absolute detection limits of elements by <i>in situ</i> laser ablation ICP-AES .....	168
6.5 Some recent literature detection limits by conventional laser ablation ICP-MS. ....	171
7.1 Calculated detection limits for different masses of spherical particles in the micrometer range.....	188



## LIST OF FIGURES

FIGURE	PAGE
1.1 Schematic diagram for a generic DSI Device.....	15
2.1 Schematic diagram of the direct sample insertion-inductively coupled plasma- atomic emission spectrometry (DSI-ICP-AES) with Ar-N <sub>2</sub> (2%) plasma.....	30
2.2 Schematic diagram of the modified Fassel torch for DSI-ICP-AES.....	36
2.3 Simplified block diagram of the auto-matching network for running the mixed gas ICP .....	37
2.4 Schematic diagram of the graphite probes used for DSI-ICP .....	39
2.5 Schematic diagram of the heating chamber.....	42
2.6a The screen copy of the DSI-ICP program for MS Windows. The acquired signals are displayed in the child windows.....	46
2.6b The screen copy of the DSI-ICP program for MS Windows. The data processing functions are shown under the Edit menu.....	47
2.6c The screen copy of the DSI-ICP program for MS Windows. The stepper motor control dialog box is shown.....	48
2.6d The screen copy of the DSI-ICP program for MS Windows. The data acquisition control dialog box is shown.....	49
2.7 32 channel signal read out electronics for DSI-ICP-AES with programmable gain selection.....	52
2.8 Signals of mixed gas DSI-ICP-AES for different elements.....	54
2.9 Effect of plasma power and % N <sub>2</sub> on the signals (peak area) with DSI-ICP- AES .....	57
2.10 Effect of observation height on the signals of Ar-N <sub>2</sub> (2%) mixed gas DSI- ICP-AES for different elements .....	58

2.11 Effect of cup surface conditions on the signals of Ar-N <sub>2</sub> (2%) mixed gas DSI-ICP-AES for different elements.....	60
2.12 Calibration curves (log-log plot) of metals in solution residue using Ar-N <sub>2</sub> (2%) mixed gas DSI-ICP-AES .....	63
2.13 Calibration curve (log-log plot) of V in aqueous standards using Ar-N <sub>2</sub> (2%) mixed gas DSI-ICP-AES .....	64
2.14 DSI signals of V in aqueous standards. (a) first insertion in the Ar-N <sub>2</sub> (2%) mixed gas plasma, and (b) the 5th insertion. ....	66
2.15 DSI signals of Al, Ba, and Mn in glass sample using uncoated cup (a), and SiO <sub>2</sub> coated graphite cups (c) with Ar-N <sub>2</sub> (2%) mixed gas plasma .....	68
2.16 Relative signal intensities of Sr, Al, Fe, Mg, Mn, and Ba in different glass samples analyzed by Ar-N <sub>2</sub> (2%) mixed gas DSI-ICP-AES with SiO <sub>2</sub> coated graphite cups .....	69
3.1 Schematic diagram of the direct sample insertion-inductively coupled plasma-atomic emission spectrometry (DSI-ICP-AES) with Ar-O <sub>2</sub> (20%) plasma.....	78
3.2 Diagram of the graphite sample probes (a) before insertion, and (b) after insertion into an Ar-O <sub>2</sub> (20%) mixed ICP for 80 seconds .....	81
3.3 Comparison of V signals for Ar-N <sub>2</sub> (2%) and Ar-O <sub>2</sub> (20%) mixed gas plasma. Signals shown are for first insertion in Ar-N <sub>2</sub> (2%) plasma (a), 5th insertion in Ar-N <sub>2</sub> (2%) plasma (b), first insertion in Ar-O <sub>2</sub> (20%) plasma (c), and the 2nd insertion in Ar-O <sub>2</sub> (20%) plasma (d) .....	82
3.4 Examples of DSI signals for several elements in a variety of sample matrices using an Ar-O <sub>2</sub> (20%) plasma. See text for discussion.....	85
3.5 Signals of Ar-O <sub>2</sub> (20%) mixed gas DSI-ICP-AES for 0.0033% V, Zr, and Ti in Al <sub>2</sub> O <sub>3</sub> . The signals shown are before (upper row) and after (lower row) blank corrections .....	87

3.6	Calibration curves (log-log plot) for solution standards (SM20) with Ar-O <sub>2</sub> (20%) mixed gas DSI-ICP-AES .....	90
3.7	Schematic diagram indicating the ashing position .....	94
3.8	Calibration curves (log-log plot) for trace elements in CONOSTAN, S21 oil standards using Ar-O <sub>2</sub> (20%) mixed gas DSI-ICP-AES .....	96
3.9	Calibration curves (log-log plot) for trace elements in low and high alloy aluminum using Ar-O <sub>2</sub> (20%) mixed gas DSI-ICP-AES.....	98
3.10	Calibration curves (log-log plot) for trace elements in Al <sub>2</sub> O <sub>3</sub> standard, TS6 (0.001% - 0.%) using Ar-O <sub>2</sub> (20%) mixed gas DSI-ICP-AES.....	102
4.1	Schematic diagram of conventional Laser Ablation Inductively Coupled Plasma Atomic Emission Spectrometry (LA-ICP-AES) System .....	116
5.1	Schematic diagram of <i>in situ</i> Laser Ablation Inductively Coupled Plasma Atomic Emission Spectroscopy System ( <i>in situ</i> LA-ICP-AES) .....	141
5.2	Detail of the graphite sample holder (a) and a schematic of the inserted sample probe (b). .....	145
5.3	Train of emission signals for 0.0005% Zn in a low alloy steel (NIST 1262) (a) and an expanded scale plot of one emission pulse (b). The laser rate was 20 Hz and the data rate was 7 kHz. The data is acquired with asynchronous mode.....	147
5.4	A single emission pulse for 0.28 ppm Ca in stainless steel (NIST 1261) acquired in the triggered mode at a rate of 8 kHz (a) and the result of averaging 100 such signals (b). .....	149
5.5	Sequences of 10 triggered emission signals for Co, Zr and Mn in an Al sample (ALCAN low alloy Al, 1SWM) acquired in a time multiplexed mode. See text for discussion.....	151

5.6 Sequences of 10 triggered emission signals for Al, V, Ti, Cu, Fe, and Zn in Al samples (ALCAN low alloy Al, 1SWM and ALCOA, SA1507-7) acquired in a time multiplexed mode. See text for discussion.....	153
5.7 <i>in situ</i> LA-ICP-AES signals with different times of averaging. The signal demonstrate that multipulse average fails when high concentration sample is analyzed with low amplifier gain ( $10^5$ ). .....	155
5.8 Diagram for the determination of particle speed in the plasma with <i>in situ</i> LA-ICP-AES .....	158
5.9 Schematic diagram of the sample plug in the observation zone with <i>in situ</i> LA-ICP-AES .....	160
5.10 Effect of amplifier's time constant on the signal intensity and peak width with <i>in situ</i> LA-ICP-AES .....	161
6.1 Two different methods used for the calculation of the standard deviation with <i>in situ</i> LA-ICP-AES. In column (a) the SD is calculated from 16 runs of a blank sample, and in column (b) 16 data points taken from an off peak base line used for calculation of the standard deviation .....	167
6.2 <i>in situ</i> LA-ICP-AES signals for trace elements in low alloy steel.....	173
6.3 Calibration curves (log-log plot) of trace elements in Al standard (both low and high alloy Al) with the <i>in situ</i> LA-ICP-AES.....	174
6.4 Calibration curves (log-log plot) for Cu, Mo, and Mn in steel standard with the <i>in situ</i> LA-ICP-AES .....	175
6.5 Some ideological methods can be used to sample in different place with the <i>in situ</i> LA-ICP-AES for eliminating sample inhomogeneity problem .....	177
6.6 <i>in situ</i> LA-ICP-AES signals for V in solution residue sample. ....	179
7.1 Schematic diagram of conventional Laser Ablation Inductively Coupled Plasma Atomic Emission Spectrometry (LA-ICP-AES) (a) and the ablation chamber (b) .....	184

7.2	Single shot LA-ICP-AES signals for a high alloy Al sample with low data acquisition speed (243 Hz/channel) .....	185
7.3	Single shot LA-ICP-AES signals for Cu (3.83 % in high alloy Al sample) (a) and the zoomed view for several spikes (b) with high data acquisition speed (26.7 kHz/channel) and small time constant (0.01 ms).....	186
7.4	Single shot LA-ICP-AES signals for Cu (3.83 % in high alloy Al sample) with different time constant. The data is acquired at a rate of 26.7 kHz/channel .....	190
7.5	Single shot signals of conventional LA-ICP-AES vs. <i>in situ</i> LA-ICP-AES.....	191
7.6	Effect of laser firing rate on signal shape and intensities with the conventional LA-ICP-AES.....	193
7.7	Blank signals of conventional LA-ICP-AES in Al (left column) and Cu (right column) channels. The signals shown are the blank signals with laser firing on a graphite rod (a and b), and the one without laser action (c and d) .....	194
7.8	Blank signals of the <i>in situ</i> LA-ICP-AES in different channels. The signals are obtained by firing the laser on a graphite rod .....	196

## **PART I**

# **DIRECT SAMPLE INSERTION INDUCTIVELY COUPLED PLASMA ATOMIC EMISSION SPECTROSCOPY (DSI-ICP-AES)**

## **Chapter 1**

### **General Introduction**

#### **1.1 Solution nebulization sample introduction for ICP**

The inductively coupled plasma (ICP) has been widely accepted as a standard elemental analytical technique, and may be considered in a stage of maturity. It has been almost 30 years since the inductively coupled plasma was first introduced to the analytical chemistry community by Greenfield [1] and Fassel [2]. The sample introduction system, however, in today's state-of-the-art ICP spectrometer is basically the same as those used by the pioneering researchers. The operating parameters and the figures of merits of today's ICP are surprisingly similar as those reported two decades ago [3, 4, 5]. Is there any room to improve sample introduction and figures of merit for ICPs?

An ideal atomic spectroscopy source should exhibit the following characteristics:

- Be able to convert any sample into gas phase atomic vapor with little or no sample pre-treatment.
- Do so for all elements at all concentrations.
- Have identical operating conditions for all elements and samples.
- Have analytical signal which is a simple function of the concentration of individual elements. i.e., no interferences, no matrix effects
- Have been well characterized and understood at a fundamental level
- Be accurate and precise
- Have low initial cost, with low maintenance and running costs
- Be simple to operate, reliable.

The ICP is a very good atom and ion source for atomic emission, elemental mass spectrometry, and atomic fluorescence. It meets or is close to meeting most of the criteria of an ideal source with the exception of the first one which is, unfortunately, a very important one because it is the linkage of the powerful source to the real world. The performance of ICP spectrometry is more often than not limited by the pneumatic nebulization sample introduction system. Such limitations are two fold: low sampling efficiency and lack of flexibility with sample form.

There is, however, nothing wrong with a solution sample. It does have features that an analytical chemist appreciates. It is easy to handle, easy to manipulate, easy to standardize, easy for matrix matching, etc. It is inherently homogeneous. A simple solution pneumatic nebulization system coupled to the ICP generates a steady dc signal that allows straight forward multielement detection that is easy to integrate in order to improve detection limits and precision, and that can be handled comfortably with low end electronics and computers. It is no surprise then that most commercial ICP spectrometers use exclusively a solution sample as the final sample form and pneumatic nebulization as the standard sample introduction system.

However, the limitations of solution sample introduction are obvious and serious. The sample introduction step has been referred to as the ICP's "Achilles' heel" [6].

The poor efficiency (typically less than 3%) is perhaps the most important drawback of pneumatic nebulization. Put otherwise, 97% of a hard earned sample literally "goes down the drain" [7]. The consequences are large sample volumes and limited sensitivity.

Second, real world samples are complicated. They could be in any form. To be analyzed by ICP the samples have to be converted into solution form. However most samples are not readily convertible, such as soil samples, alloys, geological samples, ceramics, biological samples, etc. Sample dissolution is a challenging and tedious job even for an experienced chemist.



Furthermore, some undesirable consequences may inevitably occur during the sample conversion process. These are:

(1) Loss of speciation and phase distribution information. Such information is very important, for example, in evaluating the environmental impact of inorganic pollutants or in studying a catalyst [8]. In the analysis of inorganic pollutants, speciation can be very useful since the toxicity of many metals varies widely with chemical form; in a catalyst system it is important to know in what chemical forms the catalyst exists under active and passive conditions; the oxidation state and phase distributions of the component are very important in making high temperature superconductors. It is the form of the metal that determines its biological activity and environmental effects. A striking example is the case of chromium. Trivalent chromium is an essential element and yet extremely low levels of hexavalent chromium are known to be carcinogenic. This loss of information is attributed to both the need for dissolution and the fact that the ICP emission signal is representative of the total analyte concentration and is not directly responsive to speciation.

(2) Lost of homogeneity information. This information could be important for sampling studies and for understanding the history of the samples.

(3) Lost of analyte through formation of volatile compounds and precipitates. This situation is very common for the volatile elements such as As, Cd, Se, Pb, Ge, etc., if the digestion is needed at elevated temperature. Si will be lost if HF is used for dissolution.  $\text{Ti}^{4+}$ ,  $\text{Al}^{3+}$ ,  $\text{Si}^{4+}$ ,  $\text{Fe}^{3+}$ ,  $\text{Sn}^{4+}$ ,  $\text{La}^{3+}$ , etc., could be lost by hydrolysis during the sample dilution process if only limited information about the sample is available. Furthermore, trace elements in solution samples might be lost by adsorption on the wall of containers.

(4) Because of the low nebulization efficiency, a pneumatic sample introduction system usually needs at least 1 to 2 mL of sample. However, there is not always enough sample solution available for solution ICP. The amounts in clinical, archeological, and criminological samples are often very limited.

(5) Samples are destroyed. However, in many cases the samples need to be preserved, especially in such cases as space samples, fine art, archaeology samples, criminal evidence, etc.

(6) Dissolution dilutes the often already low concentrations of the analytical elements, lowering the power of detection. Samples are usually diluted by 10 to 100 times by reagent and solvent. This limitation becomes especially serious when the trace elements in high-purity solid samples are to be analyzed. The practical determinable concentration limit of ICP-AES for solid samples is therefore about 1-100 ppm in the original solid sample.

(7) Risk of contamination is inherent in sample dissolution. Contamination is possible from a number of places such as the chemical reagent used for dissolution, the lab environment, sample containers, or from the operator. The following elements are ubiquitous in laboratories: Al, Ca, Fe, Si, Zn, K, and Na, etc.; and restricting contamination from these elements is challenging. The fact that generally accepted background levels of trace elements in botanical, zoological, and clinical samples have been steadily decreasing in recent times is a testimony to improvements in contamination prevention [9]. Human hair that is a very good collector of dust is an important source of contamination. A subtle contamination/interference from water, acids and fusion reagents used for sample decomposition encountered in wet ICP-MS spectrometry arises from the formation of polyatomic species, such as oxides, chlorides and hydroxides leading to interference peaks in the mass spectra [10].

(8) It is essential to use high-purity chemicals throughout for trace metal analysis by wet ICP. However the high cost of ultra-pure reagents may be a problem for some laboratories. This is particularly true of acids that are required in relatively large amounts in trace metal analysis. Another potential cost may arise from the recovery or recycling of hazardous chemicals before they may be discharged into the environment.

In short, direct analysis of samples by ICP spectrometry without pre-treatment is extremely desirable.

## **1.2 Alternative sample introduction systems for ICP spectrometry**

Invaluable efforts have been made for finding alternative sample introduction technique for ICPs. Most of the alternative sample introduction techniques have been targeted on the direct analysis of samples, especially solid samples. These studies bring in more choice for ICP sample introduction systems, leading to increased sensitivity and making the ICP system applicable to the direct analysis of different samples. This may act to complement pneumatic nebulization. In regards to wide acceptance, none of these alternatives is as successful as pneumatic solution sampling systems. After having studied three different direct solid sample introduction techniques (i.e., spark ablation, DSI, slurry nebulization), Broekaert *et. al.* [11] concluded that in plasma spectrometry they cannot replace the analysis of dissolved samples as the universal procedure. For some special purposes, however, they offer an appropriate alternatives. They overcome some limitations and create others.

The following is a list of the main alternative sample introduction systems for ICP and they will be briefly reviewed.

- Spark and arc ablation
- Electrothermal Vaporization (ETV)
- Powder injection
- Slurry nebulization
- Vapor introduction
- Laser ablation (LA)
- Direct Sample Insertion (DSI)

In this work both laser ablation and DSI have been studied. New approaches are used to achieve the ultimate goal: Direct analysis of all the elements in different samples. The purpose of our studies is to make laser ablation and DSI more versatile direct sample introduction techniques for elemental analysis of a variety of samples. Encouraging results have been obtained.

### 1.2.1 Spark and arc ablation

A recent study by Ivanoic *et. al.* [12] shows that spark ablation ICP-MS provides comparable results to LA-ICP-MS (Laser Ablation ICP-MS) for conductive samples. Linear calibration curves for Cu alloys were obtained without need for any sort of concentration normalization or ratioing to an internal standard. The estimated detection limit was about 1 ppm. Compared to laser ablation, spark ablation is inexpensive, simple, and has better shot-to-shot reproducibility. A very low background in the mass spectrum after cessation of spark sampling was shown as evidence of a minimum memory effect. However their evidence illustrating the minimum memory effect was not convincing. Sparking a blank sample such as graphite rod should have been used to test for a memory effect.

The potential of an arc discharge as an aerosol generator was first demonstrated by Johnes *et. al.* [13]. Although it was made for a capillary arc plasma excitation source it can be readily coupled to an ICP. The use of spark ablation for direct vaporization of metal samples for ICP spectrometry was first described by Human *et. al.* [14]. A "segregated" discharge system was described by Coleman and coworkers [15, 16], which used spark sampling followed by re-excitation with a 200-MHz pulsed radio-frequency source. Reasonable linearity and detection limits were reported.

In general, the combination of spark sampling and ICP excitation results in improved detection limits and better calibration curve linearity when compared to direct spark

emission. As well the precision obtained is better than by laser ablation. This may be a consequence of the wobbling of the spark on the sample surface which results in an averaged sampling over a relatively larger area. From their experiments, Broekaert *et al.* [11] found that a high repetition rate with a medium-voltage is preferred for spark sampling, and the ablated particles from an aluminium alloy have the same composition as that of the bulk sample under such conditions. Accordingly, it can be understood that spark ablation ICP-AES is relatively free from interferences for a wide variety of aluminium alloys [17]. A matrix effect was observed when analyzing Al-Si samples containing more than 125 mg Si/g. This was explained by the fact that the larger particles stem from crystallites that are ablated but are only partially molten, and so have a different composition than the smaller particles.

Lemarchand *et al.* [18] used spark ablation for analysis of ferrous alloy by ICP-AES. Reasonable detection limits have been obtained (1 - 20 ppm for Cr, Mn, Ni, P, Si, V, and Mo). The results also show good precision (1% RSD) and small matrix effects. They suggest that it might even be possible to use the same calibration curves for carbon in cast and pig iron.

Probably the biggest limitation of spark sampling is that the sample has to be conductive. This limitation could, in some cases, be circumvented. For example, non conductive powder samples can be mixed with carbon powder and pressed into pellets for sparking [19].

The sensitivity of spark ablation ICP usually is inferior to the LA-ICP and direct sample insertion. Some sample preparation is necessary, such as pressing powder samples into pellets and surface polishing.

### 1.2.2 Electrothermal vaporization (ETV)

By coupling electrothermal vaporization (ETV) to ICP-AES, one potentially combines the advantages of both ETV and ICP, i.e., the small sample volume, high sampling efficiency of ETV's and the high atomization efficiency, low matrix effect, wide dynamic range and multielement capability of ICP-AES.

In 1974, Nixon, *et. al.* [20] described a tantalum filament-based electrothermal vaporization sampling system for ICP-AES. Detection limits for 16 elements were in the ng/mL to sub ng/mL range for 100  $\mu$ L samples, approaching those obtained by ETV-AAS while providing multielement capability at a single set of operation parameters. The advantages of the combination are very attractive. In addition, interelement interferences and background interferences encountered in ETV-AAS are minimized and linear calibration curves of four orders of magnitude (0.001 to 10  $\mu$ g/ mL) were also obtained. The method is most suitable for liquid samples of known matrix, but it also has been examined for solid samples [21, 22, 23] and suspended particulate matter [24]. Some interferences, such as spectral interferences from a complicated matrix can be minimized, in some cases, by controlling the temperature and adding a chemical modifier to make the vaporization process time resolved for different elements. Usually 10 to 100 times better detection limits can be achieved for volatile and moderately volatile elements compared to a pneumatic nebulization sampling system. For refractory and carbide forming elements, chemical modifiers are needed to facilitate efficient vaporization [21, 25, 26]. By using a PTFE slurry as a fluorinating reagent, promising results have been obtained for Zr, V, Cr, W, Mo, B, and Ti in an aqueous sample by Huang *et. al.* [26]. The detection limits for these refractory elements were in the pg to sub ng range. Kirkbright and Snook [25] added gaseous halocarbon ( $\text{CCl}_4$ , Freon 23) into an Ar carrier gas stream to promote the efficient vaporization of refractory

compound forming elements from an electrothermal vaporizer followed by the ICP-AES atomization. Very good analytical results were obtained.

The complexity in instrumentation and problems associated with the vaporization of refractory and carbide forming elements from solid samples seems to be an important drawback of the technique. Some sample preparation such as dissolution and grinding is needed for solid samples. Transport efficiencies are in the range of 30-70%, and change with chemical form of the element [27]. The use of a modifier is the only way to successfully evaporate all impurity elements when impurities in refractory powders containing elements in carbide form or carbide-forming elements are determined [21].

Recently, Karanassios and Bateman [28] reported an electronically heated wire-loop sample introduction system for the analysis of  $\mu\text{L}$  volumes of liquid samples for ICP-AES and ICP-MS. Excellent detection limits have been obtained for trace elements. For example, with ICP-MS, the detection limits for Pb and Zn were 12 fg and 4 fg. In this sample introduction system, the ends of a W wire loop are placed into two holes of a four-hole thermocouple ceramic insulator and are press-fit against cables capable of carrying electrical power. A 10- $\mu\text{L}$  sample is pipetted onto the loop, the sample is dried and then inserted into the central tube of a modified, Fassel-type torch. The top of the loop is positioned about 10 cm below the plasma and electrical power is applied to the loop for sample vaporization.

### **1.2.3 Powder injection**

The operating principle of the method is to transport the finer particles of a powdered sample into an ICP discharge using a flowing stream of Ar. Different injection methods have been proposed. Mechanical agitators [29], fluidized-bed [30], and spark [31] have been used to suspend the particles in the Ar stream. These approaches are intended to produce continuous and stable signals that can be handled by the commercial

spectrometers built for a solution nebulization system. Small amounts of samples (0.5 to 2.5 mg) have also been introduced into an ICP through a powder injection device [32], which generates a transient signal.

Guevremont and Desilva [30] designed a powder sample delivery system for ICP-AES. The sample is placed in a small vibrating vial that is advanced linearly toward an uptake capillary. With controlled, quantitative delivery of weighed samples to the plasma (total consumption) at an optimum powder flow rate, quantitative results were obtained.

To be analyzed by this method, the sample not only has to be matrix matched with standards but also has to be ground to the same or similar particle size distribution, because the transportation, vaporization and atomization efficiency are functions of matrix, size, density, and shape of the particles [33]. Standard addition and internal standardization can be used to minimize the matrix and particle size effects, but matching in the above mentioned aspects between standard and samples is rarely realized. Memory effects result when particles stick to surfaces in the transportation system. Finally, grinding the samples into accepted particle size (or size distribution) without introduction of contamination is not a trivial job.

#### **1.2.4 Slurry nebulization**

The introduction of slurry samples into an ICP has been implemented by pneumatic nebulization through a Babington type nebulizer. It will run clog free when large size particles are present as suspended matter in the sample solution. Requiring minimum changes in hardware and operating conditions from a conventional solution nebulization system is the important advantage of this technique. The technique is of considerable interest in the direct analysis of electrically non-conducting powders, such as  $\text{TiO}_2$  and  $\text{Al}_2\text{O}_3$ ,  $\text{AlN}$ ,  $\text{SiC}$ ,  $\text{Si}_3\text{N}_4$ , or  $\text{ZrO}_2$  as used for production of ceramics. Those types of



samples are usually already prepared as very small particle size powders and with a well-controlled size distribution; yet present challenges for dissolution methods.

The analytical performance of slurry nebulization depends especially on

- the ability to keep and transport the analyte in the form of a suspension.
- the evaporation of such particles in an analytical plasma discharge [11].

Solution standards have been used to calibrate slurry samples of ultra-fine  $\text{ZrO}_2$  powders used for the production of ceramics. Because of the different vaporization efficiencies experienced by the slurry and the solution, a correction coefficient must be applied [34]. The correction coefficient is only applicable to samples of the same matrix and particle size distribution because the vaporization efficiency is strongly dependent on the particle size and matrix. Therefore the samples that have been successfully run by this technique are very limited.

By adding 7.5%  $\text{H}_2$  to the injection gas, Ebdon and Goodall [35] were able to improve the vaporization efficiency of the plasma for refractory slurry samples (firebrick). This ability to decompose refractory particles was correlated to the higher rotational temperatures of the plasma. This increase in temperature from 2200 to 3900 K was attributed to increased energy transfer from the toroid to the annular region of the ICP because of the higher thermal conductivity of hydrogen compared to argon.

However, overall, slurry nebulization lacks versatility in handling different sample forms and extensive sample preparation may be involved. The nebulization /transportation efficiency and vaporization/excitation efficiency are strongly dependent on the particle size and its distribution [36].

### **1.2.5 Vapor introduction**

This technique involves chemical reaction of samples with some reagents that can generate volatile analyte compounds. The analyte vapor produced by the reaction is then

carried into the ICP for excitation/ionization. Vapor introduction techniques are well established in AAS for the determination of elements such as As, Sb, Se, Te, Ge, Sn, Bi, Pb, etc., by forming volatile hydrides. This method has also been applied to ICP-AES with great success [37, 38]. Vapor introduction offers several advantages over conventional liquid sample introduction; it gives a transportation efficiency approaching 100% and it offers the possibility of pre-concentration. Therefore excellent detection limits can be achieved. Elimination of matrix effects is possible by selectively vaporizing the analyte. Black and Browner [39] have shown that some transition elements such as Fe, Zn, Co, Cr, and Mn can be converted into volatile metal chelates at elevated temperatures with  $\beta$ -diketone ligand (trifluoroacetylacetone and hexafluoroacetylacetone). The generated metal-chelate is then swept as a plug into an ICP with an Ar carrier gas for atomic emission analysis. Direct determination of Fe, Zn, and Cr in bovine liver and blood serum were achieved with improved sensitivity.

However, loading a large amount of foreign gas into an ICP through the central tube may disturb, if not extinguish, the plasma. The applicability of this technique is practically limited to a small range of hydride forming elements (i.e., As, Se, Sb, Sn, Bi, Pb, Ge, Te), and samples usually have to be in solution form for complete reaction.

### 1.2.6 Laser ablation

Reviews have been published for laser ablation sample introduction for both ICP-AES and ICP-MS [40] and for laser microanalysis [41] by Moenke-Blankenburg. A detailed discussion of laser ablation will be presented in Part II of the thesis: *in situ* laser ablation for ICP. The advantages and disadvantages of the technique are summarized as follows:

Pros of laser ablation

- For solid samples, both electrically conducting and non-conducting

- Virtually no sample pre-treatment
- Very small sample consumption (in the range of ng to  $\mu\text{g}$ ) while providing good sensitivity,
- Small sampling area, spatially resolved analysis capability

Cons of the conventional LA-ICP setup:

- Memory effects
- Particle size dependent transportation efficiency and particle size dependent concentration distribution make accurate quantitation difficult
- Dilution effect, i.e., the ablated sample particles are diluted (band broadened) by the large volume of the ablation chamber and transportation system due to diffusion. Therefore the sensitivity is deteriorated.

### 1.2.7 DSI

Several of the solid sample introduction techniques suffer from a common problem, that is, the vaporization and atomization efficiency is strongly particle size and matrix dependent. Large particles ( $>10\ \mu\text{m}$ ) and particles of refractory materials may experience incomplete vaporization due to the short residence time of particles in the plasma ( $\sim\text{ms}$ ). The direct sample insertion (DSI) technique developed by Salin and Horlick in 1979 [42] remedies this problem by placing a sample probe inside the plasma. A schematic diagram for a generic DSI device is shown in Figure 1.1. The operation of the system is as follows:  $\mu\text{L}$ 's of solution or mg's of solid sample is added to a sample probe (mostly a graphite cup). The sample probe is then driven into the core of the ICP by an insertion mechanism. The sample is then vaporized, atomized, excited and ionized. A drying and/or ashing step may be needed, depending on the type of sample. Figure 1.1a shows the sample probe in the home position while in Figure 1.1b the sample probe is inside the plasma.

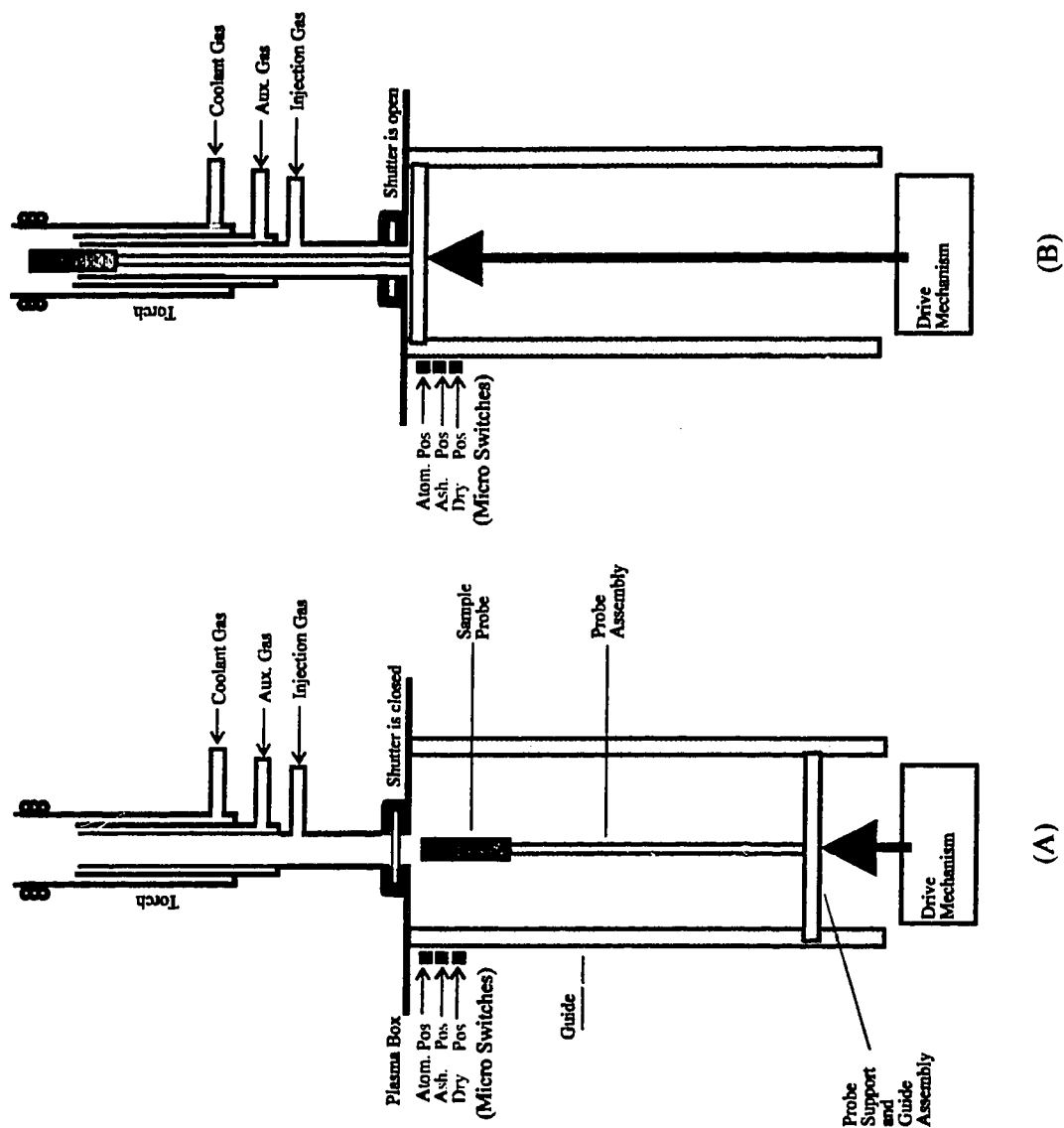


Figure 1.1 Schematic diagram of a generic DSI-ICP device

Karanassios and Horlick [7] have thoroughly reviewed this area up until 1991. The information was tabulated for convenient reference, including instrumentation, operating parameters, applications, and important analytical figures of merit.

The following is a summary of DSI-ICP applications and some important analytical figures of merit.

#### **1.2.7.1 Applications**

The DSI-ICP technique has great potential for the direct analysis of small amounts (~10  $\mu\text{L}$  or sub mg) of a wide variety of samples (solution, fluid, slurry, oil, solid (both conductive and non-conductive)). The sample can be inorganic, organic and/or biological.

Determinations of volatile elements in aqueous and botanical samples have proven to be quite successful. However the analysis of refractory and carbide forming elements and samples of refractory matrix still present challenging tasks. Chemical modifiers have been used with some success.

A subtle advantage that DSI-ICP may offer is that some matrix effects and spectral interferences may be minimized by selective volatilization if the melting and boiling points of an interfering component and analyte are different enough.

Recently, Blain and Salin [43, 44, 45] have studied the analysis of elements (both volatile and refractory) in solid sediment reference materials of complicated matrices. By choosing proper chemical modifiers and with the help of internal standardization and standard addition reasonable results were obtained.

### 1.2.7.2 Detection limits

Of all sample introduction techniques for ICP-spectrometry, direct sample insertion has the highest analyte introduction efficiency. Accordingly, it should enable the highest absolute power of detection [11]. This has already been extensively shown for dry solution residues [46-49]. For volatile elements such as Zn and Cd, detection limits are in the pg range for a 10- $\mu$ L solution sample [50]. Sing and Salin [51] reported picogram to sub-picogram detection limits for the elements studied by using a metal wire loop as a carrier for a solution residue sample. Zaray *et. al.* [52], in analyzing trace elements in  $\text{Al}_2\text{O}_3$  by DSI-ICP-AES, reported that relatively volatile elements such as Cd, Cu, Mg and Zn could be vaporized and detected down to the  $\mu\text{g/g}$  level. For titanium, which forms refractory carbides, with addition of PTFE, quantitative determinations are possible and a detection limit of 7  $\mu\text{g/g}$  was obtained. Detection limits of 0.004-0.08 ppm based on a 5-mg sample were obtained in analyzing volatile elements in Ni-based samples [53]. The detection limits for various elements in a 1-mg hair sample ranged from 0.2 to 10 ppm in the solid form [54]. Salin *et. al.* [55, 56] used a W wire loop as sample carrier to deliver 10- $\mu$ L desolvated samples for DSI-ICP analysis and found that for ICP-MS [55] detection limits are one order of magnitude lower than obtained using conventional nebulization. For ICP-AES [56], detection limits of 0.2 and 0.08 ppb for Cu and Zn, corresponding to absolute detection limits of  $2 \times 10^{-12}$  and  $0.8 \times 10^{-12}$  g, were obtained. Sub-ppm detection limits were typical for elements of high and intermediate volatility in sediment standards [44].

Detection limits can be further improved by pre-concentration methods followed by direct sample insertion. By coupling a flow injection (FI) pre-concentration system with a DSI-ICP-AES, Moss and Salin [57] claimed a 140 to 1200 times improvement in detection limit for the elements tested (Cu, Pb, and Zn) as compared to conventional nebulization. Zaray *et. al.* [58] used a cellulose collector for adsorbing and separating

trace elements followed by direct sample insertion to ICP. The detection limits of the elements investigated ranged from 4 to 150 ng/g. Habib and Salin [59] described a separation and pre-concentration technique for DSI-ICP-AES by using controlled potential electrolysis with both graphite electrodes and a hanging Hg drop electrode. Heavy metal ions in aqueous solution were determined. With a deposition time of 5 minutes the detection limits under compromised conditions are 2.4, 680, 2.0, 175, 25, and 259 ng/mL for Cu, Pb, Zn, Cd, Ni, and Co, respectively. A determination of Cu at the 63 ng/mL level in artificial sea water (3.5% salinity) was made with a 4% error.

The detection limits for DSI-ICP-AES are summarized as follows,

1. Volatile and moderately volatile elements in solution residues are in the range of ppb to sub ppb, or 10 pg to sub pg in absolute weight with a 10- $\mu$ L sample loading.
2. Volatile and moderately volatile elements in solid samples ranged in about ppm to sub ppm levels or sub ng absolute detection limits for about 1 mg sample loads. The matrix will also affect the detection limit.
3. For involatile elements and refractory samples chemical modifiers are necessary.
4. Pre-concentration techniques such as electrochemical deposition, cellulose collectors, etc., followed by direct sample insertion can significantly improve detection limits.
5. Detection limits for DSI-ICP-MS usually are 1 to 2 orders of magnitude better.

Detection limit data varies significantly with author and instrumentation, and it is felt that the data cited above are conservative. Recently, Rattray *et. al.* [60] have conducted experiments with rapid liquid sample drying in DSI cups and in electrothermal vaporizer (ETV) tubes. Inductive drying of the DSI cup has proven to be effective for maintaining cleanliness. The solvent is removed and the concentrated sample is then analyzed by DSI-ICP-AES. DSI drying rates of 0.25 mL/min have been achieved, providing detection limit improvements for ICP-AES of greater than 500 in less than three minutes.

### 1.2.7.3 Quantitation

For quantitative analysis the peak area method is preferred over peak height measurement, because peak height is more prone to alteration owing to variations in vaporization efficiency, which is dependent on sample matrix, size, and the probe's surface condition.

Calibration curves and quantitative results are good for volatile elements in solution residues, such as Zn, Cd, Pb, Ag, Mn, Cu, etc. A linear dynamic range of four orders of magnitude seems typical. For involatile and refractory solid powder samples, chemical modifiers are necessary for quantitative vaporization. Standard addition methods have proven to be effective for quantitation with DSI-ICP.

The precision of DSI-ICP is poorer than solution nebulization and spark ablation sampling. The typical precision of DSI-ICP is usually in the range of 3% to 15% RSD, with 5% being normal for solution residues with a 10- $\mu$ L sample load. Larger RSD values may be experienced with solid samples. The somewhat elevated precision values of the technique may be attributed to several facts. First, because small amounts of samples are used the errors from measuring and transferring these samples may be large. Second, sampling errors inherent in dealing with inhomogeneous samples may be serious because of the small amount of samples utilized. For some botanical samples, it is difficult to make homogeneous standards such as wheat flour. In such cases the sampling error may become dominant. On the other side of the coin, the problem can be used for studying sample homogeneity and the DSI-ICP has proven to be very powerful for such studies [61]. Third, the surface conditions of the sample probe plays an important role in affecting the precision, e.g., when a graphite cup is used as the sample probe, the surface porosity of the graphite cup can vary from cup to cup. Analyte trapped in deeper holes will be more difficult to vaporize and have a greater chance to form a carbide. Pyrolytic and surface coated graphite cups may help to remedy this problem.



### 1.2.8 Limitations of DSI and the scope of this research

The advantages that DSI-ICP may offer are attractive. There is however no commercial DSI-ICP system available. Pneumatic nebulization sampling systems still dominate the ICP realm even though people have been complaining about tedious sample treatment procedures, expensive chemicals, contamination, dilution problems, analyte loss during conversion of solid samples into solution form, the low sampling efficiency, etc.

There are deficiencies with current DSI-ICP techniques. A major criticism leveled against DSI-ICP is that it is too restricted in the limited range of elements and sample matrices it can handle. Quantitation for some elements and samples by DSI-ICP is still a challenging task. These elements and samples include: (1) elements with high boiling points (e.g., W, Mo, Zr); (2) elements forming refractory carbide (e.g., V, Ba, Ca) and; (3) elements in refractory solid samples (e.g.,  $ZrO_2$ ,  $Al_2O_3$ ).

Therefore, to fulfill its great potential it is important for a DSI-ICP system to be capable of determining elements in all sample forms, especially solid samples.

It seems the major problem with DSI-ICP is associated with the sample vaporization step. Some elements tend to form carbides. If a graphite cup is used as a carrier, and some refractory elements such as V, Ni, Zr, Mo, W, etc., are only partially vaporized, the performance of DSI is deteriorated. This is because the gas temperature of the ICP is not high enough to vaporize all the elements in a given time. The temperature of a DSI probe in an ICP measured by different methods [8, 62-64] is about 2000 °C. Chan and Horlick [65] have carried out an interesting analysis and calculation of power requirements in ICP-DSI process, and found that only a relatively small fraction (~ 100 watts out of 1500 watts) of the applied power actually was used to heat up the sample probe.

Fortunately, plenty of ideas and prior knowledge can be borrowed from the dc arc and thermal atomization literature. The use of different chemical modifiers opens a new dimension for overcoming this problem. Different halides have been used to speed up the vaporization of elements from solution residue samples [66], powdered samples [67] and geological standard samples [43]. By mixing PTFE powder with solid powdered samples, calibration curves for nonvolatile elements such as Ti in  $\text{Al}_2\text{O}_3$  standard samples has been obtained [52]. However chemical modifiers may introduce extra interferences or contamination and as well cause plasma instabilities and even extinguish the plasma, if too much gas vapor is generated in a short time. Chemical modifiers typically are not suitable for chip and block sample forms, and the grinding of samples into fine powders may introduce contamination. Unfortunately "a successful determination of carbide-forming elements (although in an oxide-matrix) without the help from thermochemical substances has not been reported until now" [21].

An increase in ICP temperature by increasing the incident power may help improve the vaporization capability, however such a change is limited by the RF generator and is often offset by the increased cooling gas.

Changing gas composition of the plasma may improve the vaporization capability of the plasma through increasing energy density (e.g., the effect of ~ 5% diatomic gas). Most importantly, the vaporization mechanism may be changed through changing the plasma gas composition (e.g., the effect of ~20%  $\text{O}_2$  in plasma).

The first part of this thesis is focused on studies of the effect of different gas compositions and ICP power on the signals of some representative elements, from volatile to nonvolatile and carbide forming elements. Analytical results for the analysis of solution residue samples by Ar- $\text{N}_2$  mixed gas DSI-ICP-AES will be given and discussed. Then an Ar- $\text{O}_2$  mixed gas DSI-ICP-AES is investigated for the direct analysis of solid powder samples with a refractory matrix, oil samples, Al chip sample, food samples.

## References

1. S. Greenfield, I. L. Jones and C. T. Berry, *Analyst*, 89, 713, (1964)
2. R. H. Wendt and V. A. Fassel, *Anal. Chem.*, 37, 920, (1965)
3. G. W. Dickinson and V. A. Fassel, *Anal. Chem.*, 41, 1021, (1969)
4. P. W. J. M. Boumans and F. J. De Boer, *Spectrochim. Acta*, 27b, 391, (1972)
5. R. H. Scott, V. A. Fassel, R. N. Kniseley and D. E. Nixon, *Anal. Chem.*, 46, 75, (1974)
6. R. F. Browner and A. W. Boorn, *Anal. Chem.*, 56, 785a (1984)
7. V. Karanassios and G. Horlick, *Spectrochim. Acta Rev.* 13, 2, 88 (1990)
8. E. R. Prack and G. J. Bastiaans, *Anal. Chem.* 55, 1654 (1983)
9. J. C. Van Loon, "Selected Methods of trace metal analysis: Biological and environmental samples", A Wiley-Interscience Publication, John Wiley & Sons, 1985
10. V. Karanassios and G. Horlick, *Spectrochim. Acta* 44B, 1361 (1989).
11. J. A. C. Broekaert, F. Leis, B. Raeymaekers and Gy. Zaray, *Spectrochim. Acta* 43B, 339 (1988)
12. K. A. Ivanovic, D. M. Coleman, F. W. Kunz, and D. Schuetzle, *Appl. Spectrosc.* 46 (6), 894 (1992)
13. J. L. Johnes, R. L. Dahlquist and R. E. Hoyt, *Appl. Spectrosc.* 25, 628 (1971)
14. H. G. Human, R. H. Scott, A. R. Oakes, and C. D. West, *Analyst* 101, 265 (1976)
15. D. M. Coleman, M. A. Sainz, and H. T. Butler, *Anal. Chem.* 52, 746 (1980)
16. M. A. Sainz and D. M. Coleman, *Appl. Spectrosc.* 43, 553 (1989)
17. A. Aziz, J. A. C. Broekaert, K. Laqua and I. Leis, *Spectrochim. Acta* 39b, 1091 (1984)
18. A. Lemarchand, G. Labarraque, P. Masson and J. A. C. Broekaert, *J. Anal. At. Spectrom.*, 2(5), 481 (1987)
19. P. M. Beckwith, R. L. Mullins, and D. M. Coleman, *Anal. Chem.* 59, 163 (1987)
20. D. E. Nixon, V. A. Fassel, and R. N. Kniseley, *Anal. Chem.* 46, 210 (1974)

21. H. Nickel, Z. Zadgordka and G. Wolff, *Spectrochim. Acta* 48B, 25 (1993)
22. D. R. Hull and G. Horlick, *Spectrochim. Acta* 39b, 843 (1984)
23. W. M. Blakemore, P. H. Casey, and W. R. Collie, *Anal. Chem.* 56, 1376 (1984)
24. A. Sugimae and R. Barnes, *Anal. Chem.*, 58, 785 (1986)
25. G. F. Kirkbright and R.D. Snook, *Anal. Chem.*, 51, 1938 (1979)
26. M. Huang, Z. C. Jiang and Yun'e Zeng, *J. of Anal. At. Spectrom.*, 6, 3, 221 (1991)
27. S. M. Schmertmann, S. E. Long and R. F. Browner, *J. Anal. At. Spectrom.*, 2, 687 (1987)
28. V. Karanassios, K. Bateman, 1994 Winter Conf. Plasma Spectrochemistry, San Diego, Paper M6 (1994)
29. H. C. Hoare and R. A. Mostyn, *Anal. Chem.* 39, 1153 (1967)
30. R. Guevremont and K. N. De Silva, *Spectrochim. Acta*, 47b, 371 (1992)
31. R. H. Scott, *Spectrochim. Acta* 33b, 123 (1978)
32. K. C. Ng, M. Zerezghi and J. A. Caruso, *Anal. Chem.* 56, 417 (1984)
33. R. Guevremont and K. N. De Silva, *Spectrochim. Acta* 46b, 1149 (1991)
34. M. Huang and X. E. Shen, *Spectrochim. Acta* 44b, 957 (1989)
35. L. Ebdon and P. Goodall, *J. Anal. At. Spectrom.*, 7, 1111 (1992)
36. B. Raeymaekers, T. Graule, J. A. C. Broekaert, F. Adams and P. Tschopel, *Spectrochim. Acta*, 43B, 923 (1988)
37. M. Thompson, B. Pahlavenpour, S. J. Watson and G. F. Kirkbright, *Analyst* (Lodon) 103, 568 (1978)
38. M. H. Hahn, K. A. Wolnik, F. L. Fricke and J. A. Caruso, *Anal. Chem.*, 54, 1048 (1982)
39. M. S. Black and R. F. Browner, *Anal. Chem.* 53, 249 (1981)
40. L. Moenke-Blankenburg, *Spectrochim. Acta Rev.* 15(1), 1 (1993)
41. L. Moenke-Blankenburg, *Prog. analyst. Spectrosc.* 2, 335-427 (1986)
42. E. D. Salin and G. Horlick, *Anal. Chem.* 51, 2284 (1979)

43. L. Blain and E. D. Salin, *Spectrochim. Acta* 47B, 399 (1992)
44. L. Blain and E. D. Salin, *Spectrochim. Acta* 47B (2), 205-17 (1992).
45. L. Blain and E. D. Salin, *Spectrochim. Acta* 47B, 1471 (1992)
46. D. Sommer and K. Ohls, *Fresenius Z. Anal. Chem.* 304, 97 (1980)
47. G. F. Kirkbright and S. J. Walton, *Analyst* 107, 276 (1982)
48. G. F. Kirkbright and L. X. Zhang, *Analyst* 107, 617 (1982)
49. L. X. Zhang, G. F. Kirkbright, M. J. Cope and J. M. Watson, *Appl. Spectrosc.* 37, 250 (1983)
50. W. T. Chan and G. Horlick, *Appl. Spectrosc.* 44, 380 (1990)
51. R. L. A. Sing and E. D. Salin, *Anal. Chem.*, 61 (2), 163-9 (1989)
52. Gy. Zaray, J. A. C. Broekaert and F. Leis, *Spectrochim. Acta* 43B, 241 (1988)
53. C. W. McLeod, P. A. Clarke, and D. J. Morthorpe, *Spectrochim. Acta* 41B, 63 (1986)
54. C. V. Monasterios, A. M. Jones and E. D. Salin, *Anal. Chem.*, 58 (4), 780-5 (1986)
55. D. W. Boomer, M. Powell, R. L. A. Sing and E. D. Salin, *Anal. Chem.*, 58 (4), 975-6 (1986)
56. E. D. Salin and R. L. A. Sing, *Anal. Chem.* 56, 2596 (1984)
57. P. Moss and E. D. Salin *Appl. Spectrosc.*, 45 (10), 1581 (1991)
58. Gy. Zaray, P. Puba, J. A. C. Broekaert and F. Leis, *Spectrochim. Acta* 43B, 255 (1988)
59. M. M. Habib and E. D. Salin, *Anal. Chem.*, 57 (11), 2055-9 (1985)
60. R. Ratteray, J.-F. Alay, and E. D. Salin, 1994 Winter Conf. Plasma Spectrochemistry, San Diego, Paper TP27 (1994)
61. L. S. Ying, X. R. Liu, B. Kratochvil and G. Horlick, "Determination of Trace Elements Agriculture Materials By Direct Sample Insertion Inductively Coupled Plasma Atomic Emission Spectrometry", in preparation.
62. N. W. Barnett, M. J. Cope, G. F. Kirkbright and A. A. H. Taobi, *Spectrochim. Acta* 39B, 343 (1984)

63. A. G. Page, S. V. Godbole, K. H. Madraswala, M. J. Kulkapni, V. S. Mallapurkar and B. D. Joshi, *Spectrochim. Acta* 39B, 551 (1984)
64. A. Lorbe and Z. Goldbart, *Analyst* 110, 155 (1985)
65. W. T. Chan, Ph.D. Thesis, University of Alberta (1989)
66. V. Karanassios, M. Abdullah and G. Horlick, *Spectrochim. Acta* 45B, 119 (1990)
67. Y. B. Shao and G. Horlick, *Appl. Spectrosc.* 40, 386 (1986)

## Chapter 2

### Mixed Gas Direct Sample Insertion System

#### 2.1 Introduction

Atmospheric pressure ICPs of different gas compositions (pure Ar, Ar-O<sub>2</sub>(50%), Ar-He(20%), Ar-H<sub>2</sub>(20%), Ar-air (20%)) were first formed and studied by Reed in 1961 [1]. Reed found that argon is the simplest gas in which to start and operate the plasma, due probably to its low heat capacity at its ionizing temperature and due to its poor thermal conductivity. With mixed gases, it was found that the plasma contracts and the power consumption increases. Reed did report [2] that diatomic gas and helium containing plasmas were more effective for growing crystals of highly refractory oxides such as ZrO<sub>2</sub>, because they provide higher heat transfer than a pure Ar plasma.

The effect of gas composition on analytical ICPs was first studied by Greenfield and coworkers [3, 4]. It was found that the emission intensity decreased in order Ar > N<sub>2</sub> > air > O<sub>2</sub> when these gases were used in the central gas. The emission intensity decreased in the order, Ar-N<sub>2</sub> > Ar-O<sub>2</sub> > He > Ar when these gases were used in outer gas. These early ICPs operated by Greenfield and his coworkers were operated at low RF frequency (7 MHz), high power (10 kW) and high gas flow rate (64 l/min. N<sub>2</sub> coolant and 15 l/min. Ar outer gas, 1.5 to 3 l/min. Ar carrier gas). They were costly to operate and did not show important gains in analytical performance compared to all Ar supported ICPs. Therefore the mixed gas plasma obtained only limited recognition. Unfortunately, it also became a general belief that mixed gas plasmas could only be operated at substantially higher power than conventional argon plasmas.

Operation of mixed gas ICPs at low power (i.e., 1-2 kW power) was reported by Truitt and Ronbinson [5, 6] in 1970. By the late 1970s several other workers had

reported studies of mixed gas ICPs [7-10] with flow rates and powers associated with standard argon ICPs. Recently, Tang *et. al.* [11] used a low power, 50% air-Ar ICP for the determination of metallic elements in waste oil diluted with xylene and nickel naphthenate diluted with MIBK. The molecular bands characteristic of organic samples such as CN and C<sub>2</sub> are largely depressed or even eliminated with air-Ar mixed gas ICPs and no carbon deposition problem was found. The detection limits for most elements tested in MIBK were 2 to 8 times better with the mixed gas ICP than those obtained with a 100% Ar ICP. Meyer and Barnes described the operation of air and nitrogen ICPs as well as their use in spectrochemical analyses of aqueous solutions and fine powders [12]. Meyer and Thompson have also measured the detection limits for 19 elements in air and O<sub>2</sub> ICPs [13]. Choot and Horlick systematically studied the spectral characteristics and analytical performance of different mixed gas ICP's [14-17] such as Ar-N<sub>2</sub>, Ar-O<sub>2</sub>, Ar-Air, and Ar-He. The developments of analytical molecular gas and mixed gas ICPs have been reviewed by Montaser *et. al.* [18]. Some mixed gas ICP studies have been focused on the effect of foreign gas on the electron density, spectral pattern, temperature, and interferences of oxides in ICP mass spectrometry, etc.; and it was found, in most cases, best results were obtained with 1- 10 % N<sub>2</sub> in the outer gas for typical ICP operating conditions (i.e., 1- 2 kW, 12-15 L/minute).

A driving force for using molecular or mixed gas ICPs with solution nebulization is to cut the operating cost of pure Ar ICPs and to improve the ICP performance. The major impact of mixed gas and molecular gas ICPs is their superior ability to decompose refractory particles and to operate with higher solvent and analyte loading compared to an Ar ICP. It has been noticed that when diatomic gases are added into the outer gas flow of an Ar ICP the plasma becomes brighter and the axial channel and the apparent luminous volume of the plasma are reduced. The reduction in axial channel diameter enhances sample-plasma interaction, thereby reducing possible solute vaporization



interference effects [16, 18]. As the plasma's volume becomes smaller the energy density of the plasma becomes higher provided the ICP's power is the same [19].

These features of mixed gas ICPs could be very important from the direct sample insertion point of view, because, as discussed in 1.2.8, *the major limitation of DSI-ICP is the limited vaporization capability for refractory elements and samples due to the limited temperature that the probe attains in the Ar plasma.* In addition to the higher energy density of a mixed gas plasma the higher thermal conductivity of diatomic gases such as N<sub>2</sub> may also help to transfer the energy from the plasma to the sample probe more efficiently [20]. Therefore the Ar-mixed gas plasma might provide a higher gas temperature that could be critical in facilitating the vaporization of nonvolatile elements from the DSI probe.

A N<sub>2</sub> mixed gas DSI-ICP system was first studied by Sommer and Ohls [21] with a Greenfield type torch at high power. There are only a few [22] studies of the effect of gas composition on the vaporization process in DSI-ICPs. Kirkbright and Zhang [23] used an Ar-0.1% Freon 23 gas mixture as the central gas to facilitate the volatilization of U, Zr, Ti, Mo, B, Cr, Zn, Ag, and Cu from a direct sample insertion device. Improvements were obtained in the detection limits of U, Zr, and Ti. High power Ar-N<sub>2</sub> mixed gas ICPs were used by Broekaert *et. al.* [24-26] for direct sample insertion. Chlorine/argon mixtures were used as the injection gas by Matousek, Satumba and Bootes [27] to enhance the vaporization of involatile elements in their ETV-ICP. The chlorine/argon mixture was passed through an electrothermal vaporization system suitable for work with corrosive atmospheres. Elements such as Cr, V, Ti, W and Zr were converted to volatile chlorides by use of the chlorine/argon mixture. Detection limits calculated from background-corrected peak heights were comparable to those obtained in a halocarbon atmosphere and ranged between 0.006 and 0.07 ng for the elements of interest.

Pettit and Horlick [22] studied the effect of Ar-O<sub>2</sub> and Ar-H<sub>2</sub> mixed gas ICPs on signal temporal behavior with their automatic DSI-ICP-AES system using a pneumatically activated transport system. The purpose of adding 1% H<sub>2</sub> to the outer gas was mainly to prevent the metal cups that were used as sample probes from deteriorating in the plasma. By adding small amounts of O<sub>2</sub> (i.e., 0.5% to 6%) to the outer gas the signals become sharper and stronger for all the elements tested (from volatile, (In, Cd, Zn) to moderately volatile, (Mn) to carbide forming elements, (Ni)).

In this chapter results are presented for a study of different mixed gas DSI-ICPs with a small percentage of foreign gas (<10%) in comparison with the pure Ar ICP. Following, in Chapter 3, the Ar-O<sub>2</sub> (20%) mixed gas DSI-ICP is studied for the analysis of a wide variety of samples.

## **2.2 System descriptions**

### **2.2.1 Hardware**

#### **2.2.1.1 The DSI-ICP-AES setups**

A schematic diagram of the DSI-ICP-AES system is shown in Figure 2.1. The nebulizer/spray chamber found in the conventional ICP system was replaced by the sample probe delivery mechanism of a DSI-ICP system. The ICP system and spectrometer are those described by Karanassios and Horlick [28], and the readout electronics and the DSI subsystem (the torch, stepper motor, and probe driving mechanism) are those described by Horlick *et. al.* [29-31]. The system is modified so that both the stepper motor and data acquisition can be controlled by an 8088 based IBM PC computer through a PCMotion™ motor control board and a DT2801-A data acquisition board that are plugged in the 8088 IBM PC expansion slot. The stepper

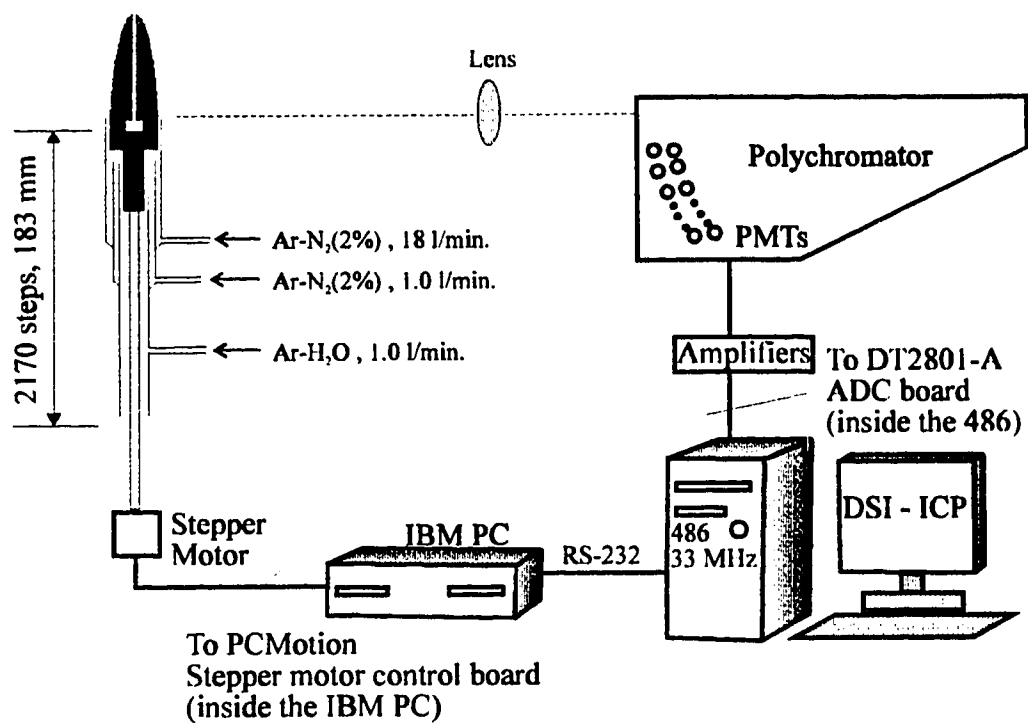


Figure 2.1 Schematic diagram of an  $\text{Ar-N}_2$  (2%) mixed gas Direct Sample Insertion System for Inductively Coupled Plasma Atomic Emission Spectrometry (DSI-ICP-AES)

motor control board can control up to four motors simultaneously, which leaves enough room for developing an automatic sampling DSI system. For example a sampling carousel could be driven by another stepper motor to achieve automatic sample change over. The readout electronics of the DSI system were built in this lab by Chan and Horlick [30]. The signals from amplifiers are now routed into a data acquisition board, DT2801-A. Up to 8 channels can be connected to the board's ADC differential input, although only 6 channels have been used. One of the disadvantages of the amplifiers is the inconvenience in changing gain. To change the gain, the resistance in the amplifier's feedback has to be changed manually. Because of the limited dynamic range of the ADC board (12 bit) the gain needed to be changed very often during the analysis of samples with a wide concentration range. Because of the transient nature of the DSI-ICP signal, it would be desirable to have fast amplifiers with programmable gain control. The amplifier's speed is especially important for *in situ* laser ablation ICP-AES as will be discussed later. There is a programmable gain amplifier on the ADC board but it only allows for limited ranges (2, 4, and 8 times). The hardware components and some system parameters are listed in Table 2.1.

This system was modified so that it could be controlled with an Intel 80486 based IBM compatible PC running at 33 MHz. The data acquisition card, DT2801-A, is now plugged into the 486 computer. However, there was a problem with the stepper motor control card. When it was plugged into the 486 computer, the computer crashed when it tried to run the stepper motor. This very likely arose from a memory conflict with the motor driving routine program. Because no source code was available for the stepper motor driving subroutine it was difficult to figure out this problem. Instead of struggling to make the card work in the 486 computer, we just simply left the stepper motor driving card in the 8088 IBM PC and controlled the old IBM PC by the 486 computer through the serial port (see Figure 2.1). An auto executive program was written for the old IBM PC. Once the computer (no keyboard and monitor are needed) is turned on the auto

Table 2.1. Hardware specification and typical operating conditions for the Ar-O<sub>2</sub> and Ar-N<sub>2</sub> mix gas ICP-DSI system.

ICP	Plasma Therm ICP 5000
ICP generator	HFS-5000D; 27.12 MHz; Max power, 5.5 kW
ICP typical operating conditions	Forward power 1.8 kW; reflected power < 30 w obs. height, 14 mm above load coil
Oxygen mix gas:	Outer gas, 18 l/min. with 20% O <sub>2</sub> in Ar; intermediate gas, 1 l/min. with 20% O <sub>2</sub> in Ar; central gas, 2 l/min. with water vapor obs.
Nitrogen mix gas:	Outer gas 18 l/min. with 2% N <sub>2</sub> in Ar; intermediate gas, 1 l/min. with 2% N <sub>2</sub> in Ar; central gas, 2 l/min. with water vapor
Spectrometer	A 1-m, Pachern-Runge mount, 29-channel direct reader with a 1200 groove/mm concave grating.
DSI system	The DSI device has been described in detail in references 1 and 5. No major modifications were made except it is controlled by an IBM PC computer instead of Apple II+
DSI probe	Graphite electrodes with different size and shape were used (see text for discussion). SPEX Industries, Inc., Edison, NJ or Bay Carbon, Inc., Bay City, MI
Stepper motor control board	PCMotion™ (Rogers Labs, 2727-E SO. Croddy Way, SANTA ANA, CA 92704) for IBM PC.
Data acquisition	DT2801-A (Data Translation, Inc., 100 Locke Drive, Marlborough, MA 01752-1192 USA) with a 12-bit ADC.
System computer	IBM compatible 486/33 MHz with 8 MB RAM, DOS 6.0 and Windows 3.1

executive program loads the motor driver routine into its memory and waits for the 486 computer to send commands and parameters for running the stepper motor. The main DSI program runs from the 486 computer and when it needs to insert or withdraw the sample probes it sends the parameters for the stepper motor, such as ash time and position, atomization time and position, etc., to the old IBM computer. Once the old IBM computer receives these data, it runs the stepper motor according to the parameters. The old IBM computer could be slaved to the 486 computer but could also be a stand alone system with stepper motor driving capability. Such a system works smoothly and later, it was found that this system provides extra flexibility. There is another direct sample insertion project for ICP-MS going on presently in the lab. This stand alone stepper motor driver module (the IBM PC with the stepper motor driving card) can be plugged/unplugged and carried around conveniently and shared by the different direct sample insertion systems. With the fast development of computer technology, yesterday's breathtaking computers are quickly becoming historical footnotes. But they still find use as intelligent instrumental control units for some specific tasks.

The gas compositions used in the normal analyses are indicated on Figure 2.1. The foreign gases are introduced into the intermediate and outer gas. The central gas is water vapor saturated Ar. The plasma would be extinguished or unstable if too much molecular gas was introduced into the central gas.

#### **2.2.1.2 The sample insertion mechanism**

The sample insertion driving system is an important component of a DSI-ICP system. It requires fast insertion, and flexible and precise control in speed, timing, and positioning. These requirements are obvious. A fast insertion speed produces sharp signals and better precision for volatile elements, thus improving analytical performance [30, 32, 33]. Precise control in timing, speed, and positioning is essential for

reproducible analytical results. While flexible programming for timing and positions of drying, ash, and atomization is very important for establishing optimum analytical conditions for different samples.

The first DSI-ICP system [34] was operated by manual insertion. Since then, different DSI systems have been developed. Except for one transverse insertion system [35, 36], in which probes were inserted transversely into the plasma cross-section just above the torch, the parallel insertion model has been exclusively used in DSI-ICP insertion mechanisms in which probes are inserted into the core of the plasma along the central tube of ICP torch. A basic schematic diagram of a DSI-ICP insertion system is depicted in Figure 1.1 [37]. A DSI device typically consists of a sample carrying probe, a torch, and a drive assembly. The positioning micro switches shown in Figure 1.1 are not necessary for our system because very precise and flexible positioning can be achieved with our computer controlled stepper motor based drive assembly.

Main hardware differences among different DSI-ICP systems are associated with the drive mechanism and sample change over mechanism. The drive mechanisms include manual insertion systems [23, 34-36, 38-42], a car aerial [43], dc motor driven insertion systems [24, 25, 29], pneumatic insertion systems [21, 22, 44, 45], and stepper motor driven insertion systems [30, 32, 46-54]. The stepper motor driven system is readily computerized while dc motor driven systems are usually stop-start switch controlled. Sample change over is accomplished manually as in most systems, but automatic carousels [22, 28] and robot control [30, 31] have been used.

Compared to other driving systems, the computer controlled stepper motor sample insertion system provides the best fit to the above mentioned requirements, i.e., fast insertion, and flexible and precise control in speed, timing, and positioning. Therefore, such an insertion system was used throughout this study. The insertion distance from home position to the final atomization position (refer to Figure 2.1) is 183 mm. or 2170

steps that take about 2 seconds with an insertion speed of 1200 steps/s. The positioning accuracy is better than  $\pm 0.1$  mm.

Most DSI-ICP studies have been carried out with AES spectrometry. There are only a few studies using mass spectrometry with DSI-ICP [32, 46, 47, 52, 53]. This is probably related to the difficulties of current ICP-MS instrumentation in handling transient signals for a wide mass range.

#### **2.2.1.3 The torch and matching network**

A modified Fassel torch with a big central tube that guides the sample probe into the plasma is used and is shown in Figure 2.2. From experience, it was found that the relatively large diameter of the central tube helps to keep the plasma stable because if the space between the central tube and sample probe is too small the plasma is extinguished upon rapid insertion of the probe into the plasma. A high outer gas flow rate is also effective in stabilizing the plasma while operating the DSI device.

Some modification of the ICP matching network may be necessary for running mixed gas ICPs if the tuning range of the capacitors is limited. The reflected power is subject to change as the plasma condition changes. When the outer gas is switched from Ar to mixed gas the reflected power level increases to over 100 W. We tried to lower the reflected power by adjusting the fine tuning capacitance on the matching network box. However, the adjustable range of this capacitance is too limited to allow lowering of the reflected power to its normal range which should be under 50 W. Additional capacitors of 150 pF total capacitance were added into the matching network to keep the reflected power level low. A schematic diagram of the matching network is shown in Figure 2.3. The added capacitor is labeled as C9 with capacitance of 150 pF that is in parallel with the other capacitors. After this change the reflected power could be kept under 20 W



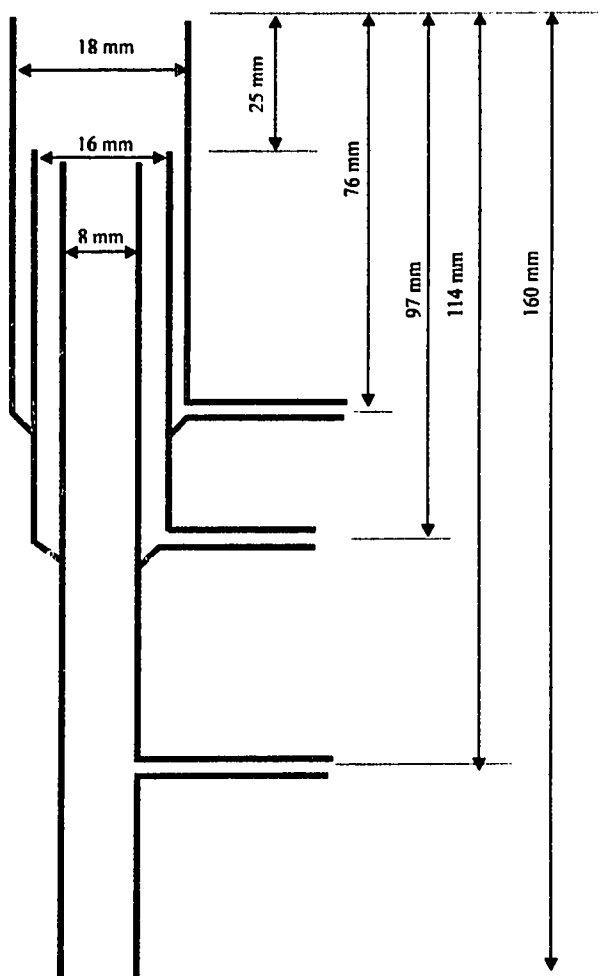
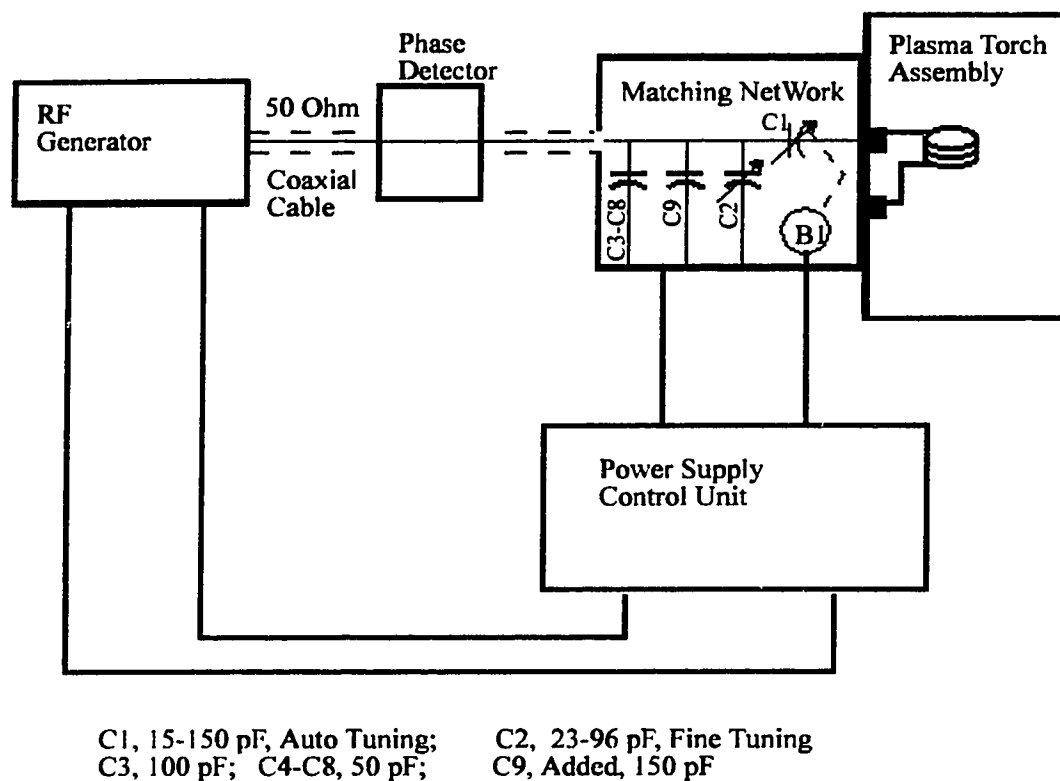


Figure 2.2 The modified Fassel torch for DSI-ICP-AES



**Fig. 2.3 Simplified Block Diagram of Automatic Matching Network  
As used in the ICP System**

when running mixed gas DSI-ICPs. However as the additional capacitance is not adjustable, it is difficult to tune reflected power to 0 W when running a pure Ar plasma.

#### 2.2.1.4 The probe

*Some requirements for the sample probe are: high thermal and chemical stability, simple matrix and spectral effects, low heat capacitance, easy to machine, and a compact surface.* Metals of high melting point such as W and Ta have been used as sample probes [22, 30, 33]; metal wire loops were found suitable for solution samples and can provide very good sensitivity [44, 45, 52, 54]. Among different probes, the graphite cup is the most widely used as a probe material. Diagrams of different graphite cups that have been used in our study are shown in Figure 2.4. The size of a graphite cup can have a significant effect on the DSI signal's profile and precision. A smaller cup (4.5 mm outer diameter) is preferred over a larger one (6 mm) because it is less disruptive of the plasma and therefore may lead to better precision [29]. This was confirmed experimentally. It was also found that the smaller graphite electrode was less affected by a change of power and gas composition. The 4.57 mm undercut graphite electrodes (see B and F in Figure 2.4) were used hereafter in this study unless otherwise indicated. Probe type (D) usually provides sharper signals, but it generates serious disturbance on the plasma. The precision of probes B, D, and F are poorer than type (A) and type (E) because they have been home modified by extending the under cut part and the precision of such a modification is limited.

Type (E) and (F) probes are usually used for analysis of liquid samples and solid samples of small loads such as 0.2 mg Al filings. Type (A) probe is used for analysis of solid samples and a large sample load such as 10 mg of rice flour can be utilized.

The density of the graphite electrodes from batch to batch may be quite different. Electrodes of higher density can provide sharper signals and better precision for a

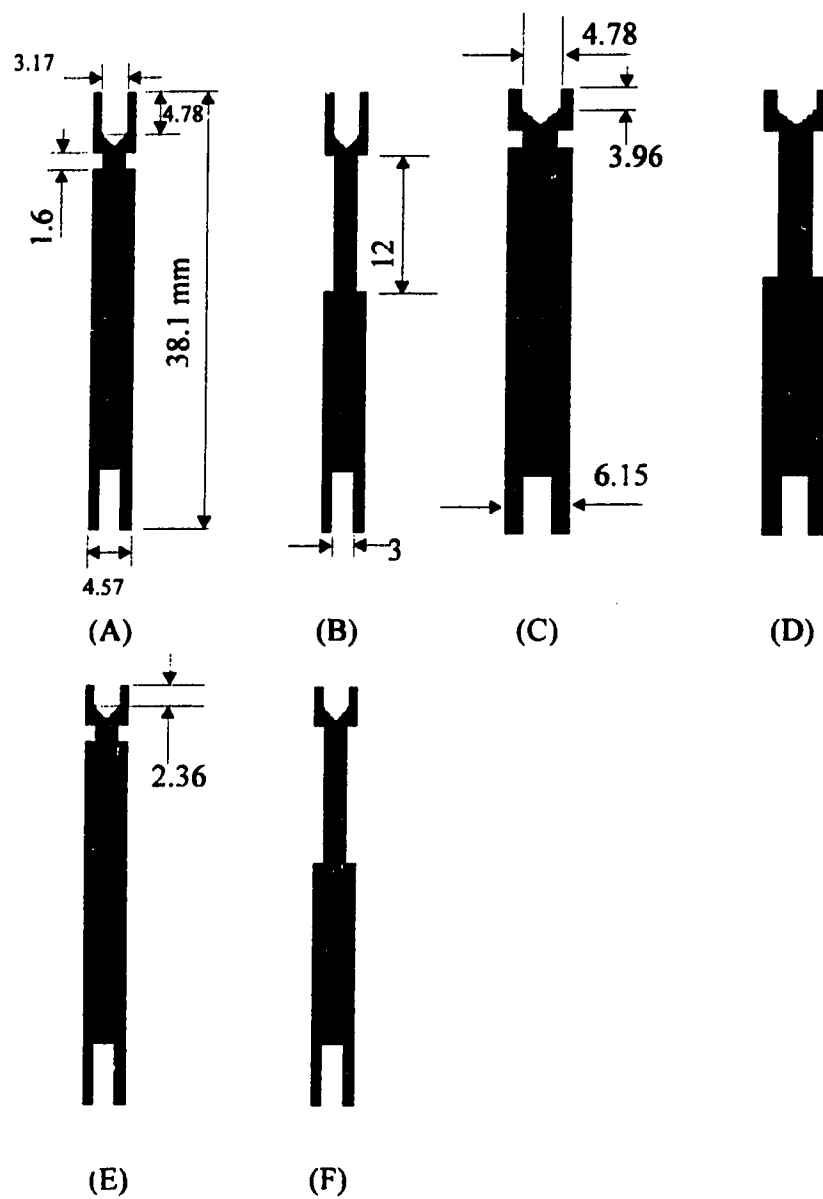


Fig. 2.4 Schematic diagrams of the graphite probes used for DSI-ICP

solution residue sample. This is probably because the surface of the electrode is more compact and analyte is less likely to soak inside the electrode. Electrodes of lower density, on other hand, may be advantageous for an efficient burn in an Ar-O<sub>2</sub> plasma and will be discussed in Chapter 3.

#### **2.2.1.5 The shutter**

Usually a shutter is employed to prevent the central and intermediate tubes of the torch from being damaged by the plasma while the sample probe is in the home position (see Figure 1.1). However, it was found that the vibration caused by opening and closing the shutter can dislodge sample powder from the probe. The ICP torch was modified to introduce the sampling gas at an angle of about 45° through a restricted injection orifice. By choosing the sampling gas flow rate properly the plasma can be run safely without the use of the shutter. By using a small outlet orifice some air may be entrained into the plasma and thus keep the plasma away from the torch tube by a thermal pinch effect. If too much air is introduced into the plasma it may become unstable. The shutter still needs to be closed during plasma ignition.

#### **2.2.1.6 The filament and carrier gas**

It has been reported that an arcing filament may form in the central tube when inserting and retracting the probe. Such a filament is even more serious when running mixed gas ICPs at higher power while using pure Ar in the central tube because of the thermal pinch effect. Originally the foreign gas was introduced into the outer gas stream only and the filaments were found in both the intermediate gas stream and the central gas stream because these two streams were pure Ar. The filament may extend to the torch box through the Tygon tube of the intermediate gas and melt the Tygon tube. This is an

important reason for introducing foreign gas into both the outer and intermediate gas streams in our system (see Figure 2.1) This problem has not been addressed by most mixed gas ICP studies with nebulization sampling systems, presumably because of the difference of solution nebulization ICP and the dry DSI-ICP. If this filament or arcing occurs in the central tube, it may spatter the sample before it reaches the plasma. Helium has been used in the central gas to reduce the arcing problem [29]. It was found that a convenient and effective way to eliminate the arcing was to pass the central Ar gas through water vapor. A very small amount of H<sub>2</sub>O vapor can effectively quench the arcing. To this end, the central gas Ar is simply passed through a bottle containing distilled deionized water.

#### **2.2.1.7 The heating chamber and drying process**

It is possible to dry the sample inside the ICP torch (*in situ* dry). However this will increase the analysis time and complexity for choosing the proper probe position. The position needs to be such that it is close enough to the plasma for efficient drying but far enough away so that there is no loss of volatile elements through pre-vaporization. We found it is easier to dry the sample externally using a hot plate or an IR lamp. However, contamination from the air dust can cause problems, especially for the elements such as Fe, Zn, Al in low concentration. A small heating chamber, as shown in Figure 2.5, was made for this purpose to enclose the probes while they were being dried. The sample probes were mounted in an aluminium plate and dried with an IR lamp for about 10 minutes with the door closed. The chamber can be ventilated or purged with gases. No detectable contamination was found for aqueous samples of 10 ppb level kept overnight in the chamber.

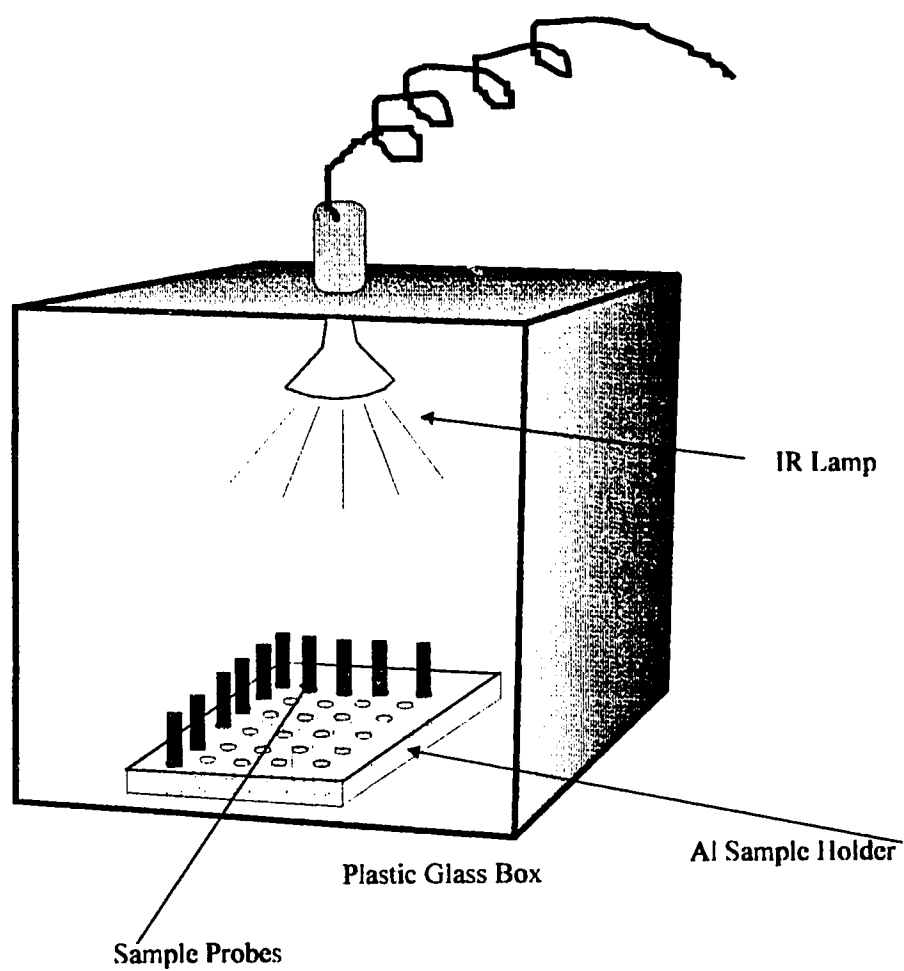


Fig. 2.5 Schematic diagram of the heating chamber. The sample probes are held in the holes on the Al sample holder.

### **2.2.1.8 The operation procedures**

Unless otherwise indicated, an undercut graphite cup of 4.57 mm diameter was used as a sample probe. The cups usually needed to be pre-burned in the plasma for about 30 seconds to remove any possible contamination. It is found that adding 10  $\mu\text{L}$  of 1 M NaF into the cup before the pre-burn step was very effective for removing some contamination elements from the graphite cups.

For aqueous or oil samples, a 10  $\mu\text{L}$  sample is added to the cup. The sample loaded cups are then dried with an IR lamp (usually 10 minutes for an aqueous sample and 20 minutes for an oil sample). If the analyte concentration is too low for accurate detection, successive aliquots of sample can be added and dried as a preconcentration step.

### **2.2.2 Software**

There are three main programs written in BASIC for pre-burning, data acquisition, and data processing. The pre-burn program simply sequences an insertion and retraction of the probe into and out of the ICP. The burn time can be controlled precisely by the computer. This is mainly for conditioning or removing possible contamination on the probe surface by pre-burning the empty probe in the plasma before the sample is loaded. The data acquisition program is the main program for doing DSI analysis. It contains some BASIC callable machine language subroutines for stepper motor control and data acquisition. The program is menu driven with a screen edit function providing for a convenient change of operating parameters, such as sample weight, ADC gain, probe position for ash and analyzing, timing for ash and analyzing, etc. The profile displaying function allows the operator to have a quick view of the results. The data is saved to disk in binary code format that saves time and disk space when large amounts of data are to be transferred. The data processing program is for post data processing and includes data



loading, displaying, plotting, both peak height and peak area calculation, different background correction modes, detection limit calculations, etc. It also provides a data format converting function that converts binary code files into text files so that the data can be read and processed by other data processing programs such as those available for the Macintosh.

There are four programmable gains that can be set for the ADC on the DT2801-A data acquisition board, and it is necessary to be able to adjust the gains for each channel and each sample to determine different concentrations. This means that the channel scan mode (in this mode the gain for all the channels must be same) cannot be used and instead the single channel convert mode must be used. However that sacrifices the total ADC speed, which is important in the case of sharp peak signals. To meet this consideration, the program was then compiled to form an executable program under the DOS system. The program can run fairly fast and is able to acquire 427 data points per second per channel. Every eight consecutive data points are then added together on line to improve the S/N ratio and compress the data size without losing useful information. In practice this provided a good compromise between the measurement of sharp peak signals (from volatile elements) and wide peak signals (from nonvolatile elements) and the data size. The data acquisition speed is mainly limited by the computer's speed. Much higher ADC speed could be obtained with higher speed computers.

An MS Windows™ based program for DSI-ICP analysis is under development using Borland® Turbo C++ for Windows. MS Windows™ 3.1 provides a good GUI (graphic user interface). Graphic user interfaces are easier to use than text-based ones because the human brain is unmatched when it comes to recognizing visual patterns. Although it is not an operating system Windows™ 3.1 does provide a user friendly operating environment with multitask capability. It also overcomes some limitations of MS DOS such as the 640 KB memory addressing limitation. On the plus side, Windows extends DOS so that programs can have a consistent, mouse-oriented graphical user interface,

complete with pop-up menus, windows, controls and dialog boxes, which, in addition to the visual interaction between user and computer, make the program easy to use. In addition, Windows makes it possible to run multiple programs simultaneously and to take advantage of all the memory available on today's PCs. Also the MDI (Multi Document Interface) function allows easy handling in opening multiple child windows that can be very useful for comparing the signal profiles of different elements (see Figure 2.6) in the same time while the computer is still driving the stepper motor and collecting the data. On the downside, Windows demands a new style of programming that at first may be a bit overwhelming, but taken in steps is really quite manageable.

Figures 2.6 (a) to (d) shows the appearance of the DSI-ICP program for Windows. It can open and display multiple DSI-ICP data files (both text and binary) by clicking the File|Open menu under the File pull down menu. Figure 2.6a shows the main window of the DSI-ICP-AES program and some child windows in which the signal traces of different samples of the DSI-ICP-AES are displayed. Signals of different elements are displayed in different colors. The displaying windows can be sized, tiled, cascaded, etc. Under the Edit pull down menu some powerful data processing function such as FFT, IFFT, and digital filtering can be found (see Figure 2.6b). Under DSID pull down menu are the main parts of the program that is the stepper motor control and the data acquisition control functions. By choosing the DSID|SetMotor menu item, a dialog box for the stepper motor is presented (Figure 2.6c). The user can specify parameters for the sample probe such as ash position/time, atomization position/time, etc. The motor can then driven, according to the parameters, by clicking the mouse on appropriate push buttons in the dialog box. By clicking the DSID|SetADC menu a dialog box for data acquisition is displayed (Figure 2.6d). The user can specify parameters for the data acquisition such as ADC speed, data number, ADC gain, ADC channels, elements, etc. Clicking the mouse on the Acquire push button, the computer drives the sample probe into the ICP torch according to the parameters specified in the SetMotor dialog box and

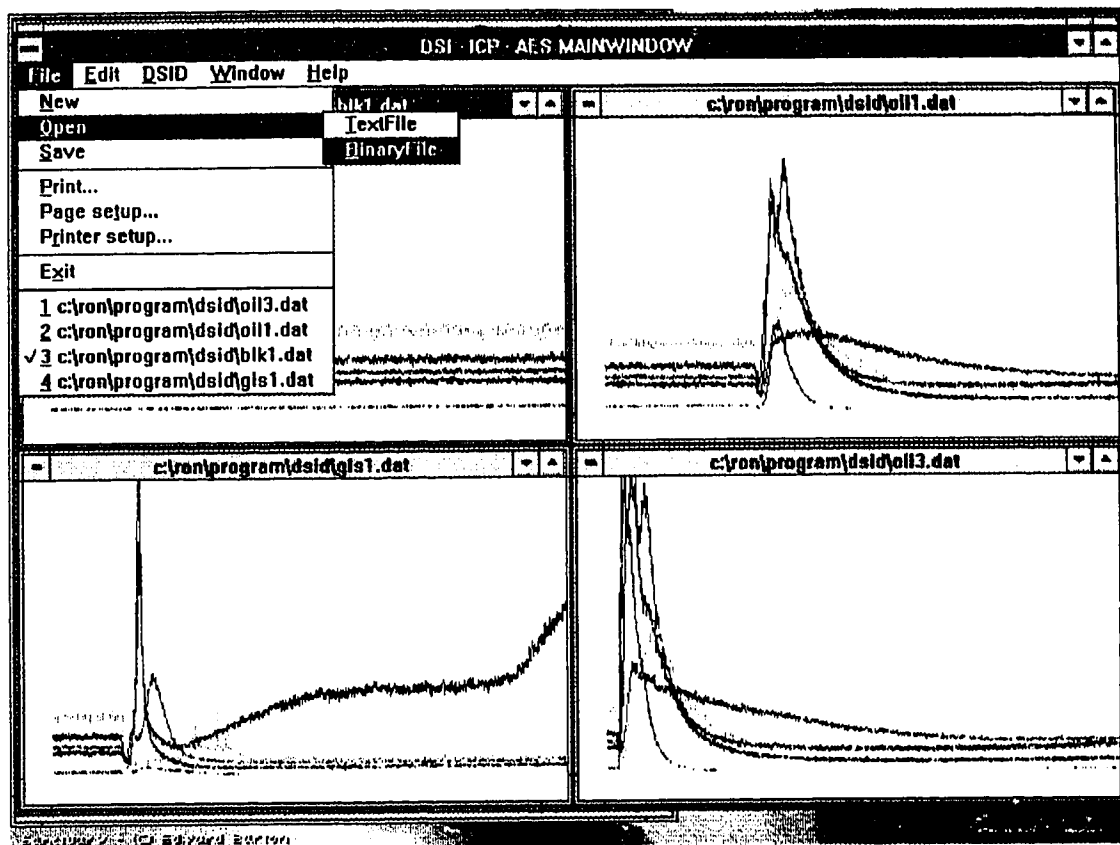


Figure 2.6a Screen copy of DSI-ICP program for MS Windows. The acquired DSI-ICP-AES signals are displayed in child windows

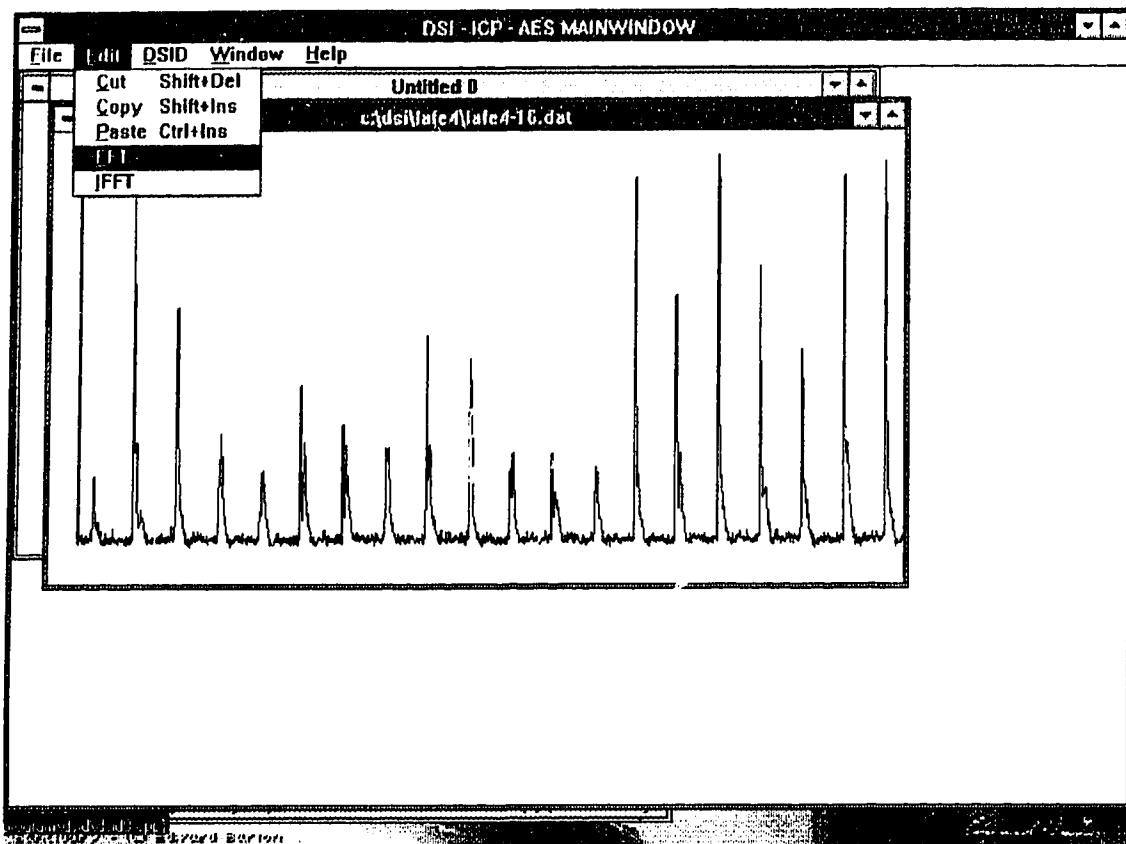


Figure 2.6b Screen copy of DSI-ICP program for MS Windows. The data processing functions are shown under the Edit menu

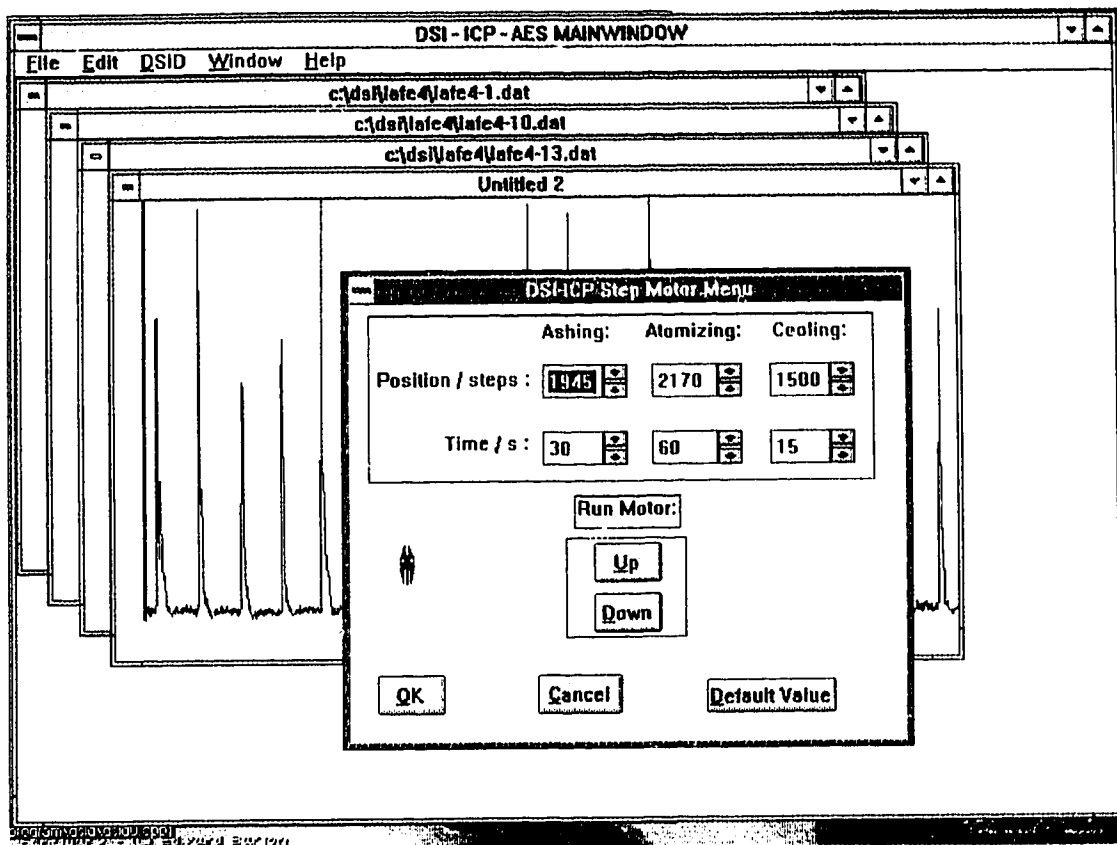


Figure 2.6c Screen copy of DSI-ICP program for MS Windows. The stepper motor control dialog box is shown.

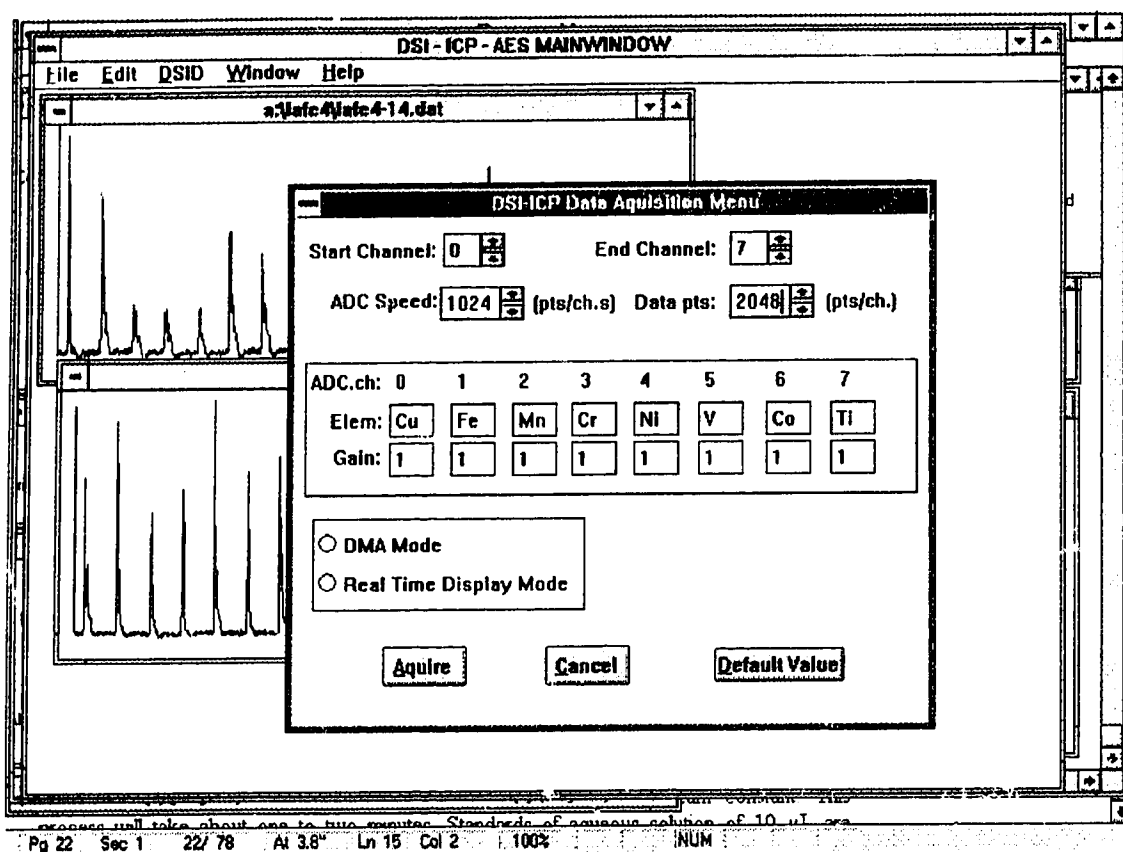


Figure 2.6d Screen copy of DSI-ICP program for MS Windows. The data acquisition control dialog box is shown.

starts the data acquisition. The default data acquisition mode is set to DMA mode and is independent of the CPU's intervention, therefore the ADC's frequency won't be changed by the interruption of other devices such as moving the mouse. Once finished, the acquired data is then displayed on one of windows (see Figure 2.6a). The data can then be saved in text mode and/or binary mode. The text formatted data can be easily exported to other data processing and presentation software.

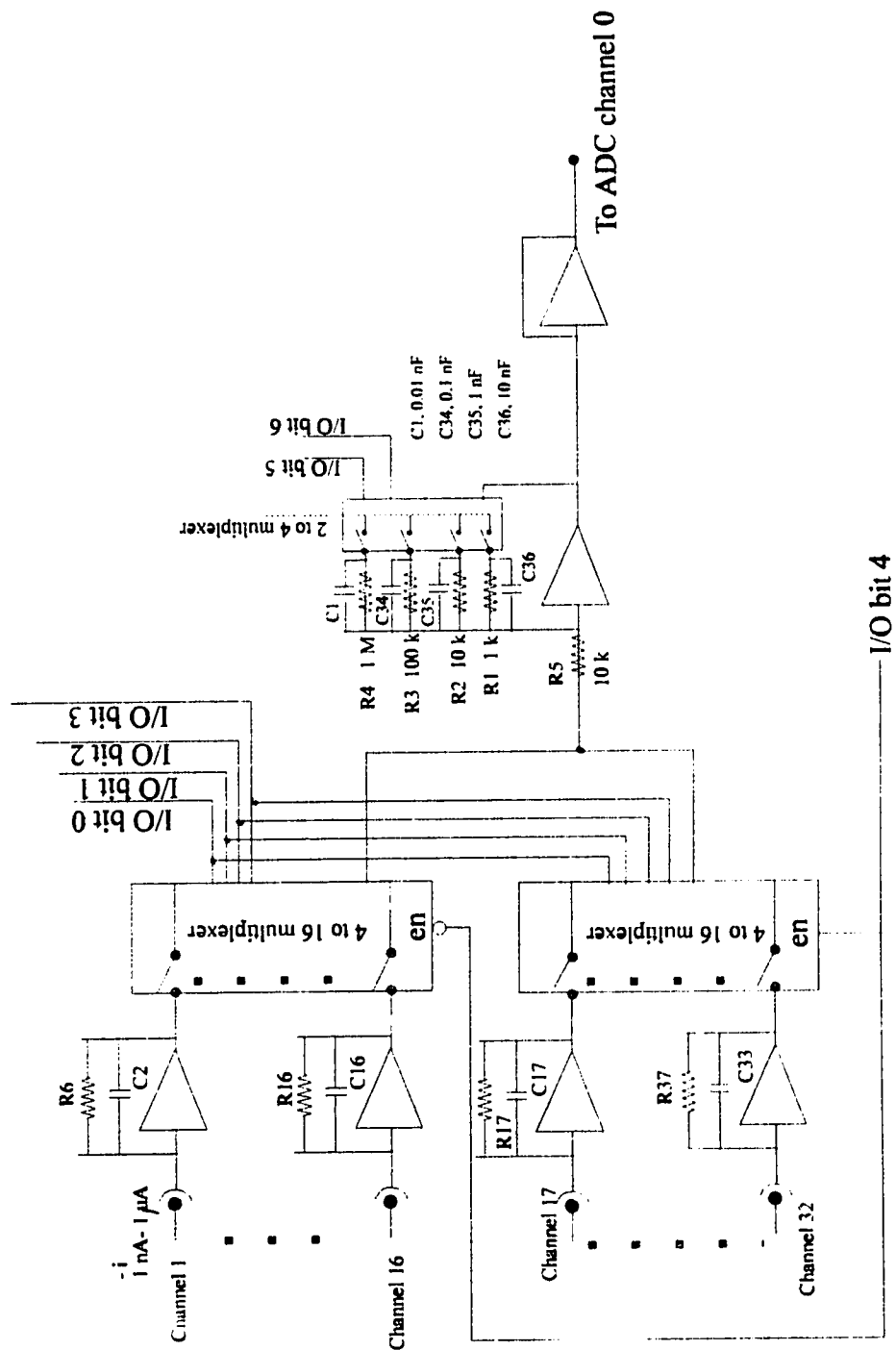
### **2.2.3 Considerations for future signal readout and acquisition subsystem**

As mentioned in section 2.2.1.1, the read out electronics of the DSI system were built in this lab by Chan and Horlick [30] with 5 input channels. Emission signals from 5 PMT channels in the spectrometer can be amplified simultaneously. The signals from the amplifiers are now routed into a data acquisition board, DT2801-A. Up to 8 channels can be connected to the board's ADC differential input, although only 6 channels (5 channel from the OPs and one from a commercial current amplifier, Keithley 427) have been used. One of the disadvantages of the amplifiers is the inconvenience in changing gain. To change the gain, the resistance in the amplifier's feedback has to be changed manually. Because of the limited dynamic range of ADC board (12 bit) the gains need to be changed very often during the analysis of samples of wide concentration range. In addition, the signal levels of an element can change several decades in a couple of seconds during a single analysis because of the transient nature of the DSI-ICPs signal. A typical situation encountered in real sample analysis is that the signals at peak positions were often out of the amplifier and/or ADC's range and cut off while the base line is often limited by quantizing noise. For a totally unknown sample, it is almost impossible to get a right signal in the first shot without going through some trial-and-error game. It is a waste of time and samples. Moreover, the  $1/f$  noise becomes important as the analytical time increases. For a technique such as DSI-ICP-AES to be

able to be run by a technician in a service lab it has to be as simple as a black box: put in sample and get the answer. The operator should not worry about anything such as adjusting the gains. It is highly desirable to have fast amplifiers with programmable gain control. Not only it is necessary to change the gains to match the concentration of the sample but also desirable to dynamically adjust the gain to amplify the signals from different parts in the profile into the proper range for the ADC. The amplifier's speed is especially important for *in situ* laser ablation ICP-AES, as will be discussed later. There is a programmable gain amplifier on the ADC board but it only allows for change in very limited ranges (2, 4, and 8 times). A new signal readout circuit was designed and new ADC sequences proposed to overcome the above mentioned drawbacks of the current system. The circuit is shown in Figure 2.7 and the operations are explained as follows.

The current signals from the PMTs are routed into the array of the 32 current-to-voltage amplifiers. The outputs of the 32 amplifiers are connected to two 4-to-16 analog multiplexers. Five DIO lines of DT2801-A DIO Port 0 (bit 0 to 4) are used to select one line out of 32 outputs of the first stage amplifiers into the second stage amplifier. The first four DIO lines (bit 0 to 3) are connected to the address lines of both multiplexers. The DIO bit 4 is used to ensure that only one multiplexer is enabled at a time. The signal from the selected channel is routed to the second stage amplifier for further amplification with appropriate gain. Four different gains, i.e., 0.1, 1, 10, 100 times, can be selected by programming the 2-to-4 multiplexer. The gain multiplexer is controlled by bit 5 and 6 of the DIO Port 0. Since the current from a PMT is negative, a voltage follower is added after the second stage amplifier to make the input of ADC positive. The ADC is set to unipolar mode with 5 volts full scale (4096). In analysis the program outputs a byte to the DIO Port 0 to select one of the 32 PMT channel and gain. The signal is digitized and registered after normalized to gain. Another byte is then outputted for selecting different channel and gain, and so on. The gain can be adjusted dynamically based on the signal level of the last point in the same channel.





$R6=R7=...=R37=0.1\text{ M}\Omega$   
 $C2=C3=...=C33=0.01\text{ nF}$

Figure 2.7 32 channel signal read out electronics for DSI-ICP-AES with programmable gain selection

In practice we found the amplifier generates noisy oscillation during switching between channels and gains. Some modifications are necessary, such as using an independent amplifier for different gain instead of using same amplifier but different resistance for different gains. A commercial ADC board with 16 bit and on board programmable gain amplifiers of wide range (such as 1, 5, 50, 500) are highly recommended (such as National Instruments AT-MIO-16X) for future work.

### **2.3 Effect of incident power and gas content on the DSI signal**

Mixed gas plasmas are established by first lighting an all-Ar plasma and then slowly adding the foreign gas to the outer and intermediate gas flows [14]. The foreign gas is added to the Ar using a pair of rotameters and a mixing tube. The flow rate is adjusted such that the foreign gas is increased to an appropriate reading on its flow meter while keeping the total flow rate of the outer and intermediate streams constant. This process takes about one to two minutes. The central gas (Ar only) is passed through a plastic bottle containing water in order to add water vapor to this Ar flow. As mentioned earlier, this prevented and/or quenched arcing of the plasma to the DSI probe during insertion and retraction. It is also possible to avoid arcing by adding a small amount of He to the central gas [29], but the water vapor addition proved to be a simple solution to this problem. Aqueous solution standards (10  $\mu$ L) were added to the graphite probes and dried for about 10 minutes with an IR lamp in the heating chamber. The probe is manually loaded onto the supporting rod of the DSI delivery system and driven into the ICP torch by the computer controlled stepper motor for analysis according to the programmed parameters such as ash position, ash time, atomization position and time.

The time resolved signal profiles for V, Cr, Fe, and Mn in different mixed gas ICPs are shown in Figure 2.8. Signals for other elements such as Ni, Co, Zn and Ag were also measured and their general characteristics were similar to that for the elements shown in

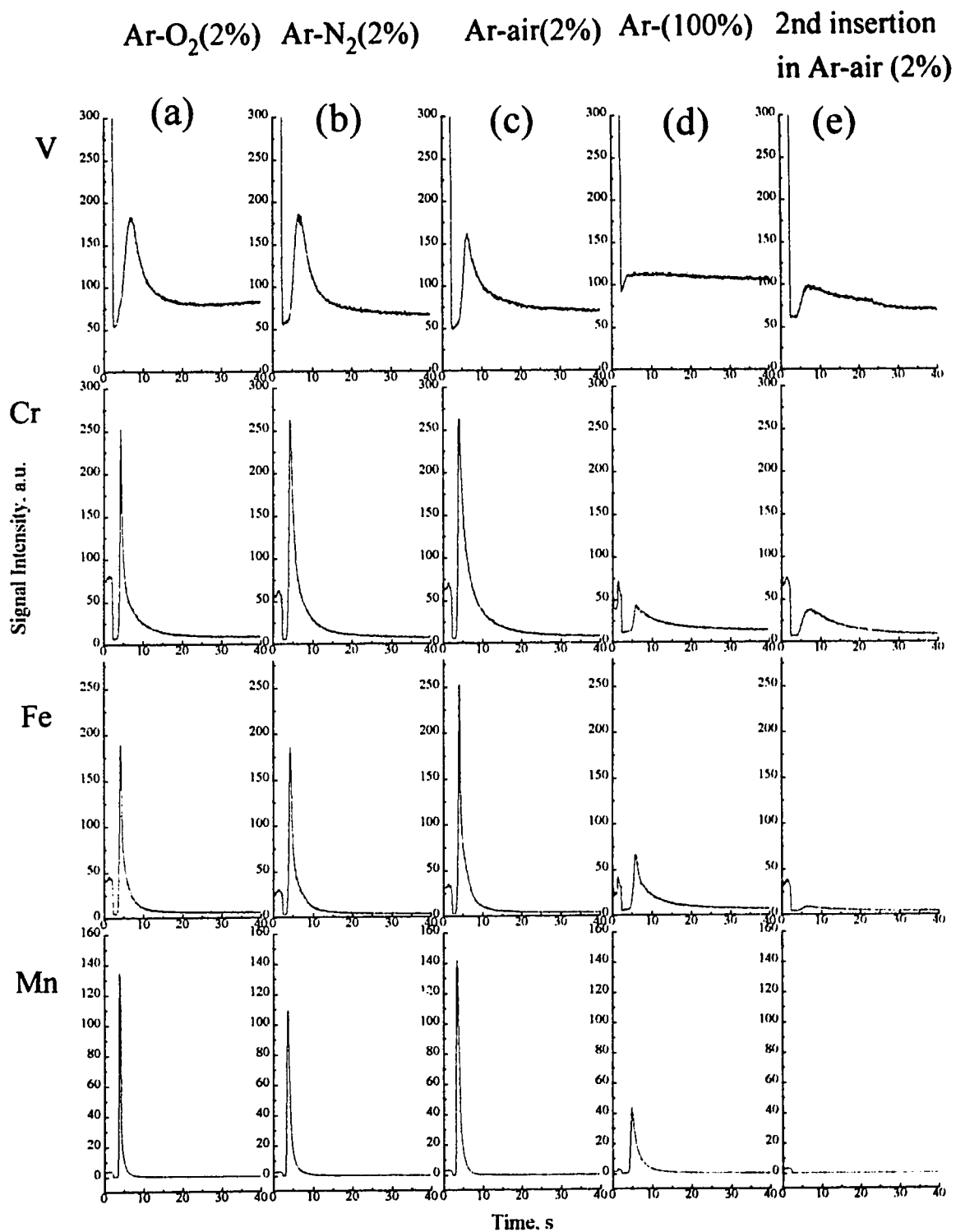


Fig. 2.8 Signals of mixed gas DSI-ICP-AES with different gas composition. Column (a), Ar-O<sub>2</sub>(2%); Column (b), Ar-N<sub>2</sub>(2%); Column (c), Ar-air (2%); Column (d), Ar (100%)  
Column (e), 2nd insertion of the probe in Ar-air(2%) plasma after first inserted in the Ar plasma  
Sample, SM20 1ppm x 10  $\mu$ L; Power, 1.75 kW

Fig. 2.8. The sample in each case was an aqueous solution (1 ppm x 10  $\mu$ L). The foreign gases used were O<sub>2</sub>, N<sub>2</sub>, and air and all were added at the 2% level.

In every case, analyte signals were significantly enhanced by the presence of the foreign gas (see column (d) of Fig. 2.8 vs. column (a), (b), and (c)). The biggest gain is seen for V, which is both an involatile element and tends to form refractory compounds. It's boiling point is 3380°C and it forms a refractory carbide with a T<sub>bp</sub> of 3900 °C.

Listed in Table 2.2 are the boiling point data of some elements and their compounds. According to the measured temperature of DSI probes in Ar ICP (~ 2000°C) the vaporization capability of the pure Ar plasma is very limited for involatile elements and their compounds, such as Zr, Ti, Al, Sr, and V. It is expected that these elements would behave similarly to V.

Table 2.2 Boiling point data for Zr, Ti, V, Al and their oxide and carbide \*

	T <sub>mn</sub> (°C)	T <sub>hn</sub> (°C)		T <sub>mn</sub> (°C)	T <sub>hn</sub> (°C)		T <sub>mn</sub> (°C)	T <sub>hn</sub> (°C)
Ba	725	1640	BaO	1918	2000	BaC <sub>2</sub>	.....	.....
Mn	1244	1962	MnO <sub>2</sub>	.....	....	Mn <sub>2</sub> C	.....	.....
Mg	649	1090	MgO	2852	3600			
Fe	1535	2750	Fe <sub>2</sub> O <sub>3</sub>	1565	....	Fe <sub>3</sub> C	1837	
Al	660	2467	Al <sub>2</sub> O <sub>3</sub>	2072	2987	Al <sub>4</sub> C <sub>3</sub>	1400	2200(d)
Sr	769	1384	SrO	2420	3000	SrC <sub>2</sub>	>1700	
Si	1410	2355	SiO <sub>2</sub>	1720	2590	SiC	~2700	
Zr	1852	4377	ZrO <sub>2</sub>	2700	5000	ZrC	3540	5100
Ti	1660	3287	TiO	1750	>3000	TiC	3140	4820
Cu	1083	2567	CuO	.....	.....	CuC <sub>2</sub>	.....	.....
Cr	1857	2672	Cr <sub>2</sub> O <sub>3</sub>	2266	4000	Cr <sub>3</sub> C <sub>2</sub>	1890	3800
V	1890	3380	VO <sub>2</sub>	1967	.....	VC	2810	3900

\* The data are obtained from *CRC Handbook of Chemistry and Physics*, 59th Edition (1978-1979).

The signals obtained from a second insertion of the sample probe (this time into an air-Ar plasma) which had previously been inserted in a pure Ar plasma for 40 s are shown in column (e) of Fig. 2.8. There is appreciable signal observed for V and Cr

during this second insertion. These are both involatile elements that also form carbides. It appears that carbide formation (perhaps during the first insertion) is hindering vaporization of the V and Cr as the signal traces are weak and drawn out during this second insertion. Certainly, they have not recovered to the level seen in column (c). In fact, even in the 2% mixed gas ICPs the V signal can persist for over 250 seconds. In the next chapter it will be seen that by use of an Ar-O<sub>2</sub> mixed gas plasma at a 20% level of O<sub>2</sub>, these signal levels can be completely recovered.

The peak areas of the Mn, Fe, V, Cr, and Zn signals change with % N<sub>2</sub> content and power level and this is shown in Figure 2.9. The DSI probes used were graphite electrodes with a long under cut of 6.15 mm outer diameter (refer to Figure 2.4d). From the data presented in Figure 2.9 one can see that N<sub>2</sub> gas has a great effect on the signal intensity especially for the nonvolatile and carbide forming elements such as V and Cr (see Figure 2.9(a) and 2.9(b)). It is interesting to see that the mixed gas ICP also has an appreciable effect on the signal intensities of the relatively volatile elements (see Figure 2.9(c), 2.9(d) and 2.9(e)). Thus, it appears that the Ar-N<sub>2</sub> mixed gas plasma may also be generally good for enhancing the signals of all analytes by increasing the vaporization efficiency. The optimum amount of N<sub>2</sub> is power dependent. The plasma can tolerate more N<sub>2</sub> at higher powers. The data for 1.25 kW and 1.5 kW for N<sub>2</sub> content over 3% is not available because under these conditions the plasma extinguished upon the insertion of the probe. Usually a 1.75 kW to 1.8 kW power level and ~2% N<sub>2</sub> are used. If higher powers were used, torch damage became a problem.

## **2.4 Effect of observation height**

An observation height of about 14 mm above the top of the load coil was chosen based upon the experimental results shown in Figure 2.10. This position is optimum for all the elements tested. It should be noted that because the slit of the spectrometer is 10

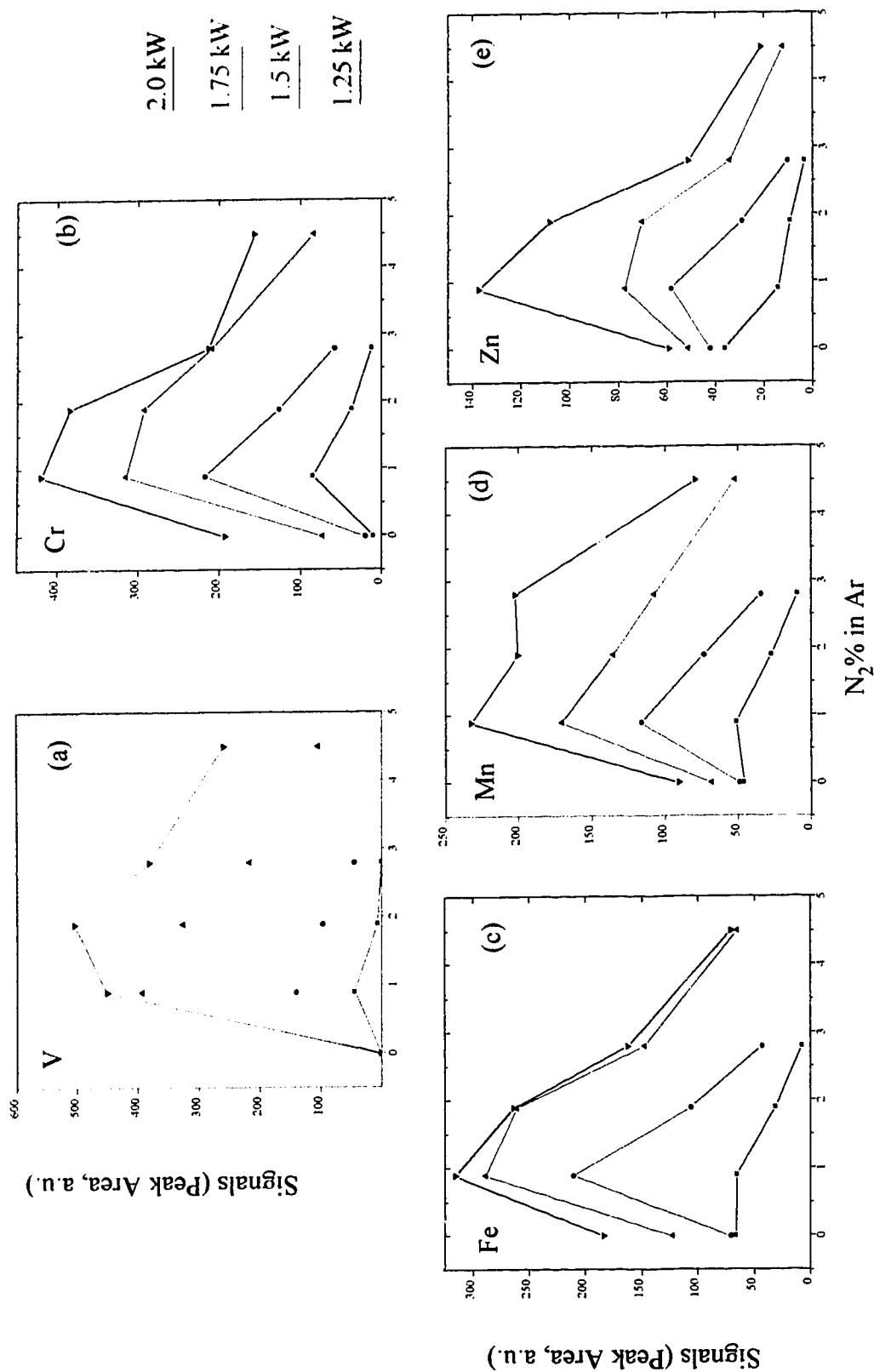


Fig. 2.9 Effect of incident power and  $N_2$  content on relative signals of different elements with DSI-ICP-AES

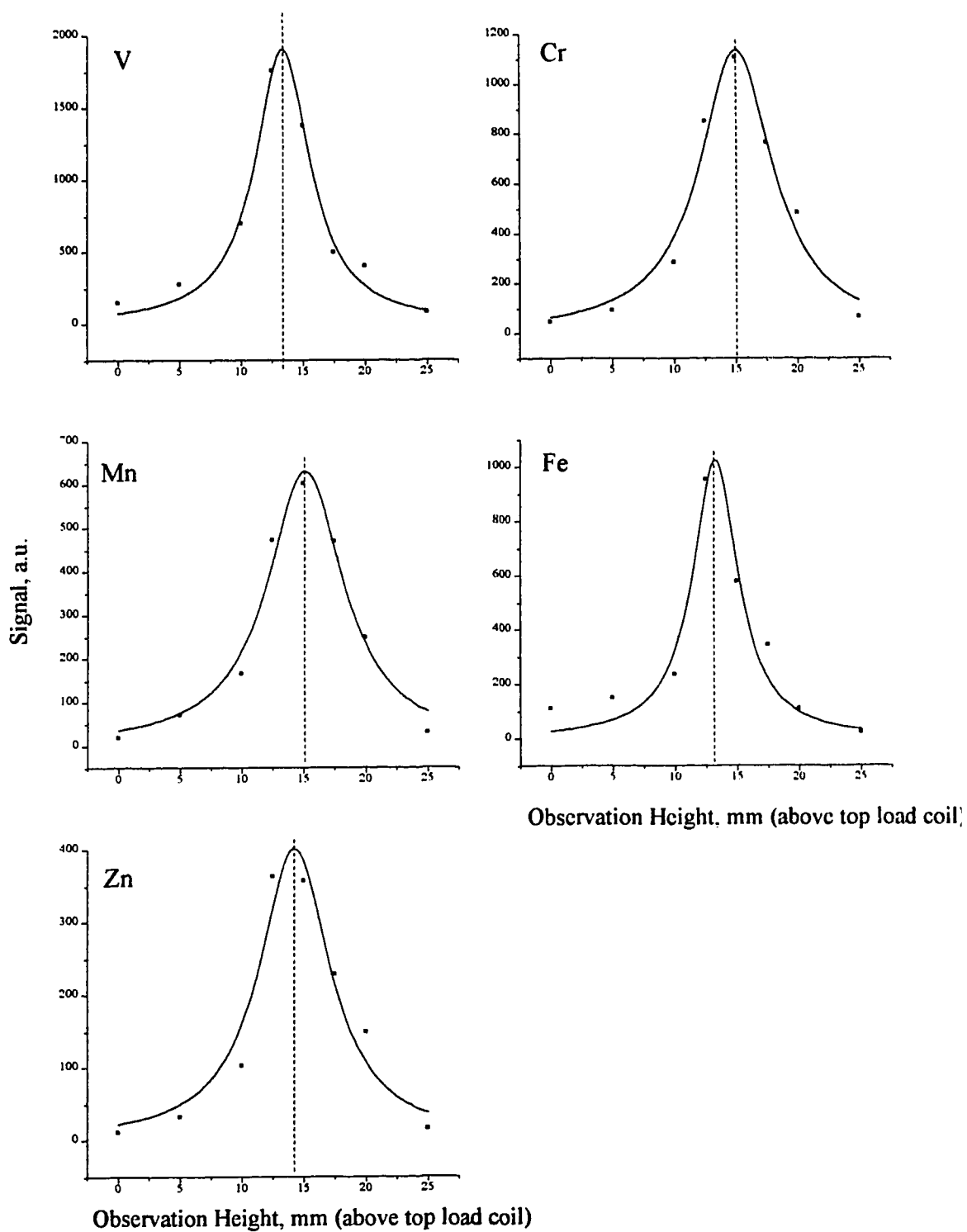


Fig. 2.10 Effect of observation height on the signal's intensities of elements with Ar-N<sub>2</sub> (2%) mixed gas DSI-ICP-AES, ICP Power, 1.75 kW, Sample, 1.0 ppm x 10  $\mu$ L

mm high the observation height is actually an observation zone of about 10 mm centered at 14 mm above the top load coil. A simple way to fine tune parameters such as  $N_2$  content and observation height is to add some steel alloy chips into a graphite cup. The cup is then driven into the plasma. A piece of steel alloy usually will last for several minutes with little change in signal intensity. The signals for different elements can then be monitored, and adjustments can be accomplished quickly by monitoring changes of the signal intensities.

## **2.5 Effect of the probe's position and history on the signal's temporal profile**

The position of the DSI probe in the plasma has a great effect on the signal [29, 38]. A final probe position in the plasma of about 2 mm above the top load coil was chosen for all the elements tested. This was a compromise as the best position did vary somewhat with element, sample, and operating conditions.

The probe's surface condition and shape affect the signal intensity and shape. For the graphite probe, usually a smaller and new electrode with a long undercut gave sharper and more intense signals. As shown in Figure 2.11, a preburned electrode produces less intense and broader signals ( see Figure 2.11(g) - 2.11(l) vs. 2.11(a) - 2.11(f)) because the surface became porous after preburning and the solution sample probably soaked into the probe. As a consequence, vaporization is more difficult and the analyte has a greater chance to form a carbide inside the holes making vaporization even more difficult. Therefore a surface coated and/or pyrolytic graphite electrode would probably help in the vaporization process.

As it will be seen in section 2.7 a silicate coated probe can significantly improve the vaporization efficiency for some carbide forming elements from solid samples.



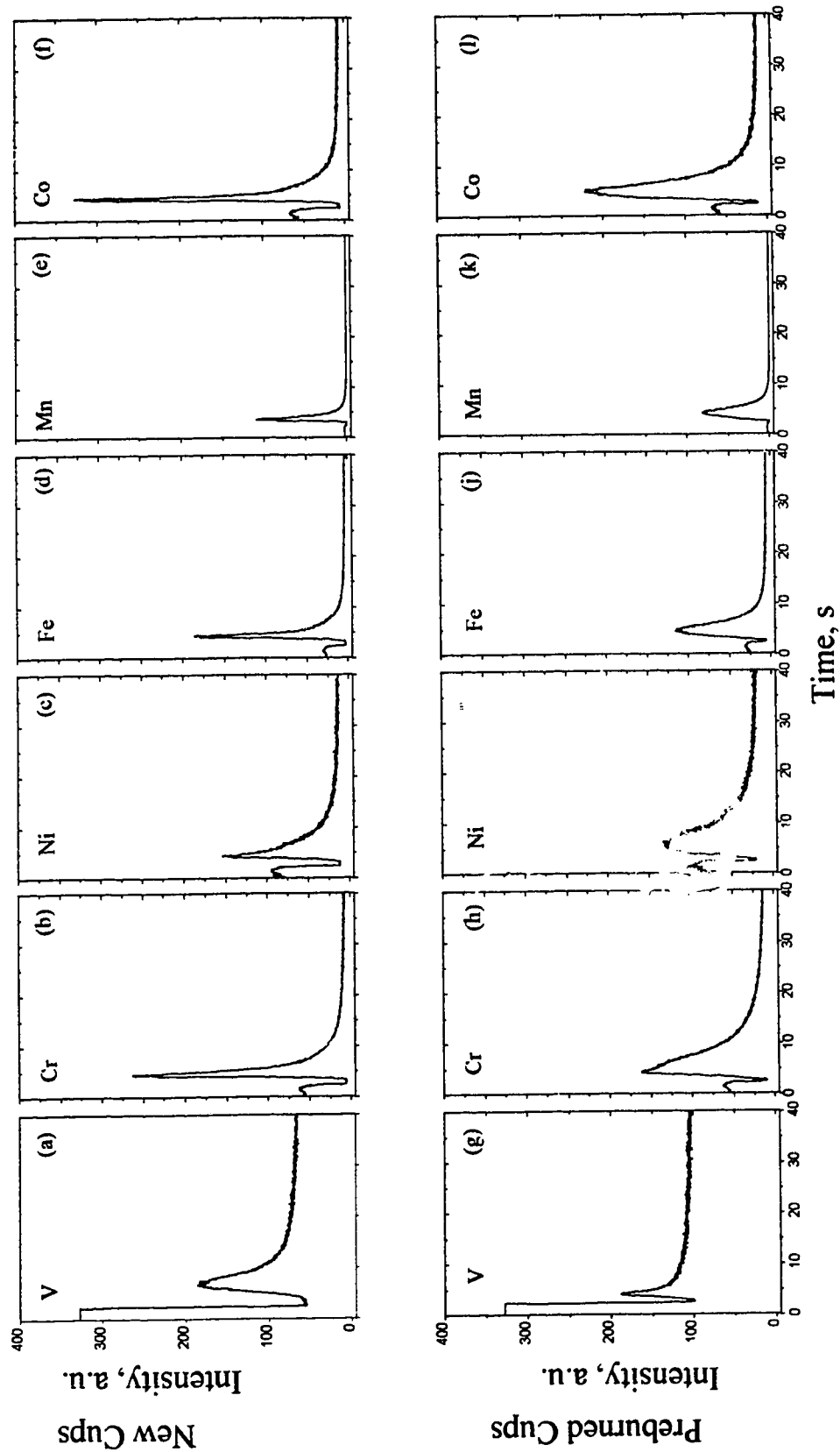


Fig. 2.11 Effect of cup surface conditions on the signal profile with Ar-N<sub>2</sub> (2%) mix gas DSI-ICP-AES  
Sample, SM20, 1 ppm x 10  $\mu$ l. Power, 1.75 kw. obs. time, 40 s

## 2.6 Studies of the mixed gas DSI-ICP-AES system with aqueous solution samples

Data of the analytical performance of the DSI system with aqueous solution residues are summarized in Table 2.3. The detection limits for 10 elements are listed in Table 2.3. The detection limits are calculated from following equation:

$$\text{D.L. (ng)} = 3 (\text{SD})_B / S.$$

Where  $(\text{SD})_B$  = Standard deviation of the peak area intensities of 11 blank samples integrated for the same intervals as the sample, and  $S$  = Sensitivities from the Calibration curves, i.e., peak area intensity/ng. The (RSD) data in Table 2.3 are a measure of the precision of the method and they are calculated from peak areas of eleven samples with 1 ng of analyte.

Table 2.3. Detection limits for the solution residue sample with Ar-N<sub>2</sub> mix gas DSI-ICP-AES

Element	$\lambda$ (nm)	Range (ng)	Slope log-log	R	D.L(pg)	Precision (% rsd)
V	292.4	1.0 - 1000	1.15	0.99745	380	55
Ni	231.6	0.1 - 1000	0.87	0.99422	418	6.6
Co	228.61	0.1 - 1000	0.92	0.99811	58	7.3
Ag	328.07	0.1 - 1000	0.98	0.99954	38	8.2
Cr	205.55	0.1 - 1000	0.98	0.99964	30	12.5
Cd	226.5	0.1 - 1000	0.95	0.99944	3.4	5.0
Cu	324.75	0.1 - 1000	0.95	0.99993	15	14.
Fe	259.94	0.1 - 1000	0.99	0.99804	11	4.6
Zn	213.86	0.1 - 1000	0.92	0.99961	4.7	9.5
Mn	257.61	0.1 - 1000	0.94	0.99981	2.8	3.6

1.  $\text{D.L.} = 3(\text{SD})_B / S$ ;  $(\text{SD})_B$  = Standard deviation of peak areas of eleven blank runs.  
 $S$  = sensitivity.
2. (RSD) calculated from peak areas of eleven 1 ng samples

The mixed gas DSI-ICP-AES system provides improved sensitivities for the nonvolatile and carbide forming elements while providing comparable detection limits for the volatile and relatively volatile elements such as Cd, Zn, Cu, and Fe compared to those values described in reference 30. It should be noted that two different spectrometers were used in these studies. In contrast to the spectrometer used in this study, the spectrometer used in reference 30 was a vacuum spectrometer and was thermostatted, which presumably would provide better sensitivities for UV lines and better precision.

The calibration curves for solution residue samples are shown in Figures 2.12 and Fig. 2.13. The linearity for most of the elements tested was good. The slopes of the log-log plots are close to unity and are listed in Table 2.3. The amounts of analyte in the standard solutions ranged from 0.1 ng to 1000 ng. The lower limit of the calibration curves is usually dictated by impurities from the probe, reagent, and laboratory environment, etc., while the upper limit is very likely determined by the dynamic range of the detector and ADC. The detectors used in our spectrometer are PMTs with a maximum operating current (anodic) of about 1  $\mu$ A. When the peak current of the signal exceeds the PMT's maximum operating current PMT saturation may occur resulting in lower sensitivities at higher concentration. Abnormally small slopes (log-log plot) of some of our early calibration curves (not shown) for sensitive elements (such as Mn, Zn) may have been the result of PMT saturation. The peak signal intensity is determined by the volatility of the vaporizing analyte species, the volatility of the sample matrix, the sensitivity of the analytical line, sample loading, plasma conditions, and some other operating parameters such as probe characteristics and probe insertion speed. To obtain appropriate signal intensity in our system the PMT's high voltage (HV) and the pre-amplifier's gain need to be properly set. The PMT's HV was chosen such that about 1  $\mu$ A of anodic current (before preamplification) corresponded to the highest peak signal. Once set, the PMT's HV should not be changed through-out one analytical task because

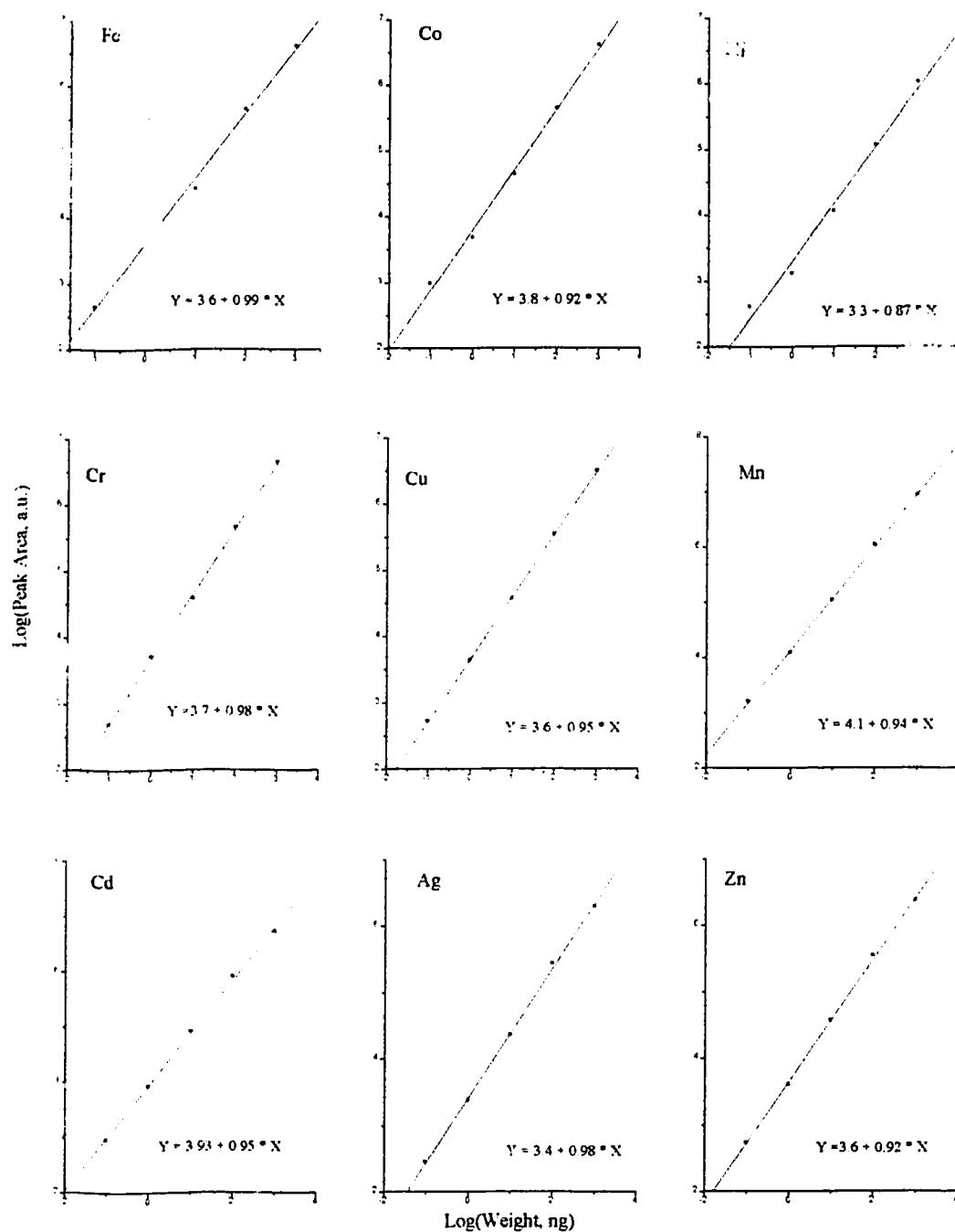


Fig. 2.12 Calibration curves(log-log plot) for aqueous standards with Ar-N<sub>2</sub>(2%) mixed gas DSI-ICP-AES

Sample, SM20 (0.01-100 ppm) x 10  $\mu$ L; Power, 1.75 kW

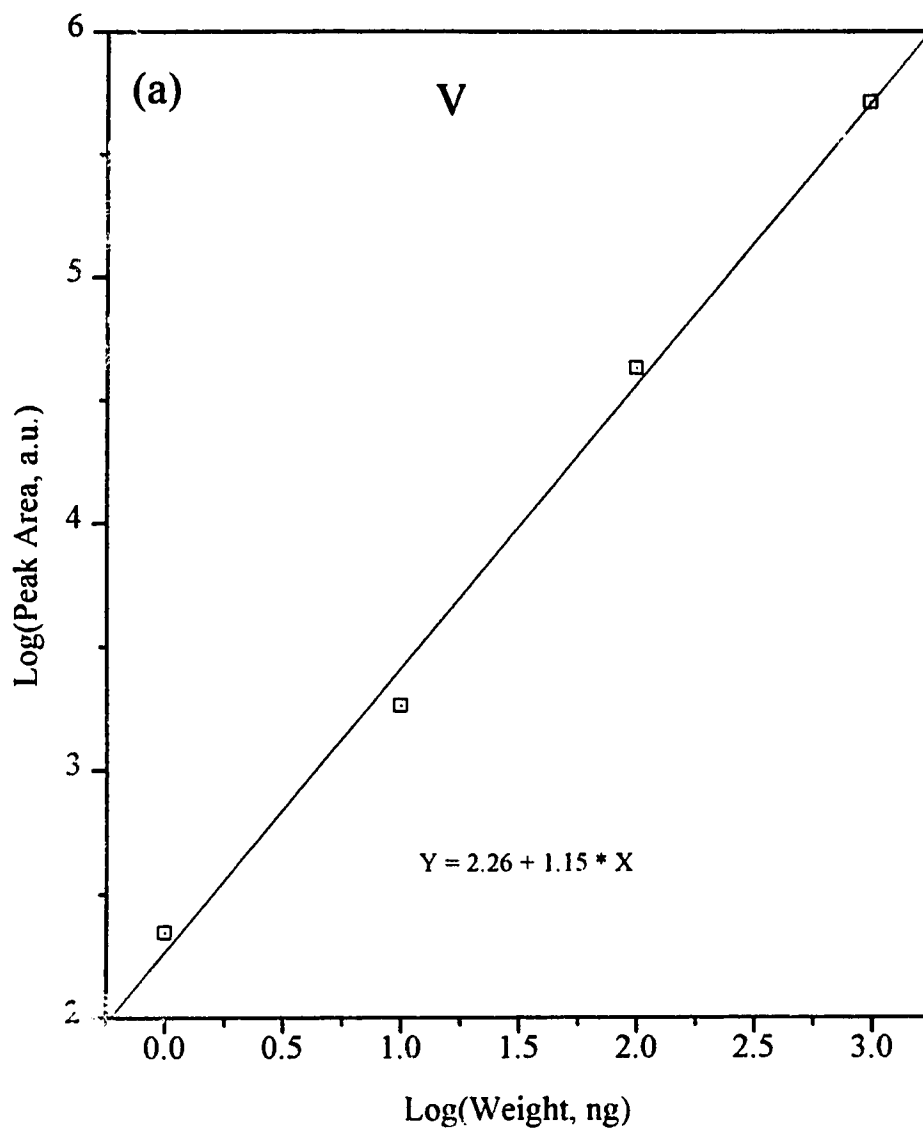


Fig. 2.13 Calibration curves (log - log) of V in aqueous standard with Ar-N<sub>2</sub> (2%) mix gas DSI-ICP-AES

Standard, SM20 (0.1 - 100 ppm) x 10  $\mu$ L. Power 1.75 kW

the sensitivity of the PMT is not a linear function of the HV. For unknown samples some trial-and-error exercises are necessary. The difficulty in handling transient signals is probably the biggest disadvantage of a DSI-ICP system as compared to a pneumatic nebulization system. Such difficulties are being relieved by the development of sophisticated computers, ADCs with wide range programmable gain controls, and improved software.

In certain ways the V calibration curve, Figure 2.13, is much better than expected. The linearity of the V calibration curve is fairly good (slope = 1.15) in the range from 1 to 1000 ng. However, the vaporization of V in the Ar-N<sub>2</sub> mixed gas ICP is incomplete within 50 seconds. Even after 5 successive insertions of the probe for an original sample load of 1000 ng a substantial V signal can still be observed (see Figure 2.14(b)). The scale of Figure 2.14(b) is expanded 10 times as compared to Figure 2.14(a) (first insertion). The "linear" calibration curve suggests that the vaporized fraction of V may be constant for a given period of time for different concentrations of the solution residue sample. If this is true, quantitative analyses of V in aqueous samples could still be possible with a N<sub>2</sub>-Ar mixed gas ICP-DSI. However, further studies are needed to characterize the vaporization of V in different samples and different matrices.

## **2.7 Studies of the mixed gas DSI-ICP-AES system with solid samples**

Standard set of botanical samples, Al<sub>2</sub>O<sub>3</sub>, Al filings and steel chunks have been tested. No satisfactory results were obtained for nonvolatile elements with the low percentage mixed gas plasma (i.e., 2% N<sub>2</sub>) used in these studies. However the determination of some carbide forming elements in solid samples has been achieved by the Ar-N<sub>2</sub>(2%) mixed gas DSI-ICP-AES with coating treatment of the probe.

The Ar-N<sub>2</sub>(2%) mixed gas DSI-ICP-AES has been used to analyze sheet glass samples. The samples are from the Edmonton RCMP lab. Six elements, Ba, Mn, Mg, Fe,

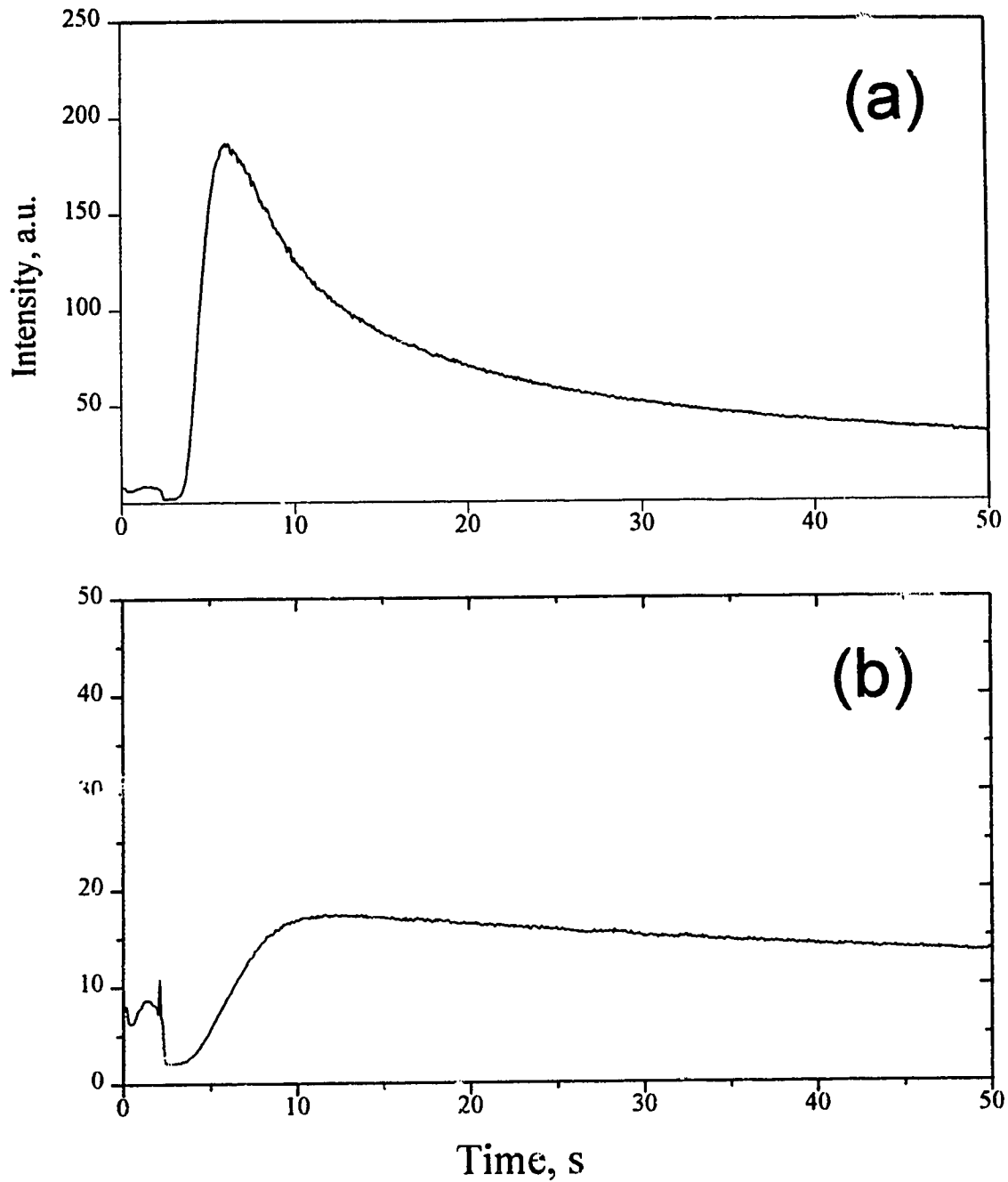


Fig. 2.14 DSI-ICP signals of 1000 ng V in Ar-N<sub>2</sub> (2%) mixed gas ICP  
(a) 1st insertion in Ar-N<sub>2</sub> (2%) plasma; (b) 5th insertion in Ar-N<sub>2</sub> (2%) plasma;  
Sample, Solution residue. Power 1.8 kW.  
All signals have been corrected to the same gain

Al, and Sr, are to be analyzed as elemental variables for the discrimination of glass samples (i.e., to assess similarity or dissimilarity between samples, usually suspects and control, of the same refractive index). The sample amount was fairly small; most of them are less than 1 g. The sample particle size varies largely in the same bottle; some are fine powders; some are particles larger than a grain of rice. The probes used were either type (A) or (E) (see Figure 2.4); they gave similar results. The probes had been pre-burned in the plasma for 30 s. About 3 mg of samples were added into the graphite sample probe. No discernible signals showed up before 80 s. This result turns out to be somewhat surprising at first glance. Another aliquot of the glass samples was therefore added to the same probe to confirm the result. This time, very strong signals for all the six elements showed up about 10 s after the insertion of the probe into the ICP. The tremendous differences of the two results indicate possible changes of the surface condition of the probe after the first insertion in the plasma. Presumably, during the first insertion in the plasma, the probe (graphite cup) surface had been coated with silicate (the matrices of the glass sample) or, more likely, with SiC. The formation of the SiC coatings prevents direct contact of the subsequent aliquot of sample with the graphite surface, which improves the vaporization efficiency significantly, especially for carbide forming elements such as Ba, Sr, and Al.

For later analysis of the glass sample the graphite probe was preburned in the Ar-N<sub>2</sub>(2%) plasma for 30 s with ~ 10 mg of pure SiO<sub>2</sub> (Spex SiO<sub>2</sub>, 99.999%). The sample was then weighed and added into the preburned (or precoated) probe for DSI-ICP-AES analysis. The signal profiles of pure SiO<sub>2</sub> and one of the glass samples in the coated probe are shown in Figure 2.15(b) and 2.15(c). Signal profiles of the same sample in an uncoated probe are shown in Figure 2.15(a) for comparison. With the coated probe not only the strongly carbide forming elements such as Ba and Al showed well-defined signals but also the moderately volatile elements such as Mn are vaporized much more quickly. With the SiO<sub>2</sub> coated probe, 12 sheet glass samples were analyzed and the



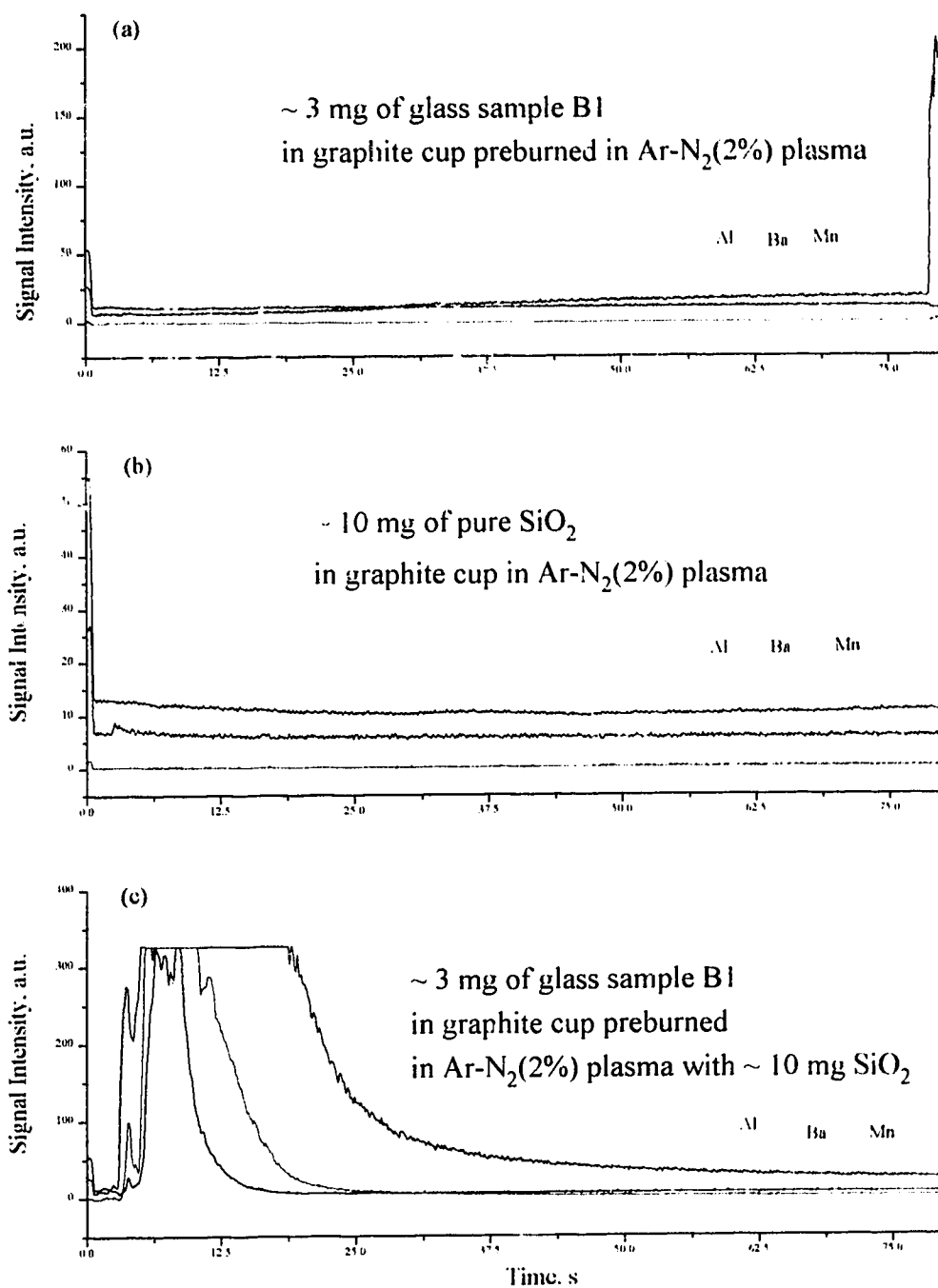


Fig. 2.15 DSI signals of Al, Ba, and Mn in glass sample using uncoated cup (a), and SiO<sub>2</sub> coated graphite cups (c) with Ar-N<sub>2</sub>(2%) mixed gas plasma

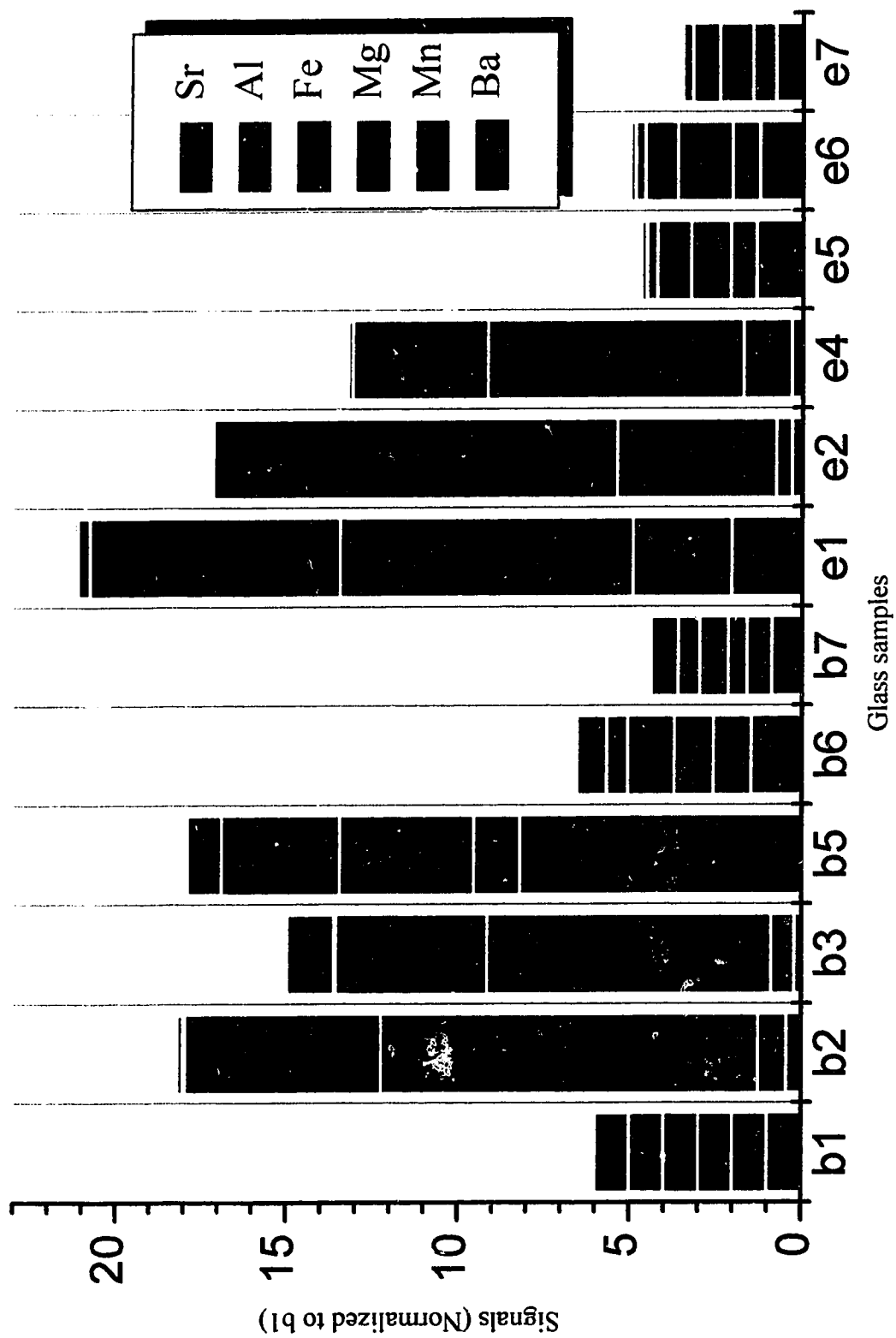


Fig. 2.16 Bar graph of the relative concentration of the elements in glass samples

**Table 2.4** Signal relative intensities (relative to b1) of 12 sheet glass samples analyzed by Ar-N<sub>2</sub>(2%) mixed gas DSI-ICP-AES with SiO<sub>2</sub> coated probe

Sample	Ba	Mn	Mg	Fe	Al	Sr
b1	1.0	1.0	1.0	1.0	1.0	1.0
b2	0.4	0.8	11	5.7	0.05	0.2
b3	0.2	0.7	8.3	4.4	0.05	1.4
b5	8.2	1.4	3.9	3.5	1.0	0.1
b6	1.5	1.1	1.1	1.3	0.6	0.9
b7	0.9	0.7	0.6	0.8	0.6	0.8
e1	2.1	3	8.6	7.0	0.4	0.1
e2	0.3	0.5	4.6	12	0.04	0.07
e4	0.3	1.4	7.5	4	0.1	0.03
e5	1.4	0.7	1.2	1.0	0.3	0.2
e6	1.3	0.8	1.6	0.9	0.3	0.2
e7	0.8	0.7	1	0.8	0.3	0.1
%RSD	16	7	14	12	8	4

results are listed in Table 2.4 and plotted as a bar graph in Figure 2.16. If the sample is too large to fit into the graphite cup, the glass samples were wrapped in clean paper and crushed to small particles with a hammer. The crushed samples were then immersed in the concentrated HNO<sub>3</sub> acid for 30 minutes and followed by washing three times with distilled and deionized water. The washed sample was then dried with an IR lamp for about 30 min. About 3 mg of the dried sample was weighed into the precoated graphite cup and proceeds to DSI-ICP analysis. The absolute elemental concentrations of these glass samples have not been calibrated due to the lack of the appropriate glass standards at this point and due to the fact that the object of this project was to answer whether the glass samples are from the same category (such as sheet glass) or whether the samples are the same/similar. The elements Ba, Mn, Mg, Fe, Al, and Sr were found a sensitive index for grouping glass samples. Table 2.4 and Figure 2.16 are the relative signal (peak area)

intensities (relative sample b1). Samples b1, b6, b7, e5, e6, and e7 are sheet glass and samples b2, b3, b5, e1, e2, and e4 are container glass. From Figure 2.16, the differences of the two types between the glass are quite obvious. Except for sample b1, each sample was analyzed two times and the results are the average peak area intensity of the two replicates. Sample b1 was run 5 replicates and was used to evaluate the standard deviation and precision (%RSD) of the method; the %RSD data are listed in the last row of Table 2.4.

Trace elements in fly ash has also been analyzed by the Ar-N<sub>2</sub>(2%) mixed gas DSI-ICP-AES with the silicate coated probe.

The silicate coated probe enables efficient vaporization of some carbide forming elements. However, refractory elements such as Zr, W, and Ti still cannot be vaporized with the coated probe, yet show strong signals with Ar-O<sub>2</sub>(20%) mixed gas plasma, as will be seen in next chapter.

## 2.8 Summary

A DSI-ICP-AES system was set up and software was designed for control, data acquisition and analysis. Different mixed gas plasmas were studied with the system to improve the vaporization characteristics of DSI. An Ar-N<sub>2</sub> mixed gas ICP was found to be useful in vaporizing, dissociating and exciting various analytes. The optimum amount of N<sub>2</sub> in the outer gas was ~ 2%(V/V) for powers of 1.75 to 1.8 kW. The effects of other foreign gases such as air and O<sub>2</sub> were similar at the 2% level. Detection limits for Fe, Cd, Zn, Mn, and Cr were in the range of pg, while V was in the ng level. The system should be very good for the simultaneous quantitative analysis of trace elements in small volumes of samples such as water, clinical fluids, and botanical samples. However the direct analysis of some nonvolatile elements, especially in refractory solid samples, was still problematic. Also the surface condition of the graphite cup can strongly affect the

precision and sensitivity attained. A pyrolytic graphite cup may help. The Ar-N<sub>2</sub> (2%) mixed gas DSI-ICP-AES with SiO<sub>2</sub> coated graphite cup has effectively eliminated the carbide forming interferences and been successfully used for analyzing different glass samples and fly ash samples. Surface coating the sample cup with some kind of polymer film could also be used. However in the next chapter it will be seen that an Ar-O<sub>2</sub> mixed gas DSI-ICP with higher levels of O<sub>2</sub> (~ 20%) can solve many of these remaining analytical limitations.

## References

1. T. B. Reed, *Journal of Applied Physics* 32(5), 821 (1961)
2. T. B. Reed, *Journal of Applied Physics*, 32, 2534 (1961)
3. S. Greenfield, I. LL. W. Jones, C. T. Berry and L. G. Bunch, *Proc. Soc. Anal. Chem.*, 2, 111 (1965)
4. S. Greenfield, I. L. Jones and C. T. Berry, *Analyst*, 89, 713, (1964)
5. D. Truitt and J. W. Ronbinson, *Anal. Chim. Acta* 49, 401 (1970)
6. D. Truitt and J. W. Ronbinson, *Anal. Chim. Acta* 50, 61 (1970)
7. A. Montaser and J. Morlock, *Anal. Chem.*, 52, 255 (1980)
8. A. Montaser, V. A. Fassel and J. Zalewski, *Appl. Spectrosc.*, 35, 292 (1981)
9. E. H. Choot and G. Horlick, Winter Conf. Plasma Spectrochemistry, San Diego, Paper #47 (1984)
10. E. H. Choot and G. Horlick, 30th Annual Conference Of The Spectroscopy Society of Canada, vancouver, paper # a3 (1983)
11. Y. Q. Tang, Y. P. Du, J. C. Shao, C. Liu, W. Tao and M. H. Zhu, *Spectrochim. Acta* 47b, 1353 (1992)
12. G. A. Meyer and R. M. Barnes, *Spectrochim. Acta* 40b, 893 (1985)
13. G. A. Meyer and M. D. Thompson, *Spectrochim. Acta* 40b, 893 (1985)
14. E. H. Choot and G. Horlick, *Spectrochim. Acta* 41b, 889 (1986)
15. E. H. Choot and G. Horlick, *Spectrochim. Acta* 41b, 907 (1986)
16. E. H. Choot and G. Horlick, *Spectrochim. Acta* 41b, 925 (1986)
17. E. H. Choot and G. Horlick, *Spectrochim. Acta* 41b, 935 (1986)
18. A. Montaser, *Crc Critical Rev. Anal. Chem.* 18 (1), 45 (1987)
19. S. Greenfield and H. McD. McGreachin, *Anal. Chim. Acta* 100, 101 (1978)
20. W. T. Chan, Ph.D. Thesis, University of Alberta (1989)
21. D. Sommer and K. Ohls, *Fresenius Z. Anal. Chem.* 304, 97 (1980)
22. W. E. Pettit and G. Horlick, *Spectrochim. Acta* 41B, 699 (1986)

23. G. F. Kirkbright and L. X. Zhang, *Analyst* 107, 617 (1982)
24. Gy. Zaray, J. A. C. Broekaert and F. Leis, *Spectrochim. Acta* 43B, 241 (1988)
25. Gy. Zaray, P. Puba, J. A. C. Broekaert and F. Leis, *Spectrochim. Acta* 43B, 255(1988)
26. J. A. C. Broekaert, F. Leis, B. Raeymaekers and Gy. Zaray, *Spectrochim. Acta* 43B, 339 (1988)
27. J. P. Matousek, R. T. Satumba and R. A. Bootes, *Spectrochim. Acta* 44b, 1009 (1989)
28. V. Karanassios and G. Horlick, *Spectrochim. Acta* 45B, 85 (1990)
29. Y. B. Shao and G. Horlick, *Appl. Spectrosc.* 40, 386 (1986)
30. W. T. Chan and G. Horlick, *Appl. Spectrosc.* 44, 380 (1990)
31. W. T. Chan and G. Horlick, *Appl. Spectrosc.* 44, 525 (1990)
32. V. Karanassios and G. Horlick, *Spectrochim. Acta* 44B, 1345 (1989).
33. V. Karanassios, G. Horlick and M. Abdullah, *Spectrochim. Acta* 45B, 105 (1990)
34. E. D. Salin and G. Horlick, *Anal. Chem.* 51, 2284 (1979)
35. A. Lorbe and Z. Goldbart, *Analyst* 110, 155 (1985)
36. I. B. Brenner, A. Lorber and Z. Goldbart *Spectrochim. Acta* 42B, 219 (1987)
37. V. Karanassios and G. Horlick, *Spectrochim. Acta Rev.* 13, 2, 88 (1990)
38. G. F. Kirkbright and S. J. Walton, *Analyst* 107, 276 (1982)
39. A. G. Page, S. V. Godbole, K. H. Madraswala, M. J. Kulkapni, V. S. Mallapurkar and B. D. Joshi, *Spectrochim. Acta* 39B, 551 (1984)
40. M. Abdullah, K. Fuwa and H. Haraguchi, *Spectrochim. Acta* 39B, 1129 (1984)
41. C. V. Monasterios, A. M. Jones and E. D. Salin, *Anal. Chem.*, 58 (4), 780-5 (1986)
42. M. M. Habib and E. D. Salin, *Anal. Chem.*, 57 (11), 2055-9 (1985)
43. C. W. McLeod, P. A. Clarke, and D. J. Morthorpe, *Spectrochim. Acta* 41B, 63 (1986)
44. E. D. Salin and R. L. A. Sing, *Anal. Chem.* 56, 2596 (1984)

45. D. W. Boomer, M. Powell, R. L. A. Sing and E. D. Salin, *Anal. Chem.*, 58 (4), 975-6 (1986)
46. V. Karanassios and G. Horlick, *Spectrochim. Acta 44B*, 1361 (1989).
47. V. Karanassios and G. Horlick, *Spectrochim. Acta 44B*, 1387 (1989).
48. M. Abdullah and H. Haraguchi, *Anal. Chem.* 57, 2059 (1985)
49. M. Abdullah, K. Fuwa and H. Haraguchi, *Appl. Spectrosc.* 41, 715 (1987)
50. L. X. Zhang, G. F. Kirkbright, M. J. Cope and J. M. Watson, *Appl. Spectrosc.* 37, 250 (1983)
51. N. W. Barnett, M. J. Cope, G. F. Kirkbright and A. A. H. Taobi, *Spectrochim. Acta 39B*, 343 (1984)
52. L. Blain, E. D. Salin and D. W. Boomer *J. Anal. At. Spectrom.* 4, 721 (1989)  
MS&AES
53. G. E. M. Hall, J. C. Pelchat, D. W. Boomer, and M. Powell *J. Anal. At. Spectrom.*, 3 (6), 791-7(1988)
54. R. L. A. Sing and E. D. Salin, *Anal. Chem.*, 61 (2), 163-9 (1989)



## Chapter 3

### Ar-O<sub>2</sub> mixed gas direct sample insertion system

#### 3.1 Introduction

As discussed in the previous chapter, when small amounts of diatomic molecular gases such as N<sub>2</sub>, O<sub>2</sub>, and air are added into the outer and intermediate stream of an ICP, the plasma shrinks and its vaporization capability increases compared to a pure Ar plasma due to the increased energy density and better thermal conductivity of the molecular gas. Air, N<sub>2</sub> and O<sub>2</sub> show a similar signal enhancement when they are added at about the 2% level. However, quantitative vaporization of refractory elements with an Ar-N<sub>2</sub> mixed gas DSI-ICP is a problem. As was seen in the last chapter (Figure 2.14), even after a 250 second "burn" of a 1 µg V solution residue sample in an Ar-N<sub>2</sub> mixed gas ICP, appreciable V signal was still observed. This problem is even more pronounced with refractory solid samples. Similar results were observed by Pettit and Horlick [1] with an Ar-O<sub>2</sub> mixed gas DSI-ICP-AES system. They reported that by adding small amounts of O<sub>2</sub> (i.e., 0.5% to 6%) to the outer gas, the signals became sharper and stronger for all the elements tested (from volatile elements such as In, Cd, and Zn to moderately volatile elements (Mn), and finally to the carbide forming elements (Ni)). In their case, the addition of O<sub>2</sub> was intended to consume the graphite cup, in an analogous manner to that of the gas composition control sometimes used with the Stallwood Jet in dc arc techniques. However with the amount of O<sub>2</sub> they added it was not possible to consume the cup in a reasonable amount of time; therefore, the function of O<sub>2</sub> probably merely increased the energy density of the plasma, not unlike the Ar-N<sub>2</sub> plasma studied in Chapter 2. In fact, their signal profiles were similar to those presented in Chapter 2.

Their largest signal enhancement was obtained with 1% O<sub>2</sub> (instead of 6%) and for Ni the signal was not very intense and had a long vaporization time [1].

Nevertheless, the idea is of great interest and it stimulated the use of a larger amount of O<sub>2</sub> in a mixed gas DSI-ICP for our studies described in this chapter. *By adding enough O<sub>2</sub> into the plasma, the role of O<sub>2</sub> in consuming the graphite cups should come into play and, presumably, the samples can be burned into the plasma efficiently to facilitate the direct analysis of elements with different volatilities in hard to vaporize matrices.* Analytical results using an Ar-O<sub>2</sub> mixed gas DSI-ICP-AES for the determination of trace elements in oil standards, Al alloy standards, botanical standards, and Al<sub>2</sub>O<sub>3</sub> base standards will be presented and discussed in this chapter.

### 3.2 System descriptions and operations

The schematic diagram of the Ar-O<sub>2</sub> DSI-ICP-AES system is shown in Figure 3.1. The same system as described in the previous chapter was used except that the mixed gas was Ar-O<sub>2</sub> instead of Ar-N<sub>2</sub>. The main hardware setup and typical operating parameters were listed in Table 2.1. The same software as described in the previous chapter was used. Now, however, about 20% O<sub>2</sub> (V/V), instead of 2%, is added to the outer and intermediate gas flows. The central gas (Ar) was run through a plastic bottle containing distilled water. The water vapor carried by the Ar gas helped to quench the arc filament that tends to form in the central tube during insertion and retraction of the sample probe.

To run a mixed gas plasma the capacitance in the ICP matching box must be changed to keep the reflected power low. By adding O<sub>2</sub> to the Ar, the plasma shrinks, thus altering the matching parameters; however the effect is not as serious as with a N<sub>2</sub> mixed gas plasma. With the addition of 20% O<sub>2</sub>, the plasma's volume is reduced about 1/3 at 1.8 kW forward power. After this more O<sub>2</sub> can be added with little change in the plasma's appearance. The O<sub>2</sub> content (~ 20%) was chosen such that the graphite cup is

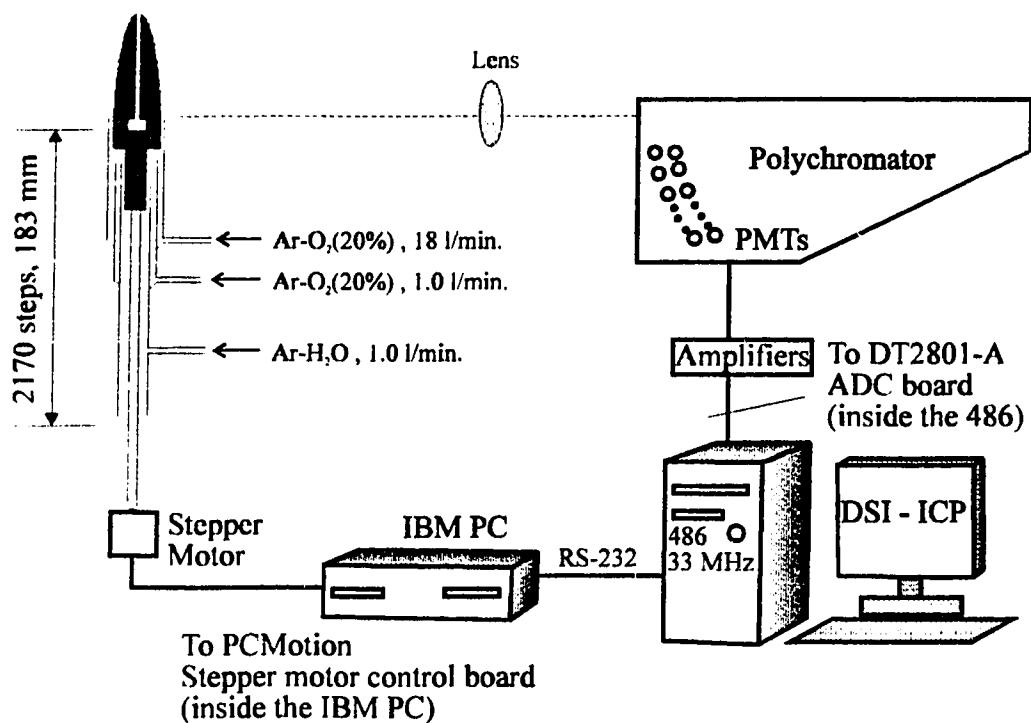


Figure 3.1 Schematic diagram of an Ar-O<sub>2</sub> (20%) mixed gas Direct Sample Insertion System for Inductively Coupled Plasma Atomic Emission Spectrometry (DSI-ICP-AES)

consumed in a reasonable time (~ 60 s). If the burning process is too slow the analysis time would be too long resulting in poor S/N ratios due to drawn out signals. On the other hand, if the burning process is too fast spattering of the sample tends to occur.

Spattering can be a serious problem with an Ar-O<sub>2</sub> mixed gas DSI-ICP-AES, especially for those samples that will react with O<sub>2</sub> at high temperature, such as Al filings, and botanical samples. A boiler cap may help to prevent sample loss from spattering [2]. However, the cap can fall off in the plasma during the burning process because the side walls of the graphite cup burn out first in the Ar-O<sub>2</sub>(20%) mixed gas plasma. Mixing a sample with graphite powder prevents the formation of glassy globules and also considerably smoothes out the burn in an Ar plasma [3, 4]. This, however, raises detection limits due to dilution and as well contamination that may occur as a result of the mixing process [4]. Heating the sample in pure Ar plasma or an Ar-N<sub>2</sub> mixed gas plasma followed by insertion of the sample into an Ar-O<sub>2</sub> plasma led to considerably smoother burns. However, switching between outer gases introduces extra complexity in the operation and causes difficulties in keeping reproducible operation parameters, which results in poorer precision. This approach has potential if one could automate the gas change over procedure.

Using smaller amounts of sample is probably the easiest way to eliminate sample spattering. For example, in the analysis of Al filings, the burning processes became very smooth when the sample load was reduced to about 0.2 mg. Examination of the probe after it was in the plasma for 10 seconds showed that the sample melted and dispersed on the inner surface of the graphite cup. This sample load is too small to be weighed accurately; therefore an internal standardization was used to correct for sample weight variations. Also special attention may have to be paid to sample homogeneity when analyzing solid samples because the rather limited sample size of the DSI system can lead to significant sampling errors when dealing with inhomogeneous samples. If the

average concentration of an inhomogeneous sample is required several replicate analyses should be performed.

For samples that have an organic matrix, an ashing step must be applied before the sample is inserted into the core of the plasma; otherwise the sample will be lost in the explosive release of vapors as the matrix is rapidly vaporized.

All graphite cups were pre-burned in the Ar-O<sub>2</sub> mixed gas plasma for about 30 seconds to remove impurities and contamination. This pre-burning step is also important in controlling the total analysis time as some of the graphite cup is burned off. This makes the cup wall thinner and it is thus easier to completely burn off the cup during an analysis run. During a run the pre-burned graphite cup is consumed within 80 seconds, resulting in the shape shown in Figure 3.2(b). For comparison, a new graphite cup used in this work is shown in Figure 3.2(a). The burning speed is also dependent on the density of the graphite cup and lower density graphite consumed more rapidly.

Samples, once loaded in the probes, were arranged in an aluminum holder placed in a plastic glass chamber with an IR lamp in the roof of the chamber for the purpose of drying if necessary. The chamber helps to effectively eliminate contamination from dust in the air. Samples may also be dried inside the ICP torch by controlling the position of the probe. However, it was found that the external drying process with the IR lamp in the chamber is more efficient and easier, especially when large numbers of samples are to be analyzed.

### 3.3 Signal characteristics with an Ar-O<sub>2</sub> mixed gas plasma

Vanadium signals for both Ar-O<sub>2</sub> and Ar-N<sub>2</sub> mixed gas DSI-ICP-AES are shown in Figure 3.3. Window (a) of Figure 3.3 shows the signal for the first insertion of 1 µg V as a solution residue in an Ar-N<sub>2</sub> mixed gas ICP; and window (b) shows the signal for the 5th insertion of the same sample into the Ar-N<sub>2</sub> mixed gas ICP (scale expanded 10

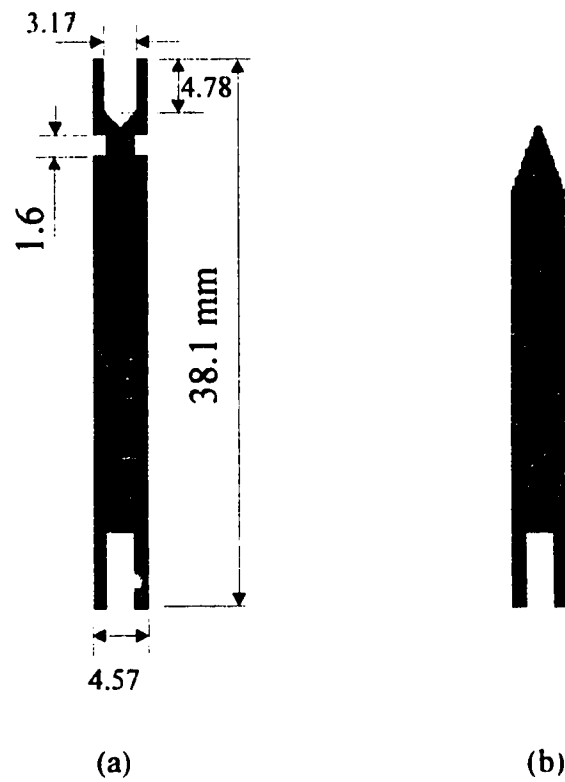


Figure 3.2 Graphite sample probes before (a) and after (b) burned in Ar-O<sub>2</sub> (20%) mixed gas plasma

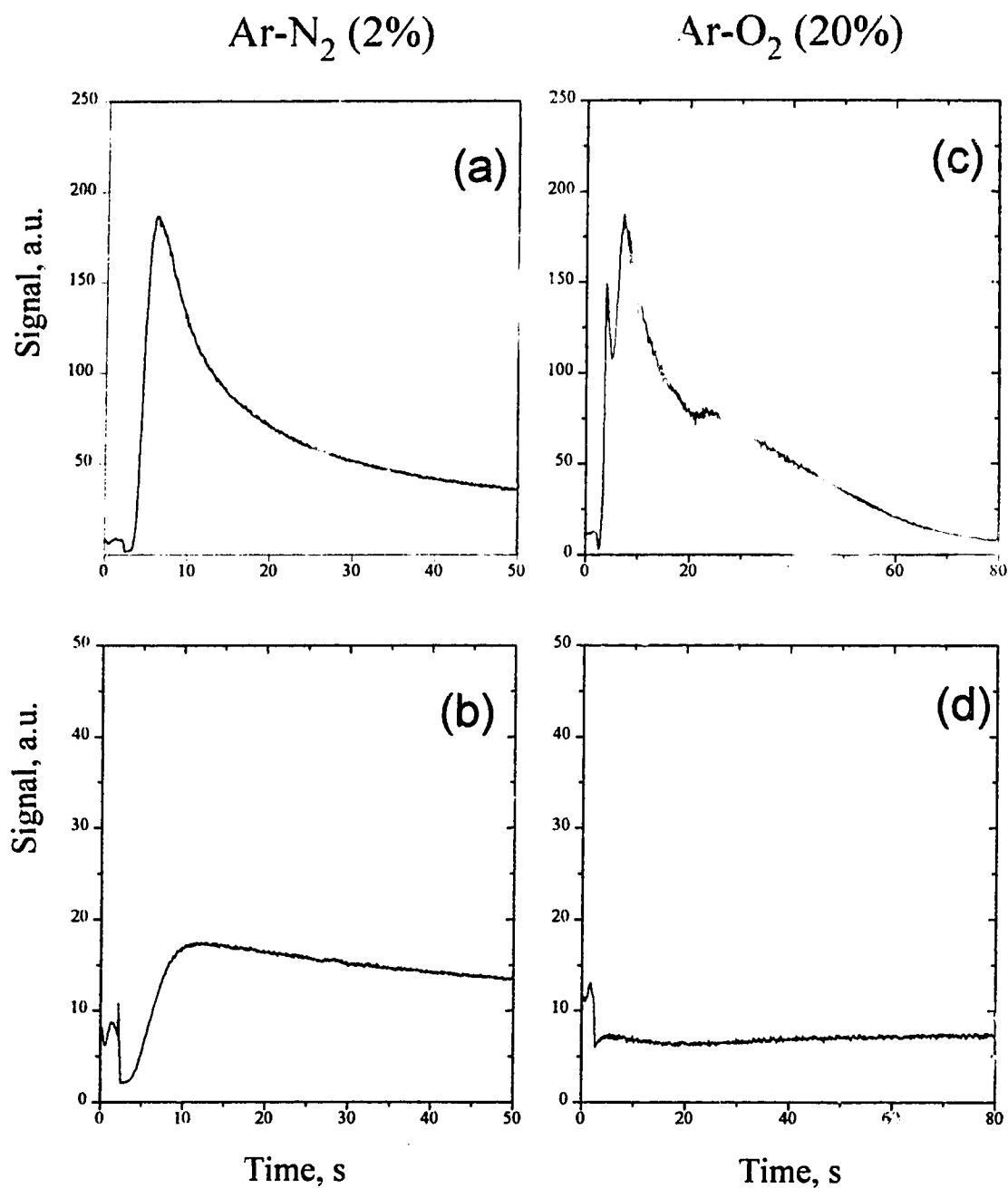


Fig. 3.3 DSI-ICP signals of 1000 ng V in Ar-N<sub>2</sub> (2%) and Ar-O<sub>2</sub> (20%) mix gas ICP  
 (a) 1st insertion in Ar-N<sub>2</sub> (2%) plasma; (b) 5th insertion in Ar-N<sub>2</sub> (2%) plasma;  
 (c) 1st insertion in Ar-O<sub>2</sub> (20%) plasma; (d) 2nd insertion in Ar-O<sub>2</sub> (20%) plasma  
 Sample, Solution residue. Power 1.8 kW.

All signals have been corrected to the same gain

times), Window (c) of Figure 3.3 shows the signal for the first insertion of 1  $\mu\text{g}$  V as a solution residue into an Ar-O<sub>2</sub>(20%) mixed gas ICP; and window (d) shows the signal for the 2nd insertion of the same sample into the Ar-O<sub>2</sub> mixed gas ICP. While the Ar-N<sub>2</sub> mixed gas plasma does help to enhance the vaporization capability of the plasma, the vaporization is still incomplete for some nonvolatile or carbide forming elements such as V. Even after 250 seconds in the Ar-N<sub>2</sub> mixed gas ICP the V signal is still appreciable (Figure 3.3b); while with the Ar-O<sub>2</sub> mixed gas ICP the V is almost completely vaporized within 80 seconds. With the Ar-N<sub>2</sub> plasma no signals were observed for elements such as Zr and Ti while in the Ar-O<sub>2</sub> mixed gas ICP most of the elements can be "vaporized" completely within 120 seconds.

Although the idea of vaporizing the sample from the probe sounds straightforward the process is likely very complicated. Some of the events that might occur are qualitatively described below.

Some solid sample will be melted upon heating in the plasma. The melted sample may wet the inside surface of the graphite cup or form beads depending on the surface tension of the melted sample; some of the melted sample may be soaked into the graphite while some may react with the probe. At the same time low boiling point components will be evaporated and yield emission signals while the refractory species will remain in the graphite cup. As the graphite cup is burned away the analyte may be carried into the plasma as a gas or in the form of fine particles. If fine enough the particles are then evaporated in the plasma. If the particles are too large, however, the evaporation may not be complete and analyte is lost. As is generally known, in an analytical ICP using pneumatic nebulization, aerosol droplets of less than 10  $\mu\text{m}$  can be completely vaporized. The acceptable particle size for dry plasmas can be slightly larger than 10  $\mu\text{m}$  depending on the matrix, plasma composition, and power. Collecting and characterizing particles from the ICP exhaust could provide useful information in elucidating the mechanism of the vaporization process in DSI-ICP. Other processes such as decomposition and



chemical reaction of the sample with graphite and plasma gases may also take place (i.e. oxide formation, carbide formation). The overall process is a complicated mixture of thermal evaporation, chemical reaction, and mechanical disintegration. The boiling points for some elements and their oxides and carbides were listed in Table 2.2. The boiling points for some refractory elements such as Zr, Ti and their carbides or oxides are much higher than 2000 °C which is the estimated thermal temperature of the DSI probe by different methods [7-10]. Therefore the vapor pressure of these elements should be very low in the plasma and direct thermal vaporization of these elements from the probe, it would seem, would be difficult. However, to simplify matters, we will still use terms such as "vaporization", "volatilization", *etc.*, even though a complex "vaporization" mechanism is likely in operation with the Ar-O<sub>2</sub> mixed gas DSI-ICP.

Signals for several elements in different samples run with an Ar-O<sub>2</sub> mixed gas DSI-ICP-AES system are shown in Figure 3.4. The x-axis is time starting from the insertion of the probe to the atomization position and the y-axis is signal intensity in arbitrary units. For easy comparison, the Y-axes are scaled the same (except for window i). The samples are oil (Figure 3.4(i)), Al base alloys (Figure 3.4(b), (e), (h)), aluminum oxide (Figure 3.4(a), (d), (g)), and botanical standards (Figure 3.4(c), (f)). Elements such as Zr, Ti, and Al are very difficult to vaporize with a pure Ar plasma yet show strong signals in a variety of samples (Figure 3.4(d), (g), (h)). Virtually all elements can be directly determined using this system.

It is no surprise to see that the same element shows very different vaporization patterns in different samples (e.g., comparing Figure 3.4(a), (b), (c), and (e) for Cu signals). The form of the element may be different in different samples and may also be changed with temperature during the vaporization process. Different matrices will also affect the vaporization pattern. With an organic matrix the vaporization of analyte takes only a few seconds resulting in strong and sharp signals (Figure 3.4(c), and (f));

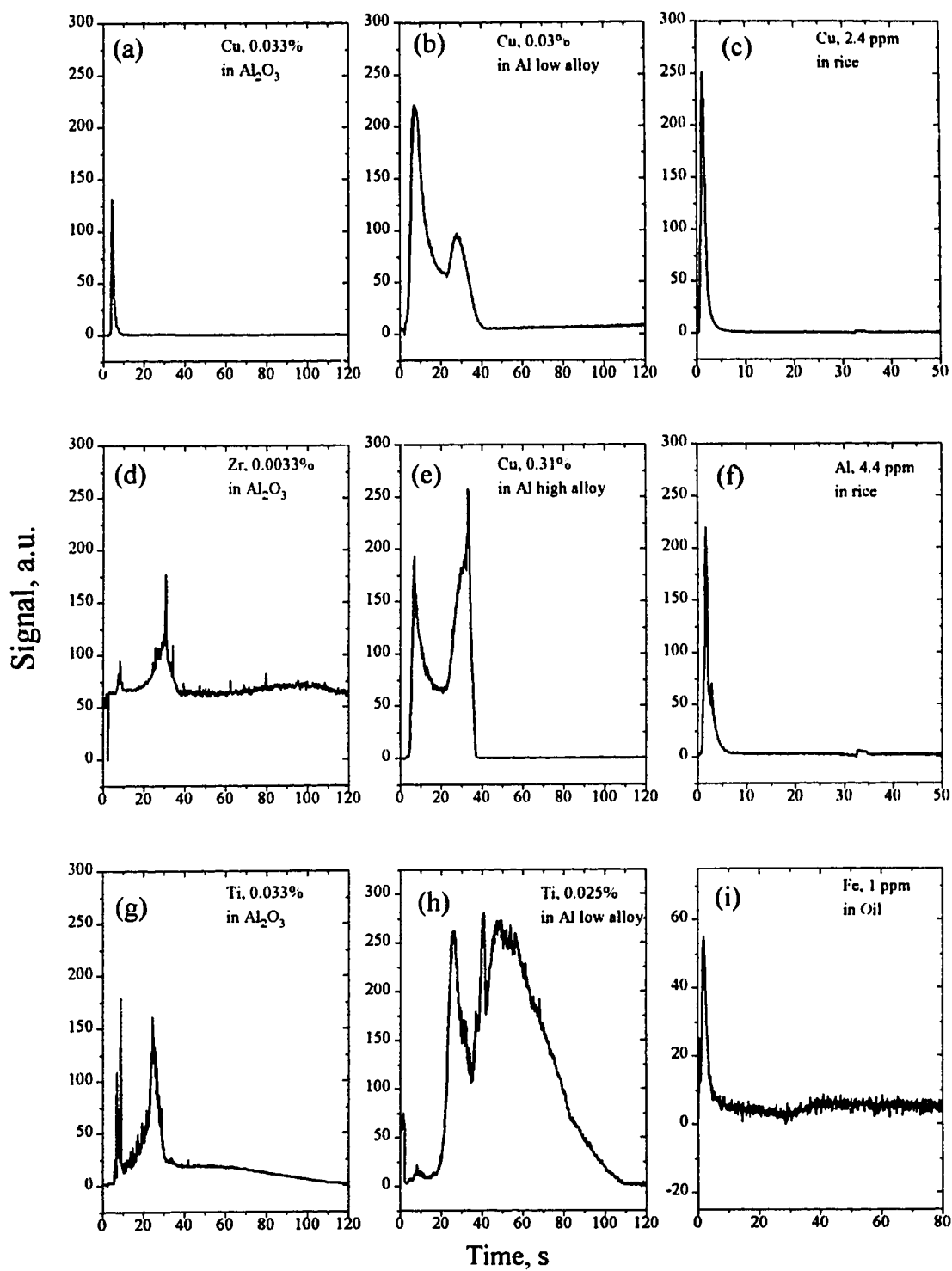


Fig. 3.4 Signal profiles of different elements in different samples with Ar-O<sub>2</sub> (2%) mixed gas DSI-ICP-AES

while with a refractory matrix the signal can last for over 100 seconds. It might be interesting, therefore, to concentrate the trace metals in some kind of organic ion exchange resin and then analyze the resin directly with the DSI-ICP-AES system. Improved sensitivity and higher vaporization efficiency can be expected.

With the Ar-O<sub>2</sub> mixed gas ICP, the base line gradually increases towards the end of a run. A probable explanation for this is that the plasma becomes brighter and brighter as the graphite electrode becomes smaller and smaller (Figure 3.2b). This may result in problems for background correction and a blank sample subtraction may be necessary. To do blank subtraction an empty graphite probe was run after, say, 10 sample runs. During data processing, both the sample signal and blank signals were normalized to the same gain and then the blank signal was subtracted (point by point) from the sample signal. However, such a subtraction may not be very accurate as the sample and blank are not analyzed at the same time and may not have identical burning processes. The ideal correction method would be to use simultaneous off-line background correction. In this case the analyte spectral line (say, ZrII 343.82 nm line) and the off-line background (say, 343.0 nm) are monitored simultaneously. Real time changes on background signals can be corrected more accurately. However, this requires spectrometers incorporating array detectors such as PDAs. An automatic sampling DSI-ICP-AES system with a PDA detector is under development in this lab but was not yet available for this work.

Signals for Zr, V, and Ti before and after blank subtraction are shown in Figure 3.5. Before blank subtraction the signals are superimposed on a rising base line (upper row of Figure 3.5) making accurate signal measurement difficult. After blank subtraction a much better defined signal profile is generated (see lower row of Figure 3.5). However, because of the limitation of such blank subtraction (as mentioned above) over and/or under subtraction may occur for individual data point. As a result, in addition to error propagation, the subtracted signals are more noisy. The overall signal profile may

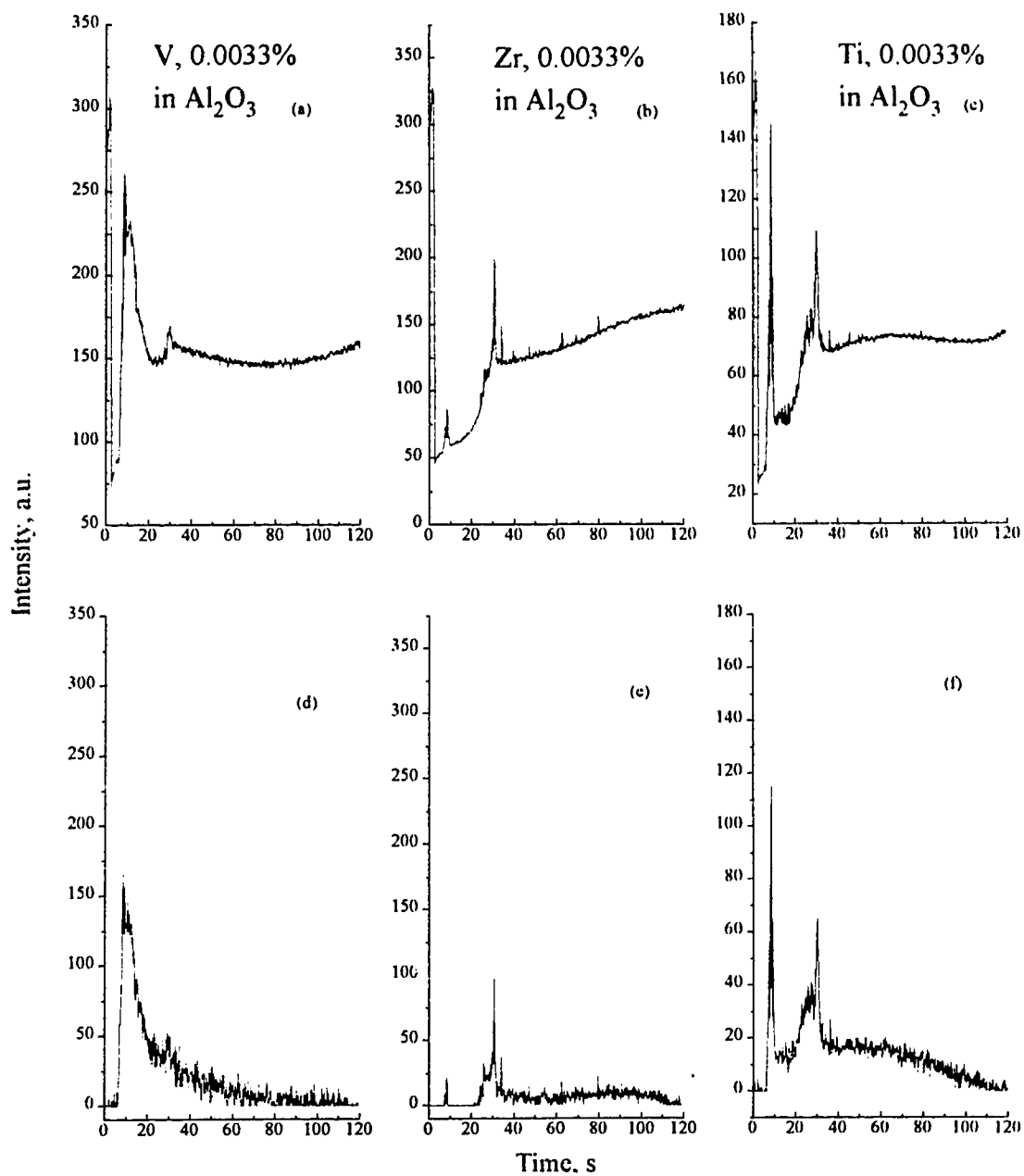


Fig. 3.5 Signal profiles of 0.0033% V, Zr, and Ti in  $\text{Al}_2\text{O}_3$  based standard (TS64) with Ar- $\text{O}_2$  mixed gas DSI-ICP-AES

Upper, without blank subtraction; Lower, after blank subtraction

also be over and/or under subtracted. For example, the subtracted signal of V (Figure 3.5(d)) should be zero after 100 s; yet a negative average signal (between 100 and 120 s) was obtained because of uncontrollable variations from run to run. Therefore, after the blank subtraction, further adjustment (or offset) of the base line may be necessary for accurate peak height or peak area measurement. The data processing program can do the blank subtraction and base line adjustment automatically.

### **3.4 Effect of probe geometry**

Probes that can provide efficient and smooth burning are the primary consideration with Ar-O<sub>2</sub> mixed gas DSI-ICP-AES. Probes (B), (D), and (F) (see Figure 2.4) with a long undercut usually provide sharp and intense signals. However the undercut part of these probes burns off too quickly, and the head of the probes then falls into the plasma resulting in loss of the sample. Usually, probe (E) was used for Al filings and liquid samples. This probe has a maximum capacity of 20 µL at a time. Probe (A) was used for botanical samples and it could hold up to 10 mg of sample. Use of probe (E) usually results in more intense and sharper signals because it is shallower than probe (A) and therefore the sample has more chance to interact with the plasma and burn off faster.

## **3.5 Quantitative analytical performance of Ar-O<sub>2</sub> mixed gas DSI-ICP-AES**

### **3.5.1 Aqueous solution samples**

Aqueous solution residue samples are the most easily studied samples with DSI. The basic performance of the Ar-O<sub>2</sub> plasma was tested using 10 µL of a multielement standard over the range of 0.1 to 100 ppm (except for Cr). With an Ar-O<sub>2</sub> mixed gas, most of the elements can be completely vaporized within 120 seconds. Calibration

curves of log-log plot for Cu, Mn, Fe, Cr, V, and Ni are shown in Figure 3.6. Linear response is indicated in all cases.

### **3.5.2 Engine oil samples**

#### **3.5.2.1 Introduction**

Of all analyses used for the determination of inorganic elements in petroleum products, the determination of wear metals in used engine oil has received the most attention. Any technique applied to the analysis of wear metals in used oils is also applicable to the analysis of additives in oil and to the analysis of trace metal content in crude oils.

The determination of wear metals and contaminating metals in used lubricating oil is of importance in preventative maintenance programs for engines. Such programs can be applied to any type of engine that uses lubricating oil, and extensive maintenance programs are used routinely in many laboratories connected with various industries (i.e. airlines, railroads). Such programs can predict engine failures from an increase in trace metal levels in the oil due to various causes, such as excessive wear, bearing failure, and radiator leaks. Problem areas and corresponding metals are listed in Table 3.1 [11]. A significant increase in concentration of the element in the lubricating oil compared to the blank value (the data in brackets of Table 3.1, for example) indicates excessive wear of the parts that contain the element. For example, when the Sn concentration is found to be higher than 15 ppm in lubricating oil, excessive wear of bearings may have occurred. The blank value of elements in lubricating oil is dependent on the type of engine and on the manufacturer. Such analytical programs not only save millions of dollars but also save lives, owing to the avoidance of impending engine failures. Also the

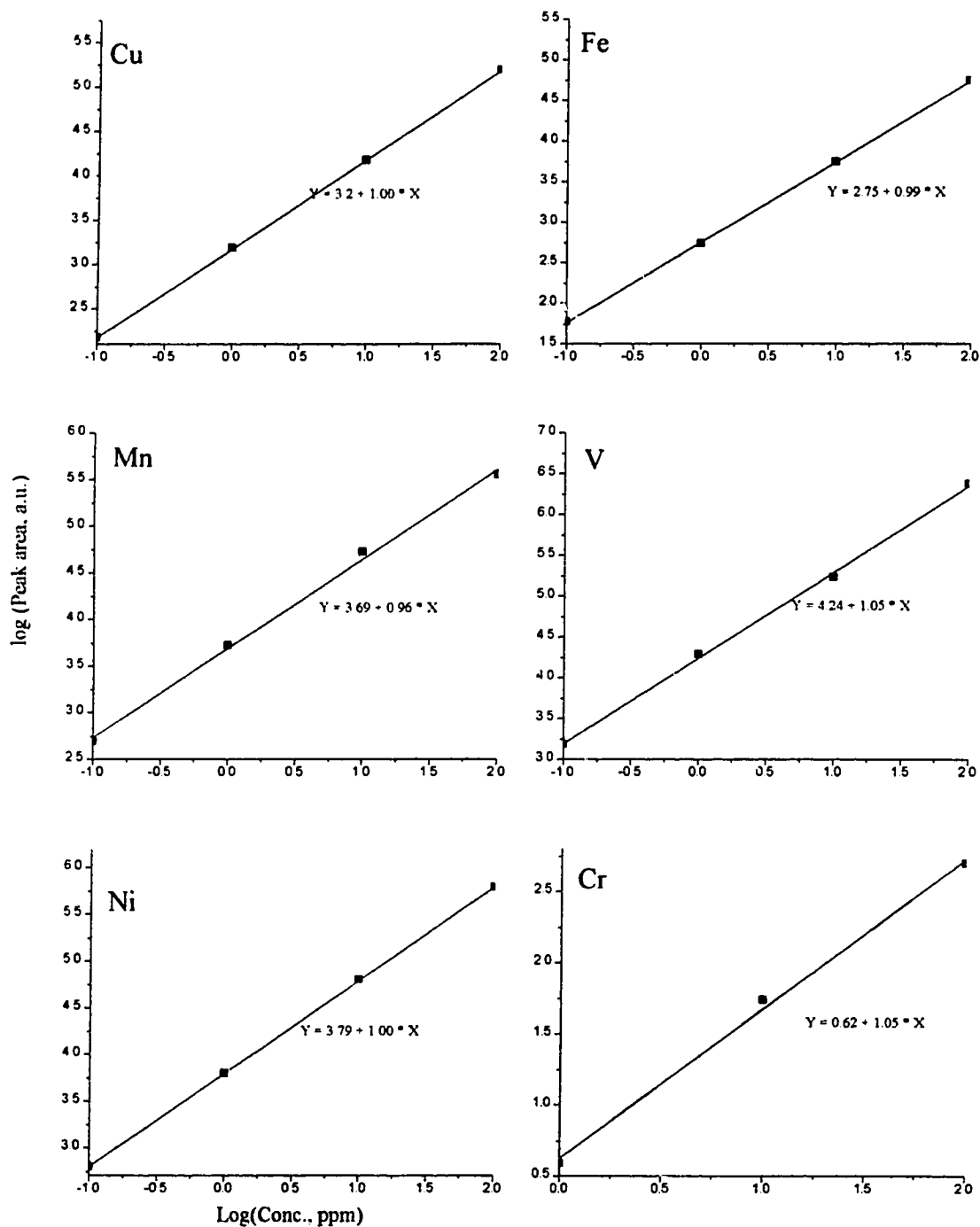


Fig. 3.6 Calibration curves of elements in solution standard sample (SM20) with Ar-O<sub>2</sub>(20%) mix gas DSI-ICP-AES.

Sample, (0.1 -100 ppm)x10  $\mu$ L , except for Cr; Power, 1.75 kW; Obs. time, 60 s;

determination of trace metals in refinery feeds may disclose those elements that may alter the refining process by acting as catalyst poisons.

Traditionally the determination of wear metals in engine oil has been performed by atomic absorption (both flame and flameless) or spark emission using a disc electrode (Rotrode) rotating in the oil. These techniques are effective for oil sample analysis due to their speed and simplicity. The spark emission method provides a very fast analysis because it requires minimum sample pretreatment and has simultaneous multielement capability. The AA method usually provides better precision and, with flameless AAS, better sensitivity but is only good for one element at a time.

Table 3.1 Metals analyzed in lubricating oils and areas associated with possible trouble [11]

Element	Possible problems with Aircraft	Possible problems with Railroad diesel engine
Ag	Ag-Plated spline	Wrist-pin bearings
Al	Lubricating pump	Bearings
B		Water leaks
Cd		Bearings
Cr	Cr-plated parts	Water leaks
Cu	Bearings	Bearings
Fe	Excess wear various parts	Excess wear various parts
Mg	Gearbox housing	
Na	Saltwater leak	
Ni	Alloy constituent (7 ppm)	Alloy constituent
Pb	Bearings	Bearings
Si	Filter failure → airborne dirt	Filter failure (8 ppm) → airborne dirt
Sn	Bearings (15 ppm)	Bearings
Oil additives		Depletion

Because of its good sensitivity and precision, ICP-AES has been applied to the analysis of petroleum products since the early 70s [12, 13]. Some sample treatment such as dilution with certain organic solvents (usually xylene) of low viscosity is necessary before the oil sample can be analyzed using a pneumatic nebulization ICP system.



Carbon deposition on the sampling tube tip is a nagging problem when conventional nebulization ICP systems are used. The analysis is frequently complicated by the presence of sediments/particulates and the analyst must determine whether these sediments/ particulates are to be included or excluded from the analysis [14]. Segregation of particulates in oil samples during the transportation stage is a serious problem affecting the accuracy of the conventional nebulization ICP method. This problem is inherent to any nebulization-spray based method. Because only about 5% of the sample passes through the spray chamber, larger particles including particulates in oil samples are selectively discarded. There has been much debate over the accuracy of flame AA methods because of this fact. If detection limits lower than those obtained by diluting the sample are required, the sample must be ashed prior to analysis and that involves several steps: forming porphyrins, burning, dissolving in HCl, *etc.*. For the determination of some volatile elements such as As and Hg, the oils may have to be wet oxidized with  $\text{HNO}_3$  and  $\text{H}_2\text{SO}_4$  prior to analysis. In the case of Hg, this wet oxidation must be performed under total reflux if the Hg is to be quantitatively retained.

The DSI-ICP method may prove to be a powerful tool for handling these kinds of samples as it may overcome many of the problems mentioned above. There is virtually no need for any sample pretreatment. One just pipettes 10  $\mu\text{L}$  of an oil sample into the graphite cup, which is dried under an IR lamp and then subjected to DSI analysis.

### 3.5.2.2 Results and discussion

An *in situ* ashing cycle right under the plasma is critical for oil samples before inserting the probe into the core of plasma for vaporization. The plasma is extinguished by the rapid release of gases that result from the vaporization of organics in the plasma if there is no ash cycle prior to the final insertion. During ashing, burning is observed inside the graphite cup after about 5 to 10 seconds in the ashing position. The flame may

extend out of the cup and may reach the bottom of the plasma body. Improperly set ashing parameters, i.e., the ashing time and ashing position, may result in sample loss due to spattering of the incompletely ashed samples and/or to the pre-volatilization of analyte during the ashing stage. The ashing time is counted from the time that the sample probe is driven into the ashing position to the end of ashing cycle. The ashing position is defined as the distance between the top of the sample cup to the top of the load coil (TLC, see Figure 3.7).

The total ashing time is normally about 20 to 30 seconds and an ashing position of 19 mm below TLC ( see Figure 3.7) is used for engine oil analysis. Under this condition the ashing process can be completed efficiently without significant loss of analyte. Compared to the ashing time used with a pure Ar plasma DSI-ICP-AES (5 minutes) [2], our ashing time is considerably shorter which is probably due to the use of O<sub>2</sub> which helps to speed up the ashing process. When ashing time is less than 10 seconds and the ashing position is farther than 23 mm below top load coil the signals are abnormally low. This is because in these conditions the ashing is incomplete and the sample is ejected from the probe upon insertion into the atomization position. The ashing position that is directly related to the ashing temperature has a more pronounced effect on the signal intensity than that of ashing time. Improper choice of ashing conditions may result in loss of volatile analytes during the ashing period. It is possible to detect the signals of volatile elements released during the ashing time. However the sensitivity may be low as it is a function of probe position in the plasma (refer to Figure 2.10). Further studies on ashing conditions are necessary for the quantitation of volatile elements such as Hg, As, *etc.*. It must be noted that the ashing conditions will change with plasma parameters such as the plasma power, gas flow rate and especially the intermediate gas flow rate which may significantly affect the plasma's position and, in turn, affect the relative distance of

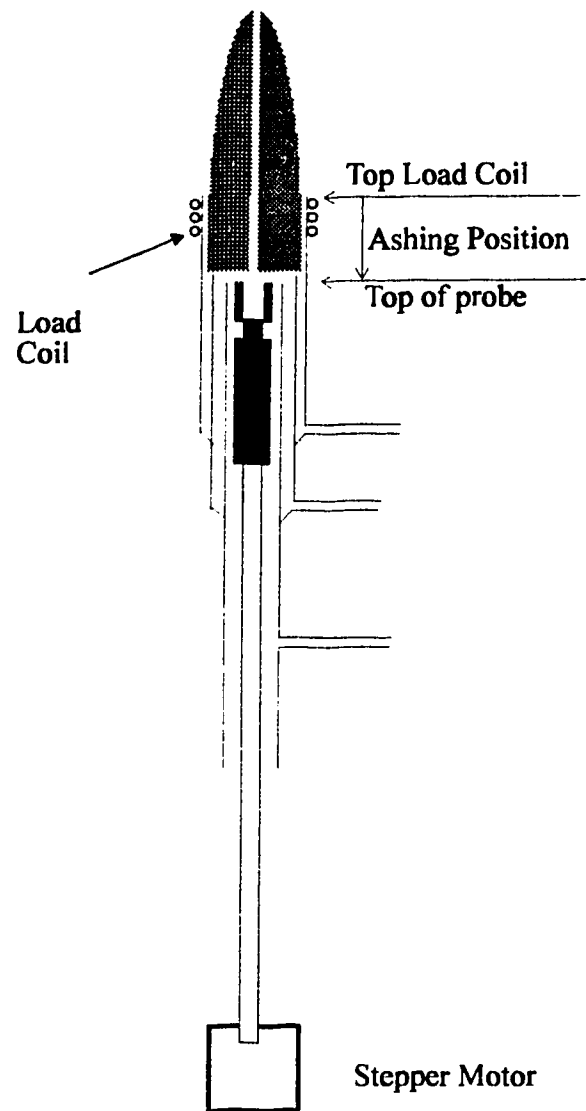


Figure 3.7 Schematic diagram for defining ashing position

the sample probe to the plasma body. Therefore the ashing parameters must be re-examined when the plasma operating conditions are changed.

Calibration curves, from 0.1 to 500 ppm, for Mn, Fe, Ni, Cu, and V in oil standards (CONOSTAN S21, CONOSTAN division, Conoco Inc., Ponca City, Oklahoma) are plotted in Figure 3.8. The standards of different concentration were made by successive dilution of the original standard (500 ppm) with base oil (CONOSTAN 75). The linearity of the calibration curves is fairly good with slopes close to unity for most of the elements. The poor slope of Mn may be the result of PMT saturation at high concentrations.

### **3.5.3 Particulate metals**

#### **3.5.3.1 Introduction**

Alloys are challenging samples for ICP-AES. In the first place many alloys are simply difficult to dissolve. Al alloys, especially low alloy Al is one of the samples that is very difficult to dissolve with normal acid digestion. High alloy Al is relatively easy to dissolve with acid digestion, but there is always some non-soluble residue of Si compounds and some Si may be lost during acid digestion by forming  $\text{SiH}_4(\text{g})$ . Therefore to be analyzed by a solution based ICP method, Al samples usually need to be dissolved in NaOH solution (with the help of  $\text{H}_2\text{O}_2$ ) followed by acidification with mineral acid before the sample can be analyzed. The basic solution can dissolve Si and other metals from the glassware, nebulizer, and ICP torch, and Si, Ti, and Sn may be precipitated out during acidification, unless all steps are carefully controlled. Therefore the development of an accurate, fast, and sensitive ICP technique that is able to analyze solid Al alloys directly would be very important for the Al industry.

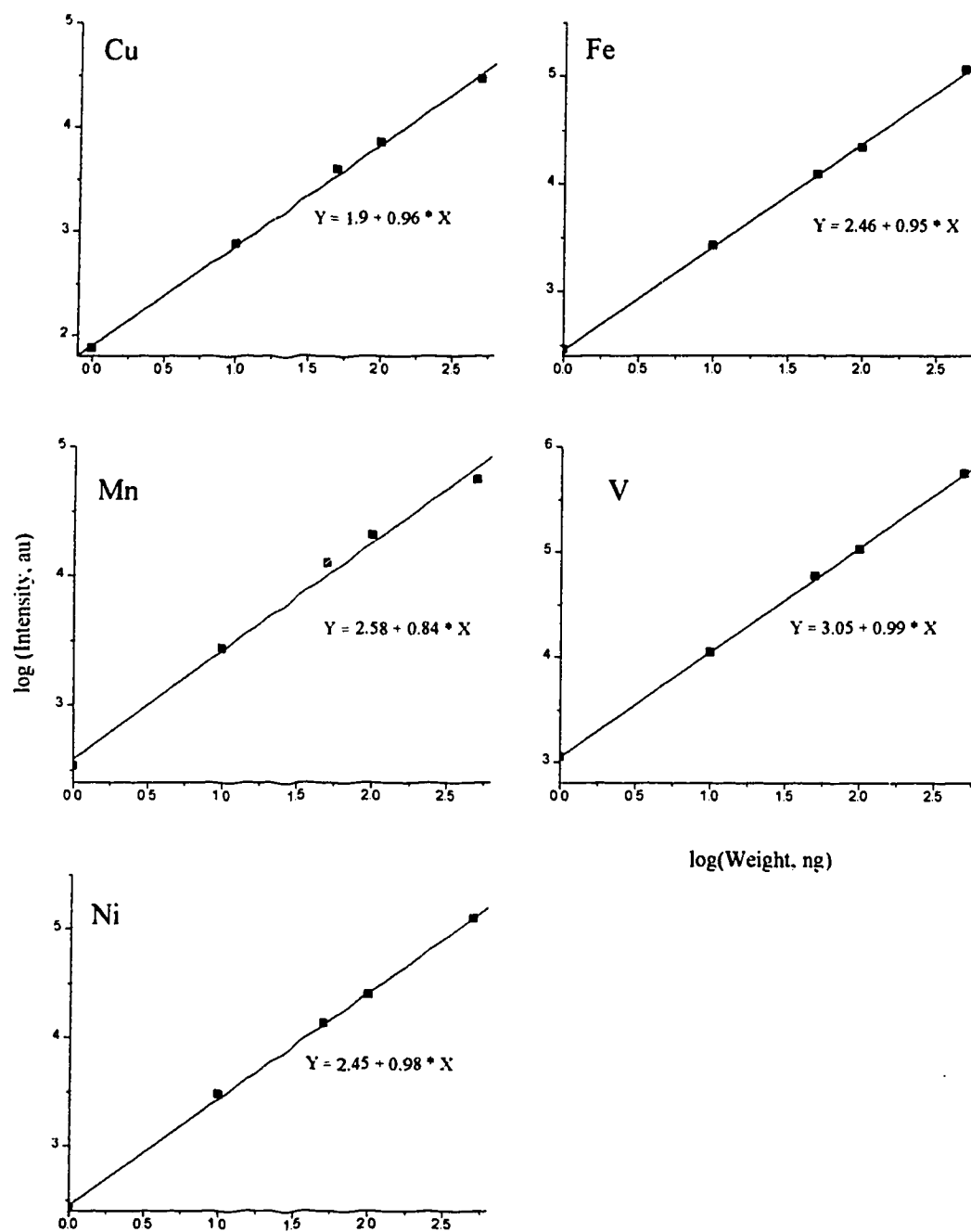


Fig. 3.8 Calibration curves (log - log) for elements in CONOSTAN, S21 by Ar-O<sub>2</sub> (20%) mix gas DSI-ICP-AES.

Sample, (0.1-500 ppm)x 10  $\mu$ L. Power, 1.75 kW. obs. time, 70 s;

### 3.5.3.2 Results and discussion

DSI-ICP-AES techniques were used to analyze Al filings and proved to be a fast, sensitive technique for the direct analysis of Al alloys. With the help of the Ar-O<sub>2</sub> mixed gas plasma virtually all of the elements in the Al samples could be determined. To analyze Al samples by DSI-ICP-AES, they had to be cut into small pieces; either filings or drillings worked just fine. There is no strict requirement for particle size, which is one of the major advantages of DSI over powder injection and slurry nebulization techniques. Samples of mg or sub mg size were weighed and added into preburned graphite cups followed by the direct insertion into the ICP for analysis. By using internal standardization the weighing procedure can even be eliminated.

Al alloy standard samples, from Alcoa and Alcan, have been analyzed with the Ar-O<sub>2</sub> mixed gas ICP-DSI system. The sample codes and specifications are listed in Tables 3.2-3.3. The results are plotted in Figure 3.9. The Y- axis is the peak area intensity ratio of the test element to the intensity of the internal standard element which was Al. The internal standard is mainly used to compensate for sample weight changes as the sample amount used was too small (in sub-mg range) to be weighed accurately. As discussed in Sections 3.2 and 3.3, if large amounts of Al were used spattering loss became a serious problem. The spattering may be attributed to reaction of the sample with O<sub>2</sub> at high temperature. There was, for example, no visible spattering with an Ar-N<sub>2</sub> or a pure Ar plasma with the same sample. From the calibration curves in Figure 3.9 one can see that both the low alloy Al and the high alloy Al samples show the same sensitivity since the data can be plotted on the same curve. This indicates that the matrix effect is small and a single calibration curve can be applied to the different aluminium samples.

These results are comparable to those obtained using a GD-MS method [15]. From the analysis it was found that the original concentration data for Ti in sample SA1170-6 from Alcoa was incorrect (see Table 3.3). It appeared as a wild point on the calibration

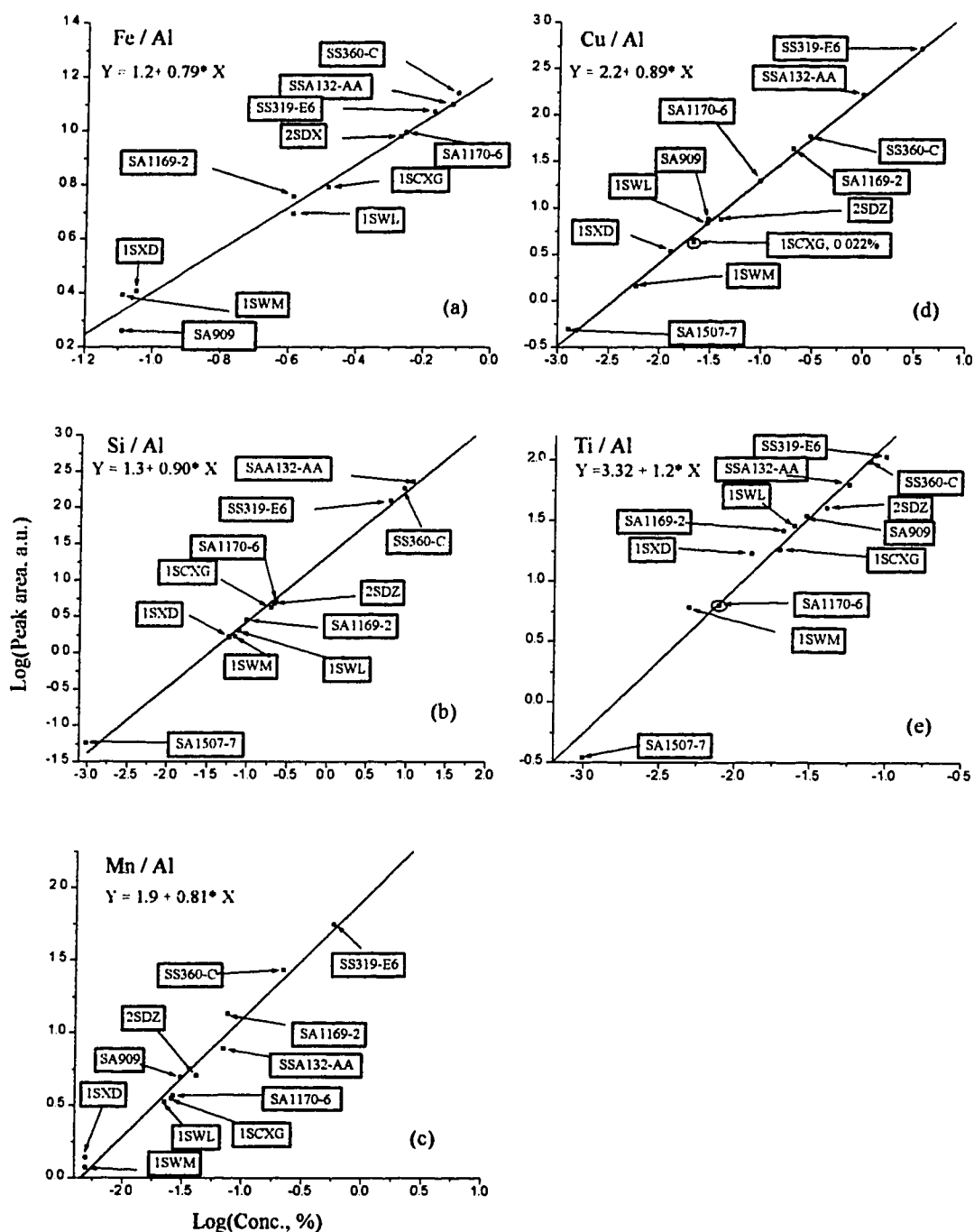


**Fig. 3.9 Calibration curves of log(peak area) vs. log(C%) of elements in Al standards (both high and low alloy A) by Ar-O<sub>2</sub>(20%) mix gas DSI-ICP-AES using Al as internal standard**  
**sample, Al particulate, ~ 0.2 mg (not weighted)**  
**ICP Power, 2.0 kW; obs. time, 120s**

curve. The calibrated value should be 0.008% instead of 0.039% (see Figure 3.9(e), the circled data point). Also the listed concentration data for Cu in sample 1SCXG from Alcan is ten times higher than it should be (see Table 3.2). The calibrated value for Cu concentration in this sample is 0.022% instead of 0.22% (see Figure 3.9(d), the circled data point). These results have been confirmed by solution based ICP-MS and GD-MS [15].

### **3.5.4 $\text{Al}_2\text{O}_3$ and $\text{SiO}_2$ based samples**

#### **3.5.4.1 Introduction**

$\text{Al}_2\text{O}_3$  and  $\text{SiO}_2$  are major components in most geological and soil samples. They are also important materials in the ceramic and glass industries. They are usually difficult-to-dissolve. Acid digestion of these samples usually involves overnight reaction using mixtures of  $\text{HF}/\text{HClO}_4/\text{HNO}_3$  or  $\text{HF}/\text{HClO}_4/\text{HCl}$ , etc. There are a number of rock forming minerals which will not be completely attacked by this dissolution procedure such as mineral zircon, mineral beryl, some garnets and spinels. Oxides such as ruby and  $\beta\text{-Al}_2\text{O}_3$  essentially can't be dissolved in any mineral acid. Fusion with strong fluxing reagents or dissolution with strong base is commonly used for attacking these samples. However the fusion method and the base decomposition method are the least desirable for ICP analysis not only because these methods may introduce a high salt content that may block the nebulizer and require large dilution, but also there is high risk of contamination from flux reagents and containers.

DSI-ICP has found its forte in the direct analysis of these difficult to dissolve samples. Calibration curves for nine volatile elements (Ag, As, Ge, Li, In, Pb, Sb, Sn, and Zn) in dc arc powdered standards, including Spex G-standards, Spex TS-6 silicon dioxide base standards, and Spex TS-6 aluminium oxide base standards, have been



Table 3.2. Sample information of ALCAN Al alloys

Elements	Concentration in sample (w%)				
	2S DZ	1S WL	1S WM	1S XD	1S CXG
Cu	0.041	0.03	0.006	0.013	0.22
Fe	0.54	0.26	0.082	0.09	0.33
Mg	0.035	0.015	0.005	0.006	0.25
Mn	0.042	0.023	0.005	0.005	0.026
Ni	0.045	0.022	0.006	0.005	0.023
Si	0.22	0.08	0.072	0.06	0.2
Ti	0.041	0.025	0.005	0.013	0.02
Zn	0.046	0.023	0.016	0.005	0.027
Bi	0.059	0.018	0.007	0.006	0.022
Cr	0.046	0.019	0.006	0.006	0.018
Pb	0.045	0.018	0.006	0.006	0.019
Sn	0.045	0.024	0.006	0.006	0.024
Be		0.029	0.0007		0.007
Ca		0.0005	0.0019		0.0058
Cd		0.006			0.018
Co		0.0013	0.004		0.02
Ga	0.022	0.012	0.01	0.001	0.015
Li		0.0019	0.00220		0.0021
Na		0.0011	0.0012		0.0026
Sr		0.0019			
V	0.007	0.019	0.004	0.001	0.008
Zr		0.013	0.018		0.034

Table 3.3. Sample information of ALCOA Al alloys

Elements	Concentration in sample (w %)						
	SS319-E6	SSA132-AA	SS360-C	SA1169-2	SA1170-6	SA909	SA1507-7
Cu	3.83	1.02	0.31	0.21	0.1	0.031	0.0013
Fe	0.68	0.77	0.8	0.26	0.56	0.082	0.001
Mg	0.18	1.26	0.52	0.038	0.009	0.030	<0.0002
Mn	0.58	0.070	0.22	0.076	0.027	0.031	<0.0002
Ni	0.2	2.52	0.26			0.034	<0.0002
Si	6.23	11.85	9.17	0.1	0.23	0.061	0.001
Ti	0.10	0.057	0.079	0.021	0.039	0.03	0.001
Zn	0.35	0.058	0.25	0.021	0.039	0.03	0.001
Cr		0.0005	0.057			0.027	<0.0002
Pb			0.16			0.03	0.001
Sn			0.062			0.026	
Ga							0.001
V							0.001

obtained by Shao and Horlick [1] using a pure Ar ICP DSI; and they found that the matrix (graphite,  $\text{SiO}_2$ ,  $\text{Al}_2\text{O}_3$ ) had little effect on the curves. However, the direct analysis of refractory elements such as Zr, Ti, and V posed a challenge. In this work, the use of the Ar- $\text{O}_2$ (20%) mixed gas ICP with direct sample insertion proved to be effective for these elements.

#### **3.5.4.2 Analysis**

A small amount of sample (~ 1mg) was added to a preburned graphite cup. The samples could be weighed or not weighed. If the sample was not weighed Al was used as an internal standard for correction of weight and other variable factors such as any possible sample loss. The samples were dried under the IR lamp in the heating chamber for about 10 min before being inserted into the plasma. The plasma power was 2.0 kW and the observation time was set to 120 s.

#### **3.5.4.3 Results and discussion**

The Spex TS-6 aluminium base standards were analyzed using the Ar- $\text{O}_2$  mixed gas DSI-ICP-AES system and the results are plotted in Figure 3.10. The linearity of the log - log plots is fairly good with the slopes close to unity. The samples were not weighed (about 0.2 mg) and Al was used as an internal standard. Similar results are obtained using weighed samples. This is a difficult sample to directly analyze for elements such as Ti, Zr, and V and the results shown in Figure 3.10 are quite encouraging.

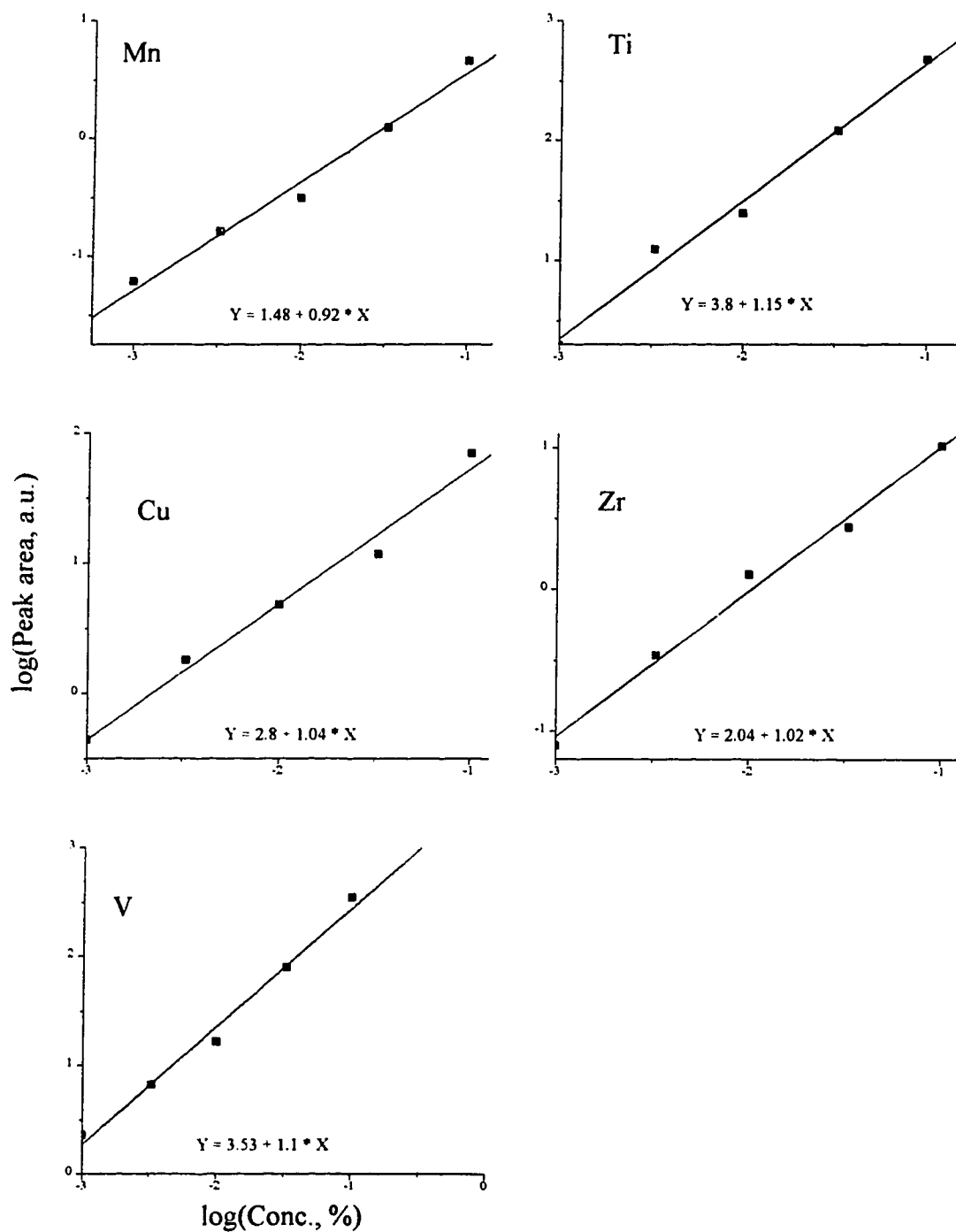


Fig. 3.10 Calibration curves (log-log) of elements in  $\text{Al}_2\text{O}_3$  std (0.001%-0.1%), TS6, with Ar- $\text{O}_2$  (20%) mix gas DSI-ICP-AES system

The samples are not weighed. Al used as internal std to correct for weight variations. Power, 2.0 kW. obs. time, 120 s.

### **3.5.5 Botanical samples (with Lishi Ying and B. Kratochvil)**

#### **3.5.5.1 Introduction**

Traditionally the elemental analysis of plant tissues and soil extracts have been performed by spark and arc atomic emission and flame atomic adsorption (FAA) techniques.

The introduction of ICPs as an excitation source for optical emission spectroscopy coincided with the growing demands for greater sensitivity in multielement techniques in the fields of agriculture, biology, and environmental sciences. Increased demand for heavy metal analysis taxed the capacity of the AAS, a single element technique. Furthermore, the spark spectrometer with its multielement capacity did not have the required sensitivity for trace elements. ICP-AES has been demonstrated to be a superior replacement for spark techniques (i.e. rotating disk methods) and a viable alternative to flame atomic absorption (FAA) for the elemental analysis of plant tissue and soil extracts [14].

However, the elemental analysis of botanical and biological material by conventional ICPs calls for the destruction of oven-dried tissue by either dry ashing or wet ashing sample treatment procedures. For the dry ash process, samples are weighed into silica crucibles and ashed with a quartz cover in an air circulating furnace at about 500 °C for about 10 hours. The residue is then soaked with HNO<sub>3</sub> or HCl for several hours before analysis. In the wet ash method, 3 mL of concentrated HNO<sub>3</sub> acid is added to a 0.5-g sample in a digestion tube (20 x 200 mm). The tube is then placed in a temperature controlled aluminum heating block and digested at 140 °C for 1 hour, followed by the addition of 2 mL of redistilled HClO<sub>4</sub>. The temperature is gradually increased to 235 °C and the sample is digested for hours or until less than 1 mL HClO<sub>4</sub> acid remains. The digested sample is rinsed and diluted with a 2M HCl solution. Not only is sample

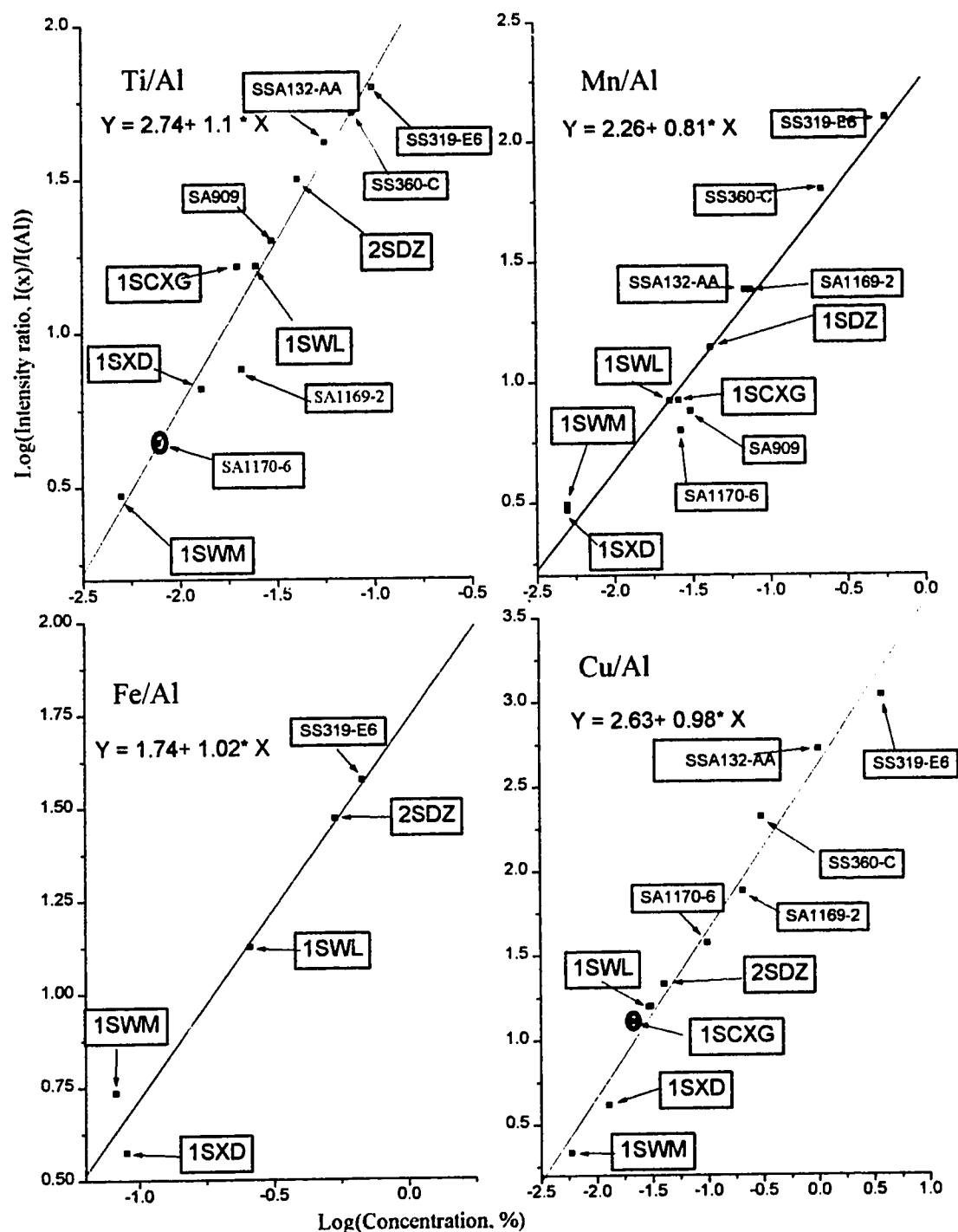


Fig. 6.3 Calibration curves of  $\log(I/I_{\text{Al}})$  vs.  $\log(C\%)$  of elements in Al standards (both high and low alloy) by *in situ* LA-ICP-AES.

Power, 1.75 KW. Analysis time, ~ 10 seconds/Sample

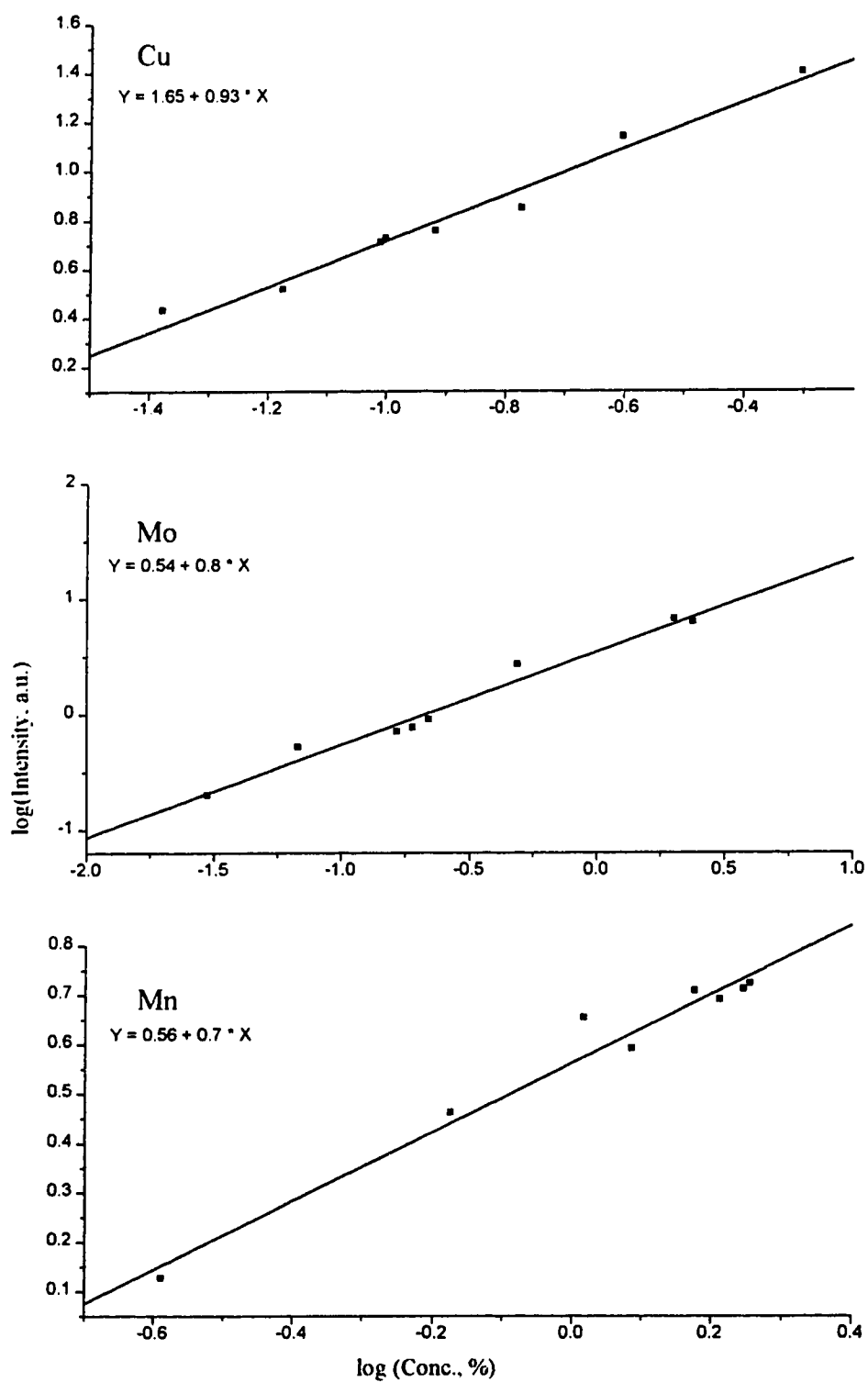


Fig. 6.4 Calibration curves for trace elements in steel standards with *in situ* LA-ICP-AES

The quality of these calibration curves can be regarded as good, but not great. However, it must be kept in mind that laser ablation methods are prone to problems associated with sample inhomogeneity. Only a small spatial section of the material is sampled. One hundred laser shots were averaged for each point, so a small depth of sample was probed, but the sample surface could not be translated relative to the laser beam as is done in some cases with external cell ablation setups. Although not tried, it should be possible to "raster" the laser beam across the surface of the sample rod with a quartz plate. This idea and others are illustrated in Figure 6.5. A glass or quartz plate can be placed in the laser beam path. By vibrating the plate randomly the laser beam will "wobble" at the sample surface randomly within a small area due to deflection of the laser by the plate. Alternatively a small tilting of the focusing lens may result in a fairly large shift of the laser spot on the sample surface. Finally it may be possible to rotate probe of the DSI. If the laser is focused off the center of the sample surface laser ablation will take place at different spots along a circle.

#### 6.4 Analyses of solution residues with *in situ* LA-ICP-AES

As discussed in Part I, DSI-ICPs is a very good method for analyzing solution residue samples. It was observed that volatile elements generate sharp signals leading to low detection limits. For refractory and carbide forming elements an Ar-O<sub>2</sub> mixed gas plasma had to be used to burn off the graphite probe with the sample. Even with the help of the Ar-O<sub>2</sub> mixed gas plasma, the signals for some refractory elements such as Zr, V, Ti, etc., still lasted on the order of 10's of seconds. Therefore a 100 times improvement in detection limit could be expected if *all* the analyte were removed and injected into the plasma in a much *shorter time* (< 1 ms). This is simply because the peak intensity will increase as the analyte is concentrated in space (or time), while the noise level increases as the square root when the integration time decreases, from 10's of

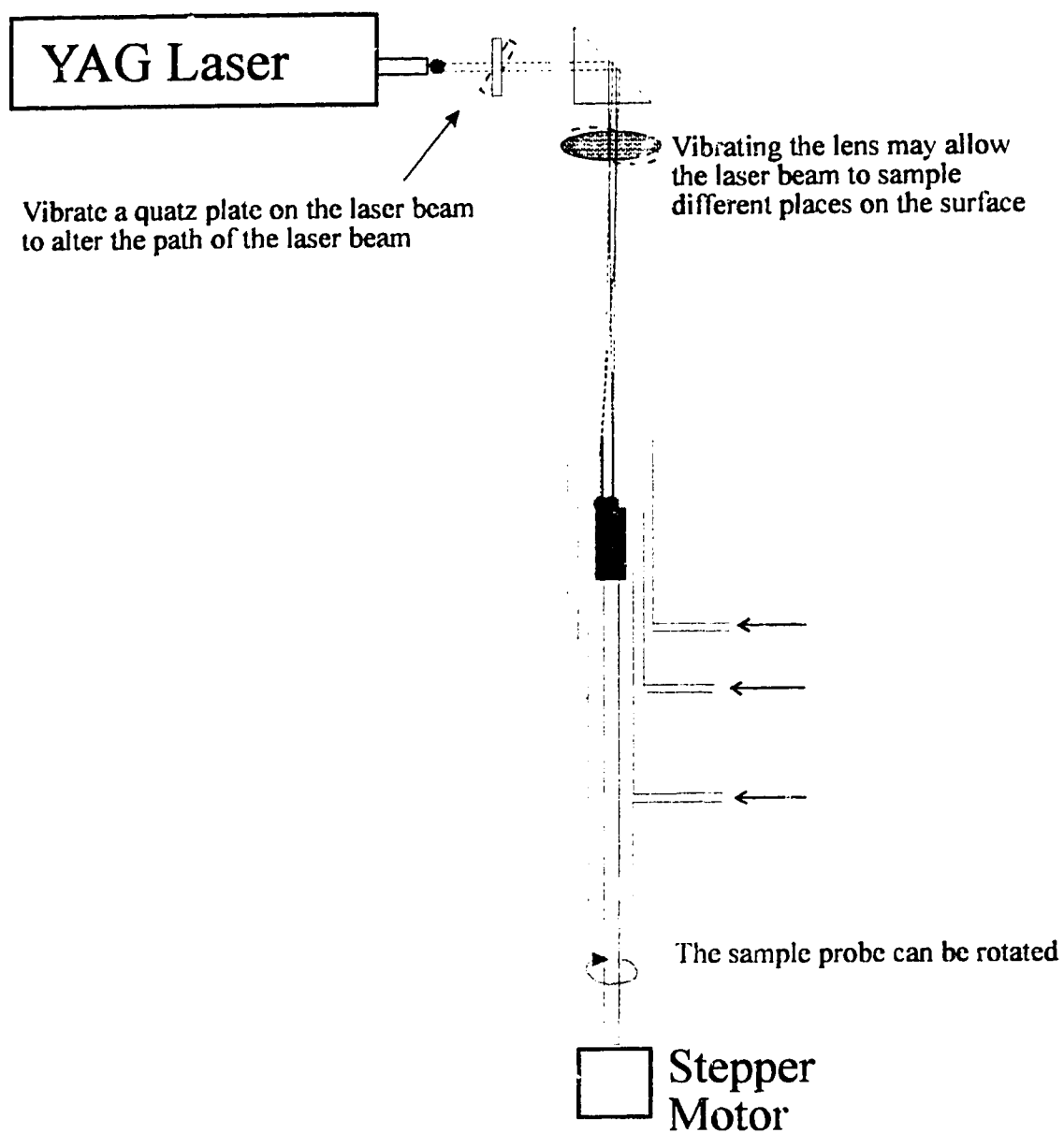


Fig. 6.5 Some methods can be used to sample in different place with *in situ* LA-ICP-AES for eliminating sample inhomogeneity problem



seconds to 1 ms. In addition, a shorter signal duration and analysis time may effectively minimize  $1/f$  noise.

*In situ* LA-ICP-AES provides a versatile technique for injecting solution residue samples into the plasma in a short time ( $< 1$  ms). For analysis, 20  $\mu\text{L}$  of a 10 ppb solution standard was added to a graphite cup and dried under an IR lamp for 10 min. Without the removal of solvent the plasma was extinguished by the fast release of solvent vapor upon ablation. The dried probe was then driven into the *in situ* position with the DSI. It was found that stronger signals were obtained when the probe was right inside the core of plasma than when the probe was under the plasma. However the tightly focused laser beam can only interact with a small portion of the sample spot. The resultant signal intensity was rather low and varied from run to run. An unfocused laser beam was then used in order to vaporize all of the sample in a single (or a few) shots. Figure 6.6 shows the *in situ* LA-ICP-AES signal for V in a solution residue sample with unfocused laser ablation. For such a low concentration (10 ppb) of a nonvolatile element the signal is fairly strong. As one can see from Figure 6.6, the V is not completely vaporized in the first shot. If all the analyte were vaporized in the first shot a much better signal to noise ratio would have been obtained. In addition to incomplete vaporization with a single shot, the precision from run to run was also fairly poor. This may have been due to the fact that the power density of the unfocused laser beam was too low and that part of the sample solution soaked into the inside graphite probe and thus could not be easily vaporized with laser action. Reasonable quantitative results have not been achieved at this stage. However, the preliminary results have demonstrated that this may be a very sensitive method for solution residue samples. A laser of high peak energy may help to improve the performance of *in situ* LA-ICP-AES for solution residue samples, and pyrolytic and/or glassy graphite cups or a quartz sample probe could be used to effectively keep all the sample on the surface of the probe.

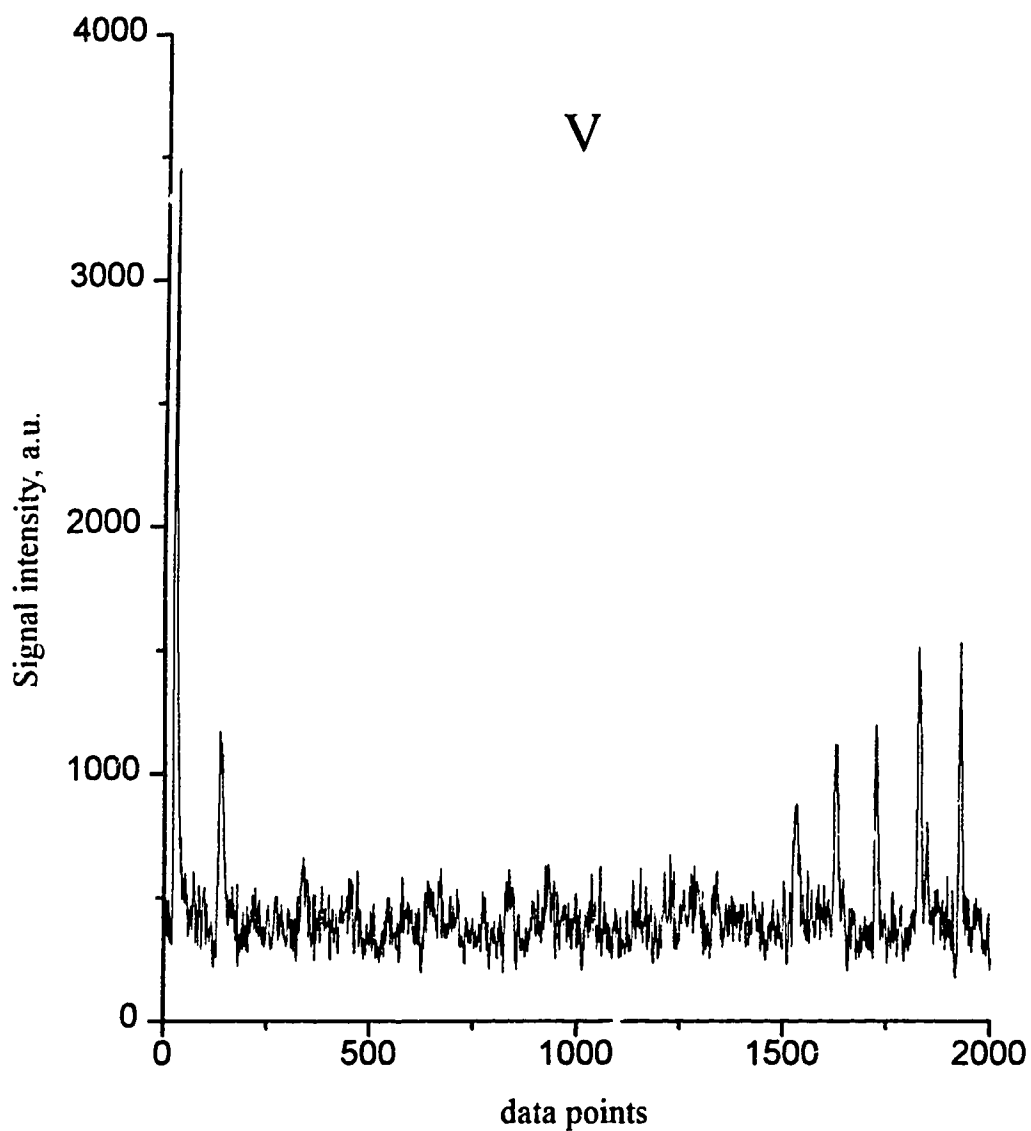


Fig. 6.6 Signal for *in situ* LA-ICP-AES of V in solution residue sample, Sample, 20  $\mu\text{L}$  x 10 ppb (SM20) in a graphite cup.

Laser, 100 mJ/pulse, firing at 20 Hz, No focus. ADC, 26.6 kHz.

## 6.5 Problems and future work

Limitations of sample size and shape, and lack of ease in translating the laser beam over the sample surface, are the most important drawbacks of the current *in situ* LA-ICPs setup.

It is also clear that the vaporization efficiency of the ICP will greatly affect the accuracy and sensitivity of the method. In conventional laser ablation ICP systems the particles transported into the ICP usually are small enough for efficient vaporization and atomization because large particles settle within the transportation system, while in the *in situ* laser ablation system presumably all the ablated particles are ejected into the plasma. The measured traveling speed in the plasma is about 35 m/s. That means the residence time of the analyte is less than 1 ms. Further studies need to be carried out to clarify such questions as; is the ICP able to vaporize all the ablated particles efficiently within such a short residence time, and how is the particle size distribution dependent on the laser power with respect to this *in situ* laser ablation system? The use of an elongated ICP torch and a higher observation position or an end-on viewing set up may help eliminate incomplete vaporization.

At the current stage of this technique, quantitative results have only been obtained for metal samples. However it is possible to analyze powder samples after pressing the sample into a pellet form or by making the sample into a glass by fusing the sample with a fluxing reagent such as  $\text{Na}_3\text{BO}_3$ . The later method has great potential. To do this, sample and fusion reagents could be weighed directly into a graphite cup. The graphite cup is then covered and heated in a muffle oven. After the probe is cooled, it could be used directly for *in situ* LA-ICP-AES analysis with no need for further transferring the sample, therefore simplifying the operation procedure and reducing the chance of contamination. The sample formed is inherently homogeneous and could be used for future analysis as standard.

## References

1. J. G. Williams and K. E. Jarvis, *J. Anal. At. Spectrom.* 8, 25 (1993).
2. W. T. Chan and R. E. Russo, *Spectrochim. Acta* 46B, 1471 (1991).
3. C. Geertsen, A. Briand, F. Chartier, J. L. Lacour, P. Mauchien, S. Sjostrom and J-M. Mermet, *J. Anal. At. Spectrom.* 9, 17 (1994).
4. J. Uebbing, A. Ciocan and K. Niemax, *Spectrochim. Acta* 47B, 601 (1992).
5. L. Moenke-Blankenburg, *Spectrochim. Acta Rev.* 15, 1 (1993).
6. A. A. van Heuzen, *Spectrochim. Acta* 46B, 1803 (1991).
7. A. A. van Heuzen and J. B. W. Morsink, *Spectrochim. Acta* 46B, 1819 (1991).
8. D. Sommer and K. Ohls, *Fresenius Z. Anal. Chem.* 304, 97 (1980)
9. X. Feng and G. Horlick, *J. Anal. At. Spectrom.* 9, XXX (1994).

## Chapter 7

### Studies of conventional LA-ICP-AES

#### 7.1 Introduction

Detection limits and overall system performance of laser ablation ICP spectrometry are difficult to compare as such a wide range of detection limits have been reported and there are a wide range of experimental systems in use. In order to directly compare the *in situ* system to a conventional system, a conventional LA-ICP-AES system was configured with the same laser and ICP. The ALCOA standards were used as the test samples with the same conditions except that an ablation chamber and transportation tube system were added.

Another reason for studying conventional LA-ICPs is the fact that most conventional LA-ICP systems are designed to deal with low speed signals with a low speed data acquisition and amplification subsystem and a lot of detail of the signal may be lost with such a system. The signals generated by LA-ICPs are discrete in nature not only because the ablation event by a pulsed laser is discrete but also the majority of analyte is present in discrete particulate form that is removed by the laser. Interestingly, Thompson *et. al.* [1] recently argued that detection limits for conventional laser ablation might be lowered by use of higher speed measurement electronics which would allow measurement of the signal pulses generated as the ablated particles were vaporized. This is quite an interesting study and they indicate that perhaps, rather than following the conventional wisdom of generating pseudo-continuum signals in conventional laser ablation, superior and more informative results may be achieved by time resolving the inherent pulsed signal. Chan and Russo [2] also carried out some measurements of laser ablation generated emission signals using higher speed measurement electronics. Bearing this

consideration in mind we have used a fast amplification and data acquisition subsystem to record the signal for the conventional system. With this system some interesting results have been obtained.

## **7.2 Instrumentation**

The schematic diagram of the conventional LA-ICP-AES system is shown in Figure 7.1a. In this system, ablation was implemented using the external ablation cell shown in Fig. 7.1b and the ablated material was transported to a conventional ICP torch via a Tygon tube (about 1m). The ablation chamber is made of quartz. A lens of 13 cm focal length is placed between the window of the ablation chamber and the laser to focus the laser beam onto the sample. The position of the lens is adjustable along the laser beam to fine tune the focus. Samples are Al alloys (ALCOA) in disc shape and no special surface processing is needed. The sample is sealed by applying a pressure to it as it is set against a rubber O-ring which is against the ablation chamber (see Fig. 7.1b). A piece of graphite rod in the center of a plastic disc was used as a blank sample. The normal ICP torch used in pneumatic nebulization ICP was used for the LA-ICP experiment.

## **7.3 Signal characterization of conventional LA-ICP-AES**

Typical single laser shot emission signals obtained with this system are shown in Fig. 7.2. These signals are for one of the high alloy standards (ALCOA SS319-E6). The amplifier time constants were set to 0.5 ms, the ADC data rate was 244 Hz, and 8 adjacent data points were added together to form one point in the final data array. The peak intensity occurred about 2s after ablation. The peak width at half maximum is about 1s.

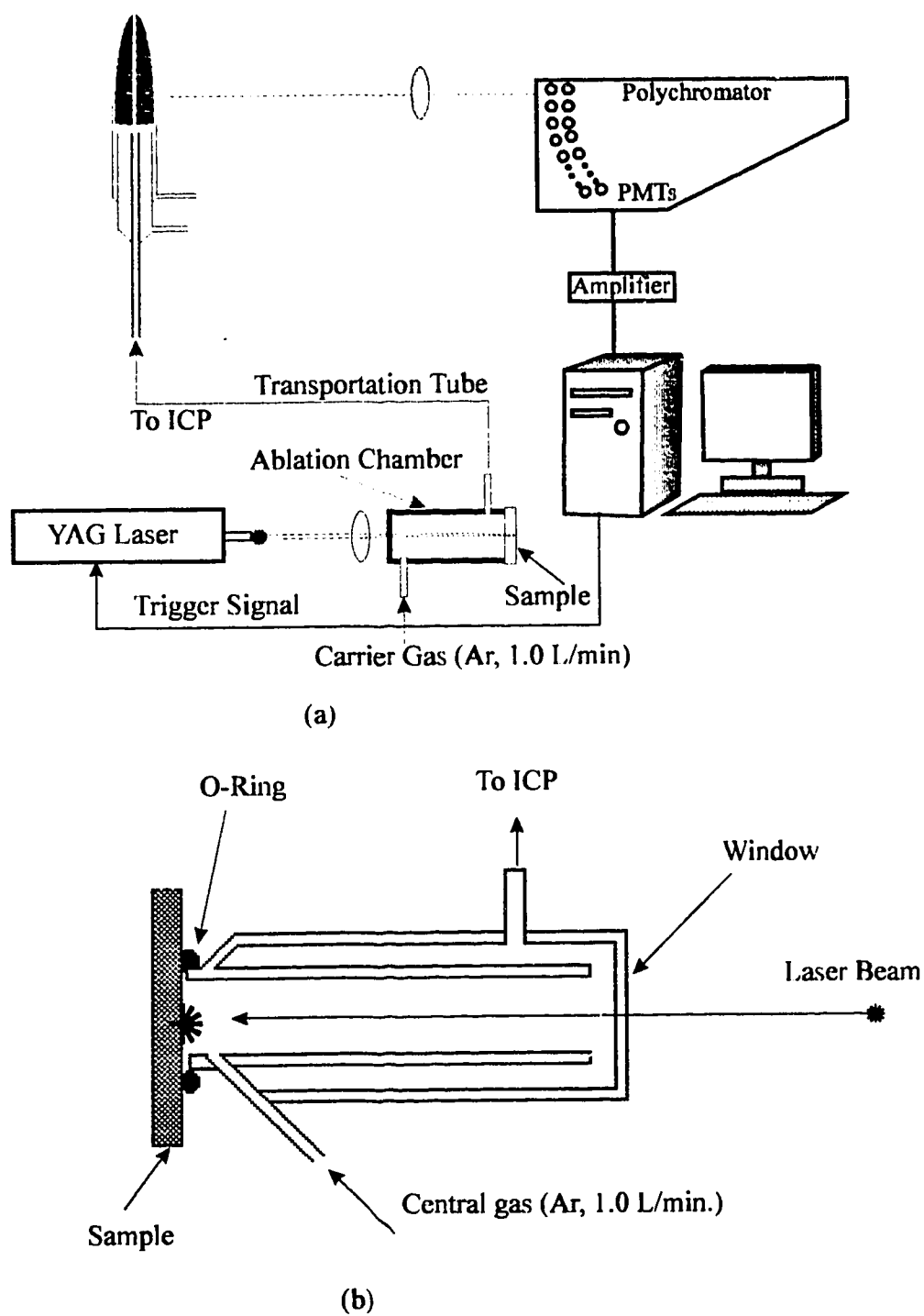


Fig. 7.1 Schematic diagram of conventional LA-ICP-AES (a) and the ablation chamber (b)

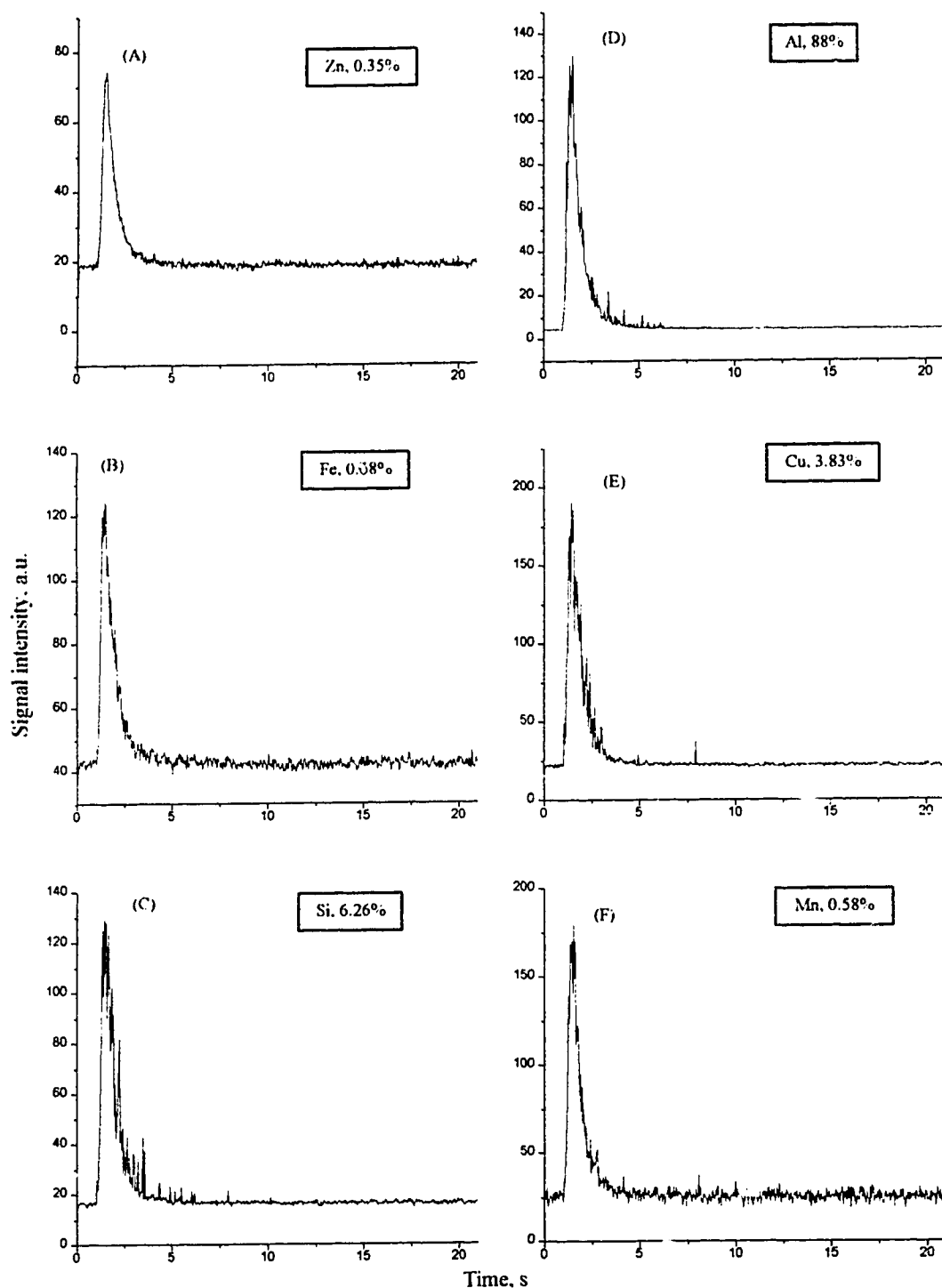


Fig. 7.2 Signal temporal profiles of single shot by conventional LA-ICP-AES  
 Sample, high alloy Al (SS319E-6);  
 Laser, Q-switched Nd:YAG, 100 mJ peak energy, single shot  
 ADC, 243 Hz/channel, 21 s obs. time  
 ICP, Ar-N<sub>2</sub> (2%) mixed gas, 1.75 kW



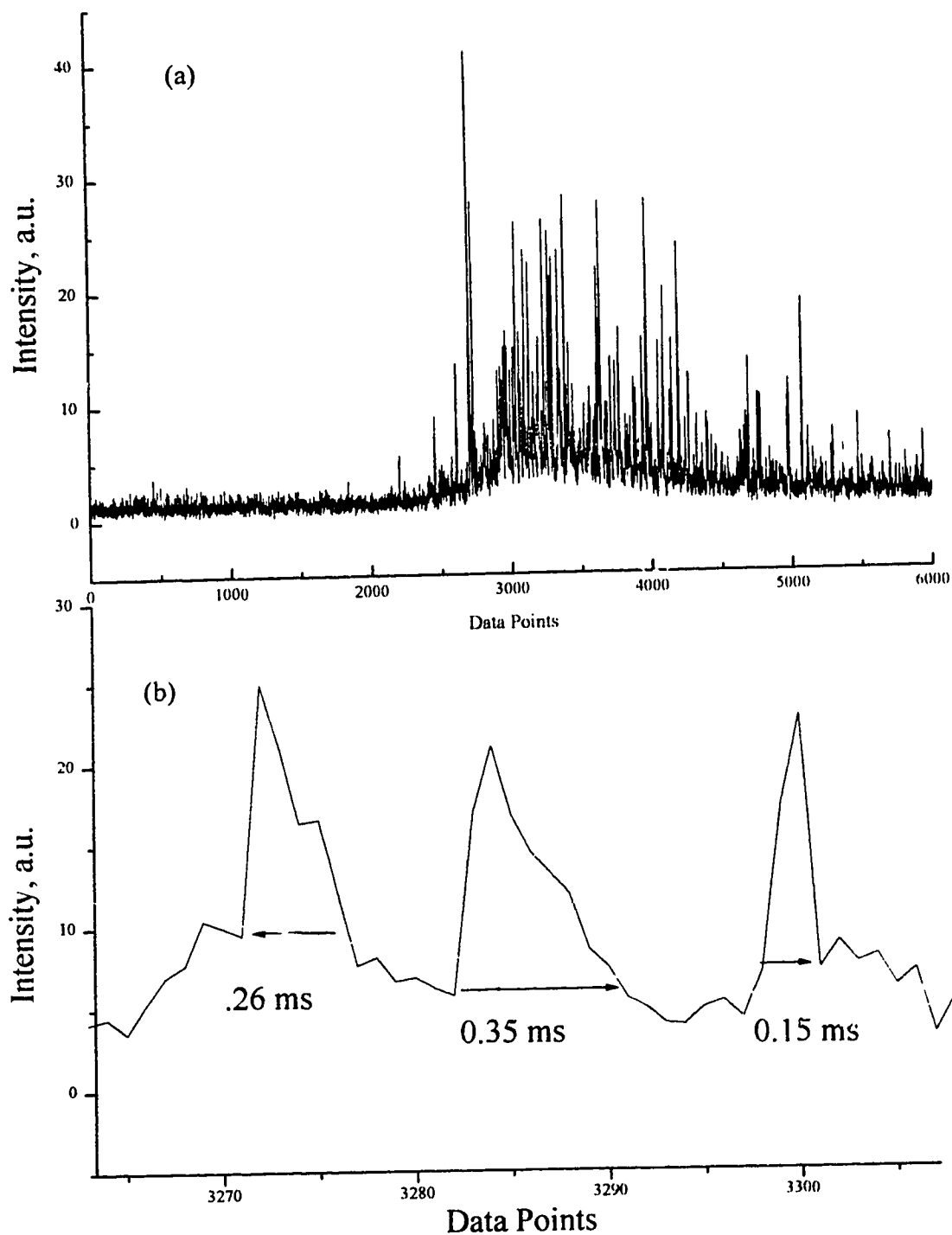


Fig. 7.3 Cu (3.83% in high Al alloy) temporal profile of single shot with conventional LA-ICP-AES  
 ADC, 26.666 kHz, 60 scans x 100 pts/scan = 6000 pts, in 3 Seconds  
 Time constant, 0.01 ms.

In contrast to Figure 7.2, Figure 7.3a shows the signals for a single shot obtained with high ADC speed (26.666 kHz). Because this ADC program had been set-up for *in situ* LA-ICP-AES analysis with 100 data points/acquisition, the signal profile shown in Figure 7.3a is discontinuous in time and consists of 60 successive 100 point acquisitions for a total of 6000 points. There is about 45 ms break between acquisitions. Signals during the break are not collected. The collected signal is therefore a representative slice of the whole signal. Otherwise a total of 79,998 data points (26666 points/s x 3 s) have to be collected for the 3 second observation time if there were no breaks. As compared to the signals shown in Figure 7.2, some characteristics of the signals in Figure 7.3 are noteworthy.

The signal in Figure 7.3a is composed of spikes superimposed on an envelope similar to the peak shape of Figure 7.2. These spike signals likely result from large particles entering the plasma. Particles entering the plasma will go through melting/vaporization, atomization, excitation and emission stages. The analyte is concentrated around the particle and therefore generates a strong signal. Signals resulting from particles separated by less than the observation window will overlap. The emission forming the envelope may be the result of the unresolved emission from the analyte in the gas phase and in small particles.

The intensities of the signal spikes can be as high as 10 times the average signal level. These signal spikes can potentially be used to improve the sensitivity of conventional LA-ICP-AES. Thompson *et. al.* [1] argued that for particle introduction sampling techniques such as laser ablation-ICPs the detection limit would be decreased as the particle size increased. Assuming that the detection limit of a given continuous solution nebulization ICP-AES system was 10 ng/mL for an analyte; and given a sampling efficiency of 1%, a sample uptake speed of 1 mL/min., and an integration time of 10 s the absolute detection limit of the system is then given by the following equation

$$D.L_{absolute} = 1\left(\frac{cm^3}{min}\right) * 1\% * \frac{10}{60} * 10\left(\frac{ng}{cm^3}\right) = 17 \text{ (pg)} \quad 4.1$$

If a particle of the same mass (17 pg) was injected into the plasma, a peak signal of 1 ms duration would be produced. That means the analyte is concentrated 10,000 times in time, from 10 s to 1 ms, and the peak intensity of the signal is expected to be 10,000 times stronger than the signal level of the continuous nebulization system. Because an integration of 1 ms is used with the peak signal, versus 10 seconds in a continuous nebulization system, the noise level is therefore expected to be 100 ( $\sqrt{10000}$ ) times higher than that of the continuous nebulization system provided it is white noise dominated. Therefore the net S/N improvement is  $10,000 / \sqrt{10000} = 100$ . The absolute detection limit with the particle injection method will then be 100 times better, i.e., 0.17 pg. Listed in Table 7.1 are the calculated detection limits for different masses of spherical particles in the micrometer range [1]. The detection limit is calculated assuming a density of 8.0 g/cm<sup>3</sup> for the particle and a concentration detection limit of 10 ng/mL.

Table 7.1. Calculated detection limits for different masses of spherical particles in the micrometer range.

Diameter (μm)	mass (pg)	detection limit (% w/w)
0.5	0.52	33
1.0	4.2	4
2.0	34	0.5
5.0	520	0.03
10.0	4200	0.004

The results in Table 7.1 indicate a cubic decrease in detection limit with an increase in particle size. However, from the stand point of laser ablation ICPs, such improvement is very limited and practically impossible for quantitation with conventional LA-ICP-AES. With conventional LA-ICP-AES only small particles have high transportation efficiency, the large particles being segregated at the bottom of the ablation chamber and the transportation tube. Furthermore, the signal is band broadened by the ablation chamber and transportation system, leading to a thousand times effective dilution. The ultimate detection limits can be obtained only when all the particles/analytes generated in a laser shot can be carried into the plasma within a short time (less than 1 ms). This has been realized with *in situ* LA-ICP-AES, as discussed in the last chapter.

The shape and width of emission spikes are strongly affected by the time constant of the amplifier. The second column of Figure 7.4 shows the zoomed views of selected parts of the signals in the first column of Figure 7.4. The label on the x-axis indicates which part was selected. The labeled values are the peak widths in ms. When larger time constants are used, the signal becomes smoother and lower in amplitude (see Figure 7.4c and 7.4d). When the time constant approaches the analyte residence time in the observation window (which is about 0.7 ms, refer to Sections 5.5 and 5.6) spike signals waned both in number and intensity (see Figure 7.4c and d).

The signal for a single laser pulse lasts for about 3 to 5 seconds. This accounts for the lower sensitivity of conventional LA-ICPs compared to *in situ* LA-ICPs. Because the laser pulse is only 18 ns and the analyte residence time over the observation window in the plasma is about 1 ms (refer to section 5.5) band broadening is mainly attributed to the diffusion of the analyte in the ablation chamber and transportation tube.

Figure 7.5 shows the signals for a single laser pulse for both conventional and *in situ* LA-ICP-AES. The sample used in conventional LA-ICP-AES is a high alloy Al and the one used in *in situ* LA-ICP-AES is a low alloy Al. In the first column of Fig. 7.5 are the emission signals for a single laser shot for the conventional laser ablation system. In the

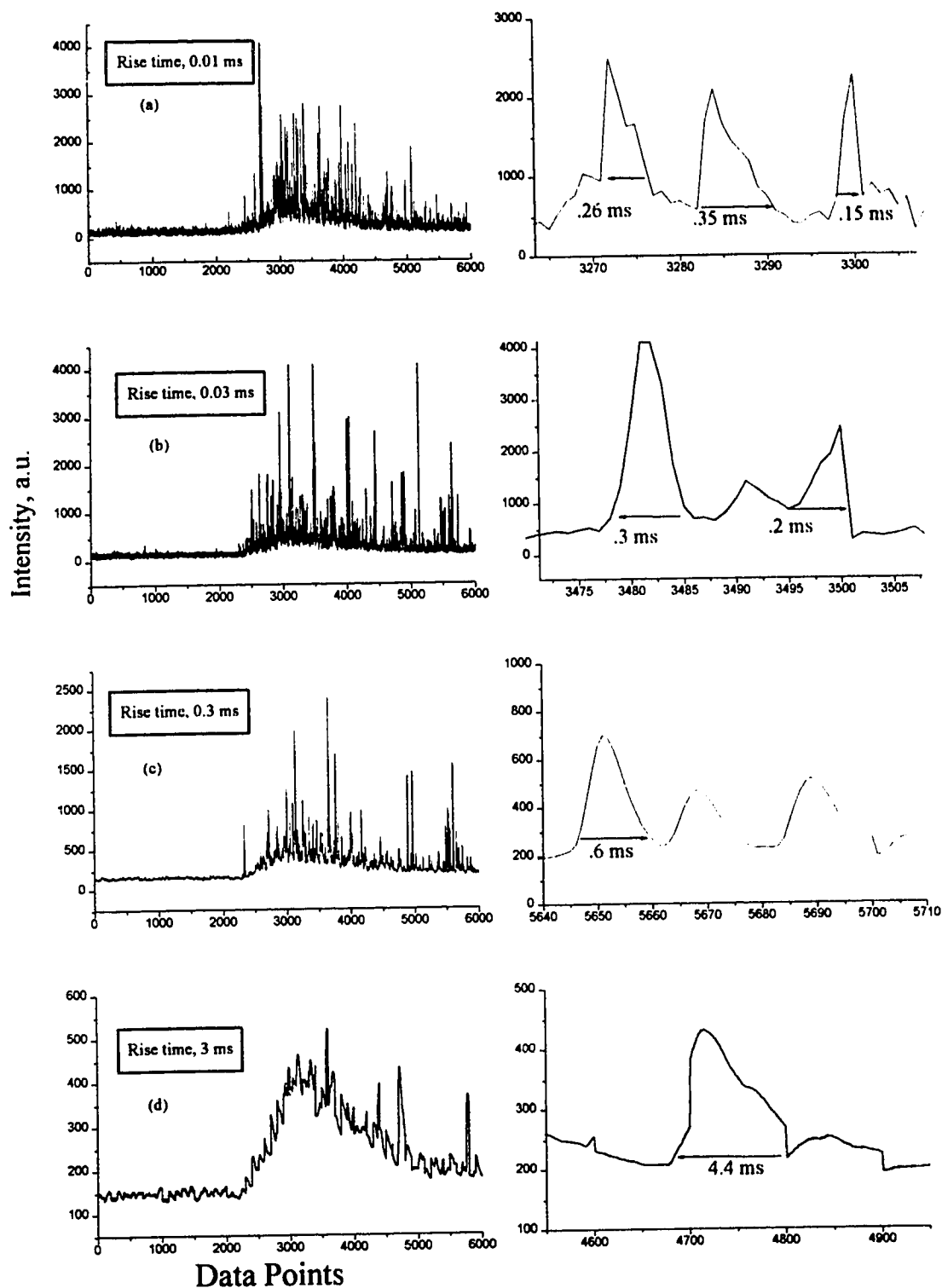


Fig. 7.4 Cu (3.83%, in high Al alloy) temporal profile of of single shot with LA-ICP-AES with different time constant  
 ADC, 26.666 kHz, 60 scans x 100 pts/scan = 6000 pts, in 3 Seconds

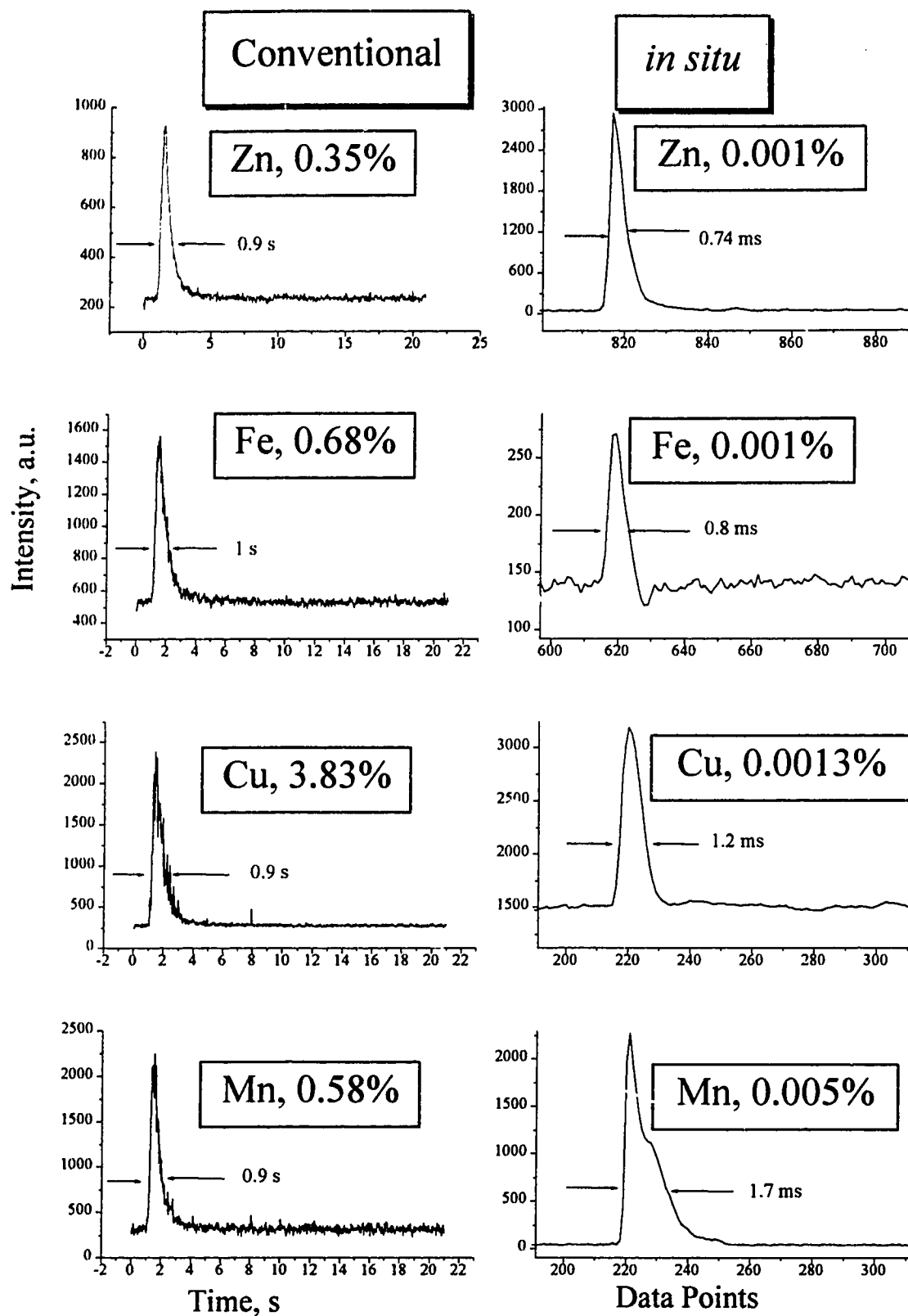


Fig. 7.5 Temporal profiles of conventional vs *in situ* LA-ICP-AES  
 Sample, Al alloy.  
 Laser, Q-Switched Nd:YAG, 100 mJ peak energy, single shot

second column of Fig. 7.5 single laser shot emission signals are shown for the *in situ* laser ablation system. The differences between these two columns are striking when one considers that the concentrations in the sample used for the *in situ* measurements are 100 to 3000 times lower than in the sample used in the conventional counterpart. Almost all the tested element channels show better S/N with *in situ* LA-ICP-AES. The data presented in Fig. 7.5 clearly indicate the importance of rapidly injecting sample when using pulsed or discrete sample introduction systems for ICP spectrometry. Sensitivity gains on the order of thousands are realizable and it is this feature that provides unique capability to *in situ* laser ablation.

The dependence of signal profiles on the laser firing frequency with conventional laser ablation is shown in Figure 7.6. As the laser firing rate increases to 5 Hz, the peaks start to overlap and a so called quasi stable signal is achieved as the laser frequency approaches 10 Hz. Also note that the signal level increases with laser firing frequency, because the sample amount removed per unit time increases with laser firing rate. Therefore a higher firing rate is advantageous in improving sensitivity, precision and in providing a quasi DC signal which is easy to handle with conventional measurement electronics.

Memory effects exist in conventional LA-ICP systems. Figure 7.7 shows the blank (graphite) signals in an Al channel (first column) and Cu channel (second column) after an Al sample had been run and the system purged for 5 minutes. The blank signals are quite different with and without laser action. The traces shown in Figures 7.7c and 7.7d are the blank signals in the Al channel and Cu channel without firing the laser on the graphite blank. The background is very clean and the background signal drops to the baseline level quickly after the laser is turned off. The signals shown in Figures 7.7a and 7.7b were obtained by shooting the laser on the graphite sample. Numerous signal spikes are observed. In examining the ablation chamber, one can see that there are particles visible on the bottom of the ablation chamber after hundreds of shots on the Al standards.

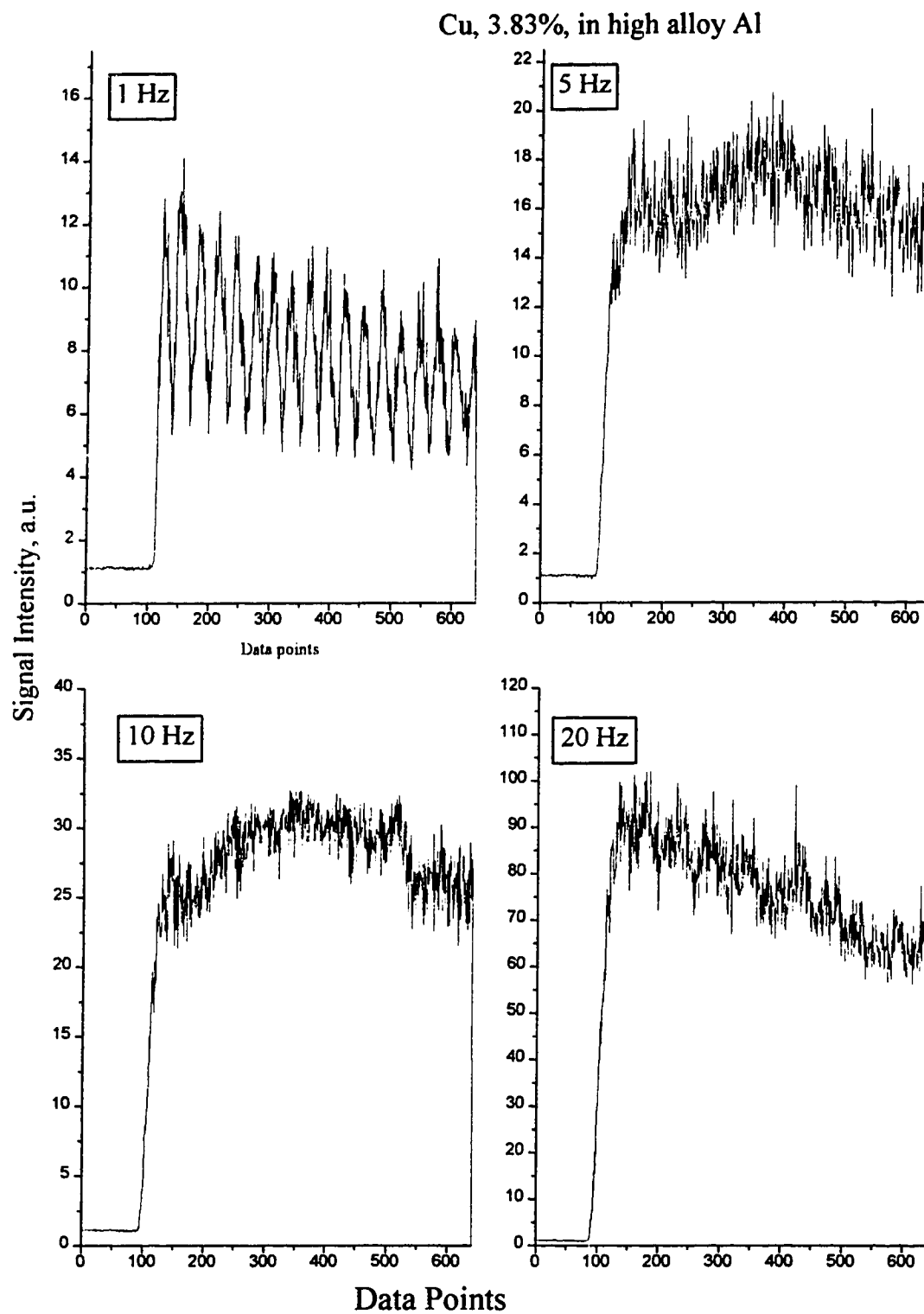


Fig. 7.6 Effect of laser frequency on signal shape and intensities with conventional LA-ICP-AES. Sample, high alloy Al (SS319E-6) ADC, 256 Hz/channel, obs. time, 20 s.



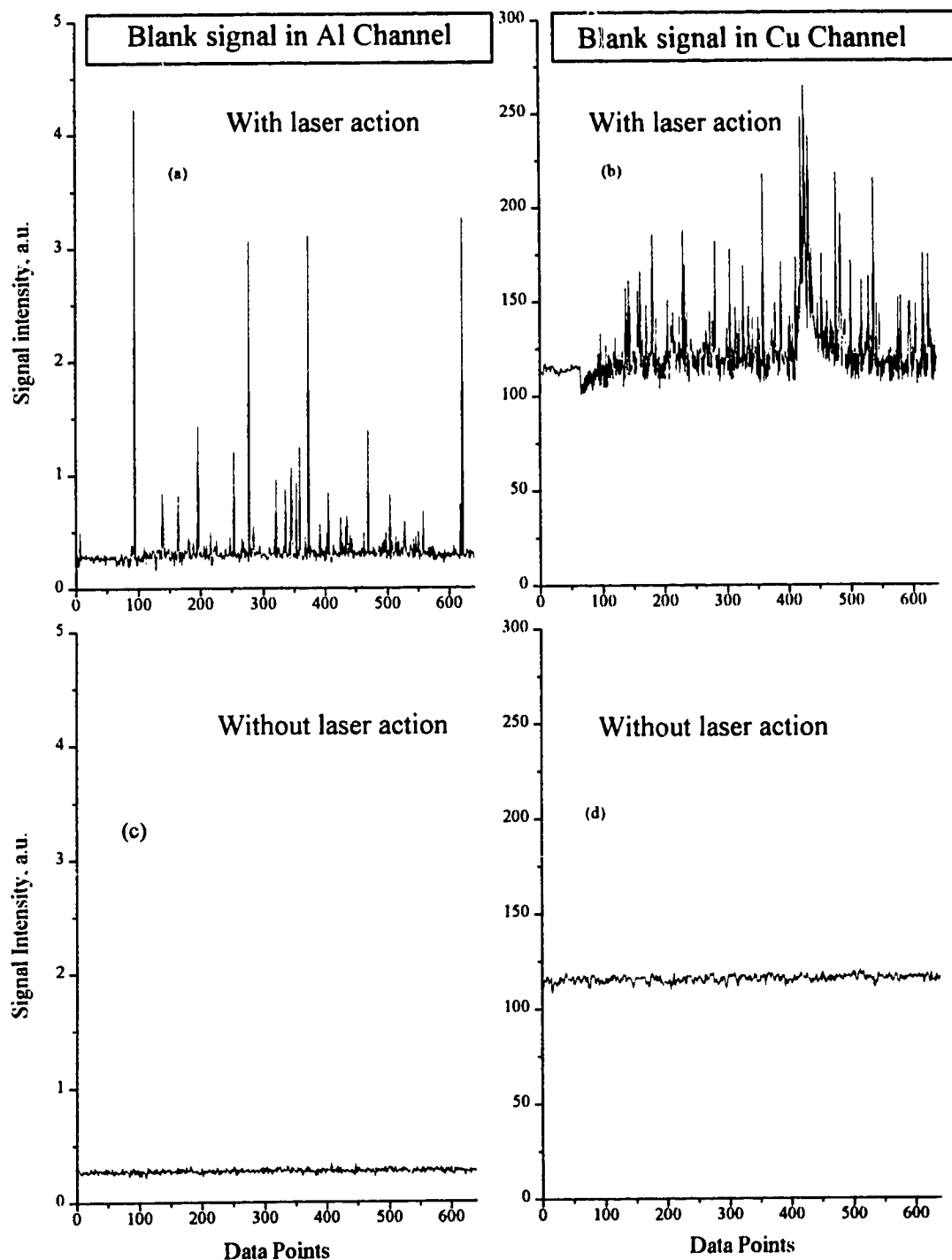


Fig. 7.7 Blank signals of conventional LA-ICP-AES  
Blank sample, graphite rod; A low alloy Al sample  
(SA909) was run in the system before blank sample.

These particles stay there without laser action, but when the laser is fired they are mobilized due to the mechanical vibration resulting from shock waves associated with the laser action. Such a process seems to release the particles from the surface of the ablation chamber and transportation tube. The results suggest: (1). A clean up (purging) cycle of several minutes is necessary when analyzing trace elements with conventional LA-ICPs; (2) In evaluating detection limits of conventional LA-ICPs, the method used to evaluate the standard deviation of the blank sample is critical. Misleading results may be obtained by running blank samples without laser action.

For comparison, Figure 7.8 shows the blank signal profiles of graphite with the *in situ* LA-ICP-AES system. The blank run was taken right after running a high alloy Al sample in the system. The graphite rod had been preburned in an Ar-N<sub>2</sub> (2%) mixed gas plasma for 60 seconds to burn out the impurities. The signal traces show no evidence of a memory effect. It should also be noted that firing the laser on the blank samples does not generate significant fluctuations on the baseline.

#### 7.4 Summary

Conventional LA-ICP was studied with fast signal amplification and data acquisition. The same parameters for the laser and ICP were employed as those used with *in situ* LA-ICP-AES. The results reinforced the merit of *in situ* LA-ICPs. *In situ* LA-ICPs realizes the ultimate sensitivity achievable with LA-ICPs. However employing fast electronics interesting signal profiles can be obtained in conventional LA-ICP. The following areas may be potentially explored in the future using a fast data acquisition subsystem with ICPs.

- Analyze individual particles for major and minor constituents.
- Improve bulk detection limits of solid-injection methods such as laser ablation and slurry nebulization ICPs.

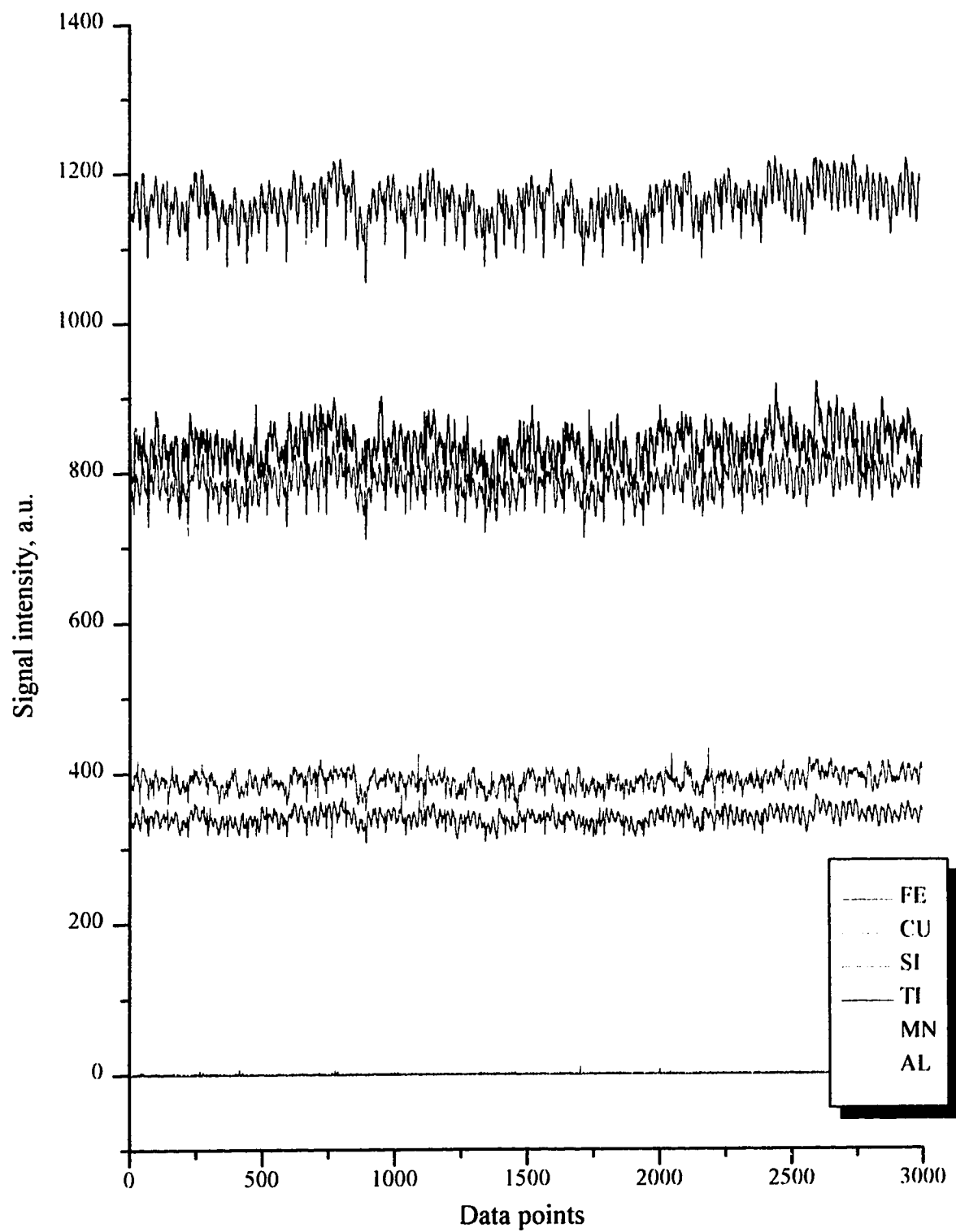


Fig. 7.8 Blank signals of *in situ* LA-ICP-AES in different channels.  
The signals were obtained by firing the laser on a graphite rod.  
ICP power, 1.75 kW; Laser, 20 Hz; ADC speed, 1.5 kHz/channel  
Observation time, 2 s.

- Determine the composition and mass of individual particles in a mixture.
- Simultaneously determine analyte in liquid and suspended phases in samples such as paint, oil, powder, dusts, metallurgical materials, etc.,
- Obtain sample homogeneity information
- Use particles as probes in fundamental studies such as particle size distribution, vaporization, and excitation processes in ICP

The development of fast modern electronics and computers make such studies readily feasible and affordable.

## References

1. M. Thompson, C. D. Flint, S. Chenery and K. Knight, *J. of Anal. Atomic Spectrometry*, 7, 1099 (oct. 1992)
2. W. T. Chan and R. E. Russo, *Spectrochim. Acta* 46B, 1471 (1991).

## **Chapter 8**

### **Summary and future work**

Two solid sample introduction techniques, direct sample insertion and laser ablation, have been studied in this thesis.

#### **8.1 DSI-ICP**

The first parts of the thesis address the main problems found in the direct sample insertion, which is the incomplete vaporization in the Ar (100%) plasma for non-volatile and carbide forming elements, especially in refractory solid samples.

An Ar-N<sub>2</sub>(2%) mixed gas ICP was then studied in order to improve the vaporization ability of the DSI-ICP. It was found that the Ar-N<sub>2</sub>(2%) mixed gas DSI-ICP provided increased vaporization capability. The optimum amount of N<sub>2</sub> in the outer gas was ~ 2%(V/V) for powers of 1.75 to 1.8 kW. The effects of other foreign gases such as air and O<sub>2</sub> were similar at the 2% level. Improved detection limits, pg to ng, and calibration curves were obtained for solution residue samples. The Ar-N<sub>2</sub> (2%) mixed gas DSI-ICP-AES with SiO<sub>2</sub> coated graphite cup has been studied and found to effectively eliminate carbide forming interferences. It was successfully used to determine carbide forming elements in different glass and fly ash samples.

However, the direct analysis of some nonvolatile elements, especially in refractory solid samples, is still problematic. Therefore, an Ar-O<sub>2</sub> mixed gas plasma with higher level of O<sub>2</sub> (~ 20%) was studied with DSI-ICP for the direct analysis of different elements in different samples. Satisfactory results were obtained for a variety of matrixes, such as solution residues, botanical samples, engine oils, Al<sub>2</sub>O<sub>3</sub> powders, and Al alloy drillings.

Applying the mixed gas DSI-ICP to the analysis of different types of samples is one of the important areas that should be pursued in the future. The Ar-O<sub>2</sub> mixed gas DSI-ICP has effectively extended the DSI-ICP technique to difficult-to-vaporize elements, refractory compounds, and refractory samples. The Ar-O<sub>2</sub> mixed gas DSI-ICP-AES system could be readily used for a wide variety of applications in elemental analysis which are difficult and time consuming for other methods. It is very suitable for biological and clinical samples. Oils and geological samples can also be analyzed readily without pretreatment.

Sample spattering is a serious problem with the Ar-O<sub>2</sub>(20%) mixed gas DSI-ICP. Spattering usually occurs in the first 10 seconds after insertion. More experiments are needed to characterize the processes that occur during vaporization and atomization for the Ar-O<sub>2</sub> mixed gas DSI-ICP. Some methods that may help to eliminate the spattering problem have been proposed in section 3.2 of Chapter 3.

Standardization for direct analysis of solid samples is always a challenging task. More attention should be paid in the future to the development of accurate and simple standardization methods for unknown samples. Perhaps synthetic standards prepared by soaking a matrix powder with solution standards can be a viable approach. The standard addition method could be a useful alternative. However, the vaporization efficiency could be different for the analyte in the spiked standard and in the original sample. More studies need to be carried out to characterize the vaporization efficiency of the analyte in different forms.

The multielement capability of the current system is quite limited. There are only eight differential input channels on the data acquisition board. A multiplexer may be used to connect more element channels, as discussed in section 2.2.3 of Chapter 2. Such a multiplexer can be obtained commercially. The complex and diverse vaporization behavior of different elements in different samples imposes the necessity for recording the

signal profiles for the entire vaporization process. This, in turn, demands faster data acquisition and processing and a larger storage medium.

Because of the transient nature of the DSI-ICP signals, the background signal is also changing with time. Therefore it is important to do real time background correction for DSI-ICP analysis. Sensitive and fast solid state array detectors should be ideal for DSI-ICP analysis due to their true multichannel capability and true off line background monitoring and correction capability.

Because of the elimination of the sample preparation step the analysis time of the DSI-ICP is much shorter and the system has the capability for massive sample through put. However, there are some steps in the current system that need manual interaction and should be automated in the future for high sample throughput.

First of all, the sample change is done manually; an autosampler needs to be interfaced to the DSI-ICP system. An autosampler similar to the one described in reference 1 but driven by a car aerial is under development in this lab. After the sample carousel, which holds up to 24 samples, is loaded the system would then be able to do DSI-ICP analysis without attendance.

Secondly, the gain of the signal amplifier of the system needs to be adjusted manually during analysis with the current system. As discussed in section 2.2.3, an amplifier with programmable gain setting is necessary to make the system easy to use. Because of the transient nature of the DSI-ICP signal, the gain should be adjusted dynamically for each data point. This idea has been discussed in section 2.2.3 of Chapter 2 and tested with a home made amplifier. A better designed amplifier or a commercial ADC board with 16 bit, on-board programmable gain amplifiers of wide range (such as 1, 5, 50, 500) is highly recommended (such as National Instruments AT-MIO-16X) for future work.

Thirdly, because of the complex temporal profiles of the DSI-ICP signals, the data processing is time consuming and usually needs interactive selection for some parameters

such as the background correction points and integration intervals. However, it is possible to automate the data processing procedure with better software.

Direct sample insertion techniques for ICP-MS have several advantages [2, 3] such as better sensitivity and reduced background and spectral interferences. This is primarily due to the elimination of water in DSI systems. However, there are some technical problems associated with the interfacing of DSI with ICP-MS. First, the horizontal setup of the ICP torch in ICP-MS demands special care to prevent solid samples from dropping out of the sample probe. Second, the rather slow scan speed with the current quadrupole mass spectrometer limited the multielement capability. Interfacing the DSI-ICP to a vertical time-of-flight mass spectrometer would be of great interest for future work.

## 8.2 LA-ICP

In the second part of the thesis an *in situ* laser ablation ICP-AES system is developed and characterized. The elimination of the ablation chamber and sample transportation system has led to substantial improvement in performance over conventional laser ablation ICPs. In addition to the features of laser ablation sampling present in conventional LA-ICPs systems, the *in situ* LA-ICPs totally eliminates memory effects, generates strong and sharp transient signals, and provides low detection limit.

The main limitations to the current system and ideas for future work have been discussed in section 6.5 of Chapter 6 and can be summarized as follows:

- (1) The sample is not rotated and therefore is subject to the sample inhomogeneity effect.
- (2) Some shaping of the sample is necessary in order to deliver the sample to the *in situ* position by the DSI mechanism.
- (3) The multielement capability of the system is limited due to the fast transient signal and the relatively slow ADC speed.

To overcome the sample inhomogeneity effect some methods have been proposed and discussed in section 6.3 of Chapter 6.



To extend the multielement capability, a faster ADC board is needed. Use of an array of gated integrators would be a practical alternative. The signal is integrated over the gating signal, which can be generated by the laser trigger signal. Therefore only one peak area data is collected for each channel in each laser pulse.

As discussed, DSI-ICP standardization is always a challenging task for direct analysis of solid samples. However, compared to DSI-ICP, the *in situ* laser ablation virtually is a nondestructive technique. Therefore well calibrated samples can be used as secondary standards for future analysis. Other standardization methods have been discussed in section 6.5 of Chapter 6 and should be studied in future work.

As discussed in section 6.4 of Chapter 6, the *in situ* LA-ICP could be very sensitive for solution residue samples. However more work needs to be done in the future to get quantitative results.

It is expected to see the high power diode laser find its niche in such applications as *in situ* laser ablation analytical spectroscopy. Such compact lasers may facilitate the development of portable laser analyzers for remote or on-site analysis.

Conventional LA-ICP was studied with fast signal amplification and data acquisition and the results were compared with the *in situ* LA-ICP. Interesting signals were observed for the conventional LA-ICP by fast electronics. More studies should be carried out on potential analytical applications of the spike signals observed with particle sample introduction techniques, such as LA-ICP by fast electronics.

**References**

1. W. E. Pettit and G. Horlick, *Spectrochim. Acta 41B*, 699 (1986)
2. V. Karanassios and G. Horlick, *Spectrochim. Acta 44B*, 1387 (1989).
3. V. Karanassios and G. Horlick, *Spectrochim. Acta 44B*, 1361 (1989)